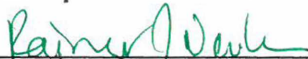PORPHYRY COPPER, COPPER SKARN, AND VOLCANOGENIC MASSIVE

SULFIDE OCCURRENCES IN THE CHANDALAR COPPER DISTRICT,

ALASKA

RECOMMENDED: _____

Mary J. Keskinen
_____

_____
Chairman, Advisory Committee

_____
Department Head

APPROVED: _____
Dean, College of Natural Sciences

_____
Dean of the Graduate School

4/27/90
_____
Date

PORPHYRY COPPER, COPPER SKARN, AND VOLCANOGENIC MASSIVE

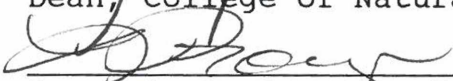SULFIDE OCCURRENCES IN THE CHANDALAR COPPER DISTRICT,

ALASKA

A

THESIS

Presented to the Faculty of the University of Alaska

in Partial Fulfillment of the Requirements

for the Degree of

MASTER OF SCIENCE

By

Lisa Nicholson, B.S.

Fairbanks, Alaska

May 1990

ABSTRACT

Metamorphosed porphyry copper, copper skarn, and volcanogenic massive sulfide (VMS) occurrences have been found in 5 key prospects within Devonian rocks of the Chandalar copper district, Alaska. The Venus, Victor, Eva, and Evelyn Lee prospects contain "proximal" porphyry copper/copper skarn mineralization, whereas the Luna prospect contains "distal" Cu-Zn skarn and Cu-Zn VMS mineralization. Porphyry copper mineralization is recognized by granodiorite composition meta-intrusives; zoned potassic, sericitic and propylitic alteration; and $del^{34}S$ values of -1.5 to -0.6 per mil. Skarns consist of andraditic garnet (Ad_{30-100}) and diopsidic pyroxene (Hd_{9-46}), and have $del^{34}S$ values of -4.7 to -1.1 per mil. Alteration types in intrusive rocks and adjacent skarn are generally compatible. VMS occurrences contain chloritic and silicic alteration, and massive sulfides have $del^{34}S$ values of -0.8 to 6.9 per mil, consistent with values from known Devonian VMS deposits.

TABLE OF CONTENTS

LIST OF FIGURES

LIST OF TABLES

LIST OF APPENDICES

ACKNOWLEDGMENTS

support I needed to finish this thesis. I especially want to thank Tim Weglarz, who gave me a lot of ideas and constructive criticism and, more importantly, who stuck with me through many thesis anxiety attacks.

CHAPTER I - INTRODUCTION AND BACKGROUND

INTRODUCTION

The Chandalar copper district, in the south-central Brooks Range, is an approximately 500 square kilometer, east-west trending belt of metasedimentary and metaplutonic rocks (Figure 1). Sporadic copper mineralization, occasionally accompanied by lead and zinc, occurs in meta-plutonic rocks, calc-silicate rocks and calcareous schists. The copper prospects in the district are located within 35 kilometers of the Dalton highway. Consequently, they are potentially more amenable to mining than many mineral prospects in Alaska, which are often located hundreds of kilometers from established roadways.

Due to the multiple deformational and metamorphic events which have affected the area, the nature of the Chandalar occurrences is complex. Some previous workers have called these mineralized bodies deformed porphyry copper and skarn occurrences (DeYoung, 1978). Others have suggested that they are regionally metamorphosed calc-silicate deposits with a skarn-like appearance, in which the mineralization is volcanogenic in origin (Croff and Bressler, 1980). The presence of either porphyry copper/copper skarn deposits or stratabound volcanogenic massive sulfide (VMS) deposits would imply that the area

1

Figure 1. Location map of the Chandalar copper district
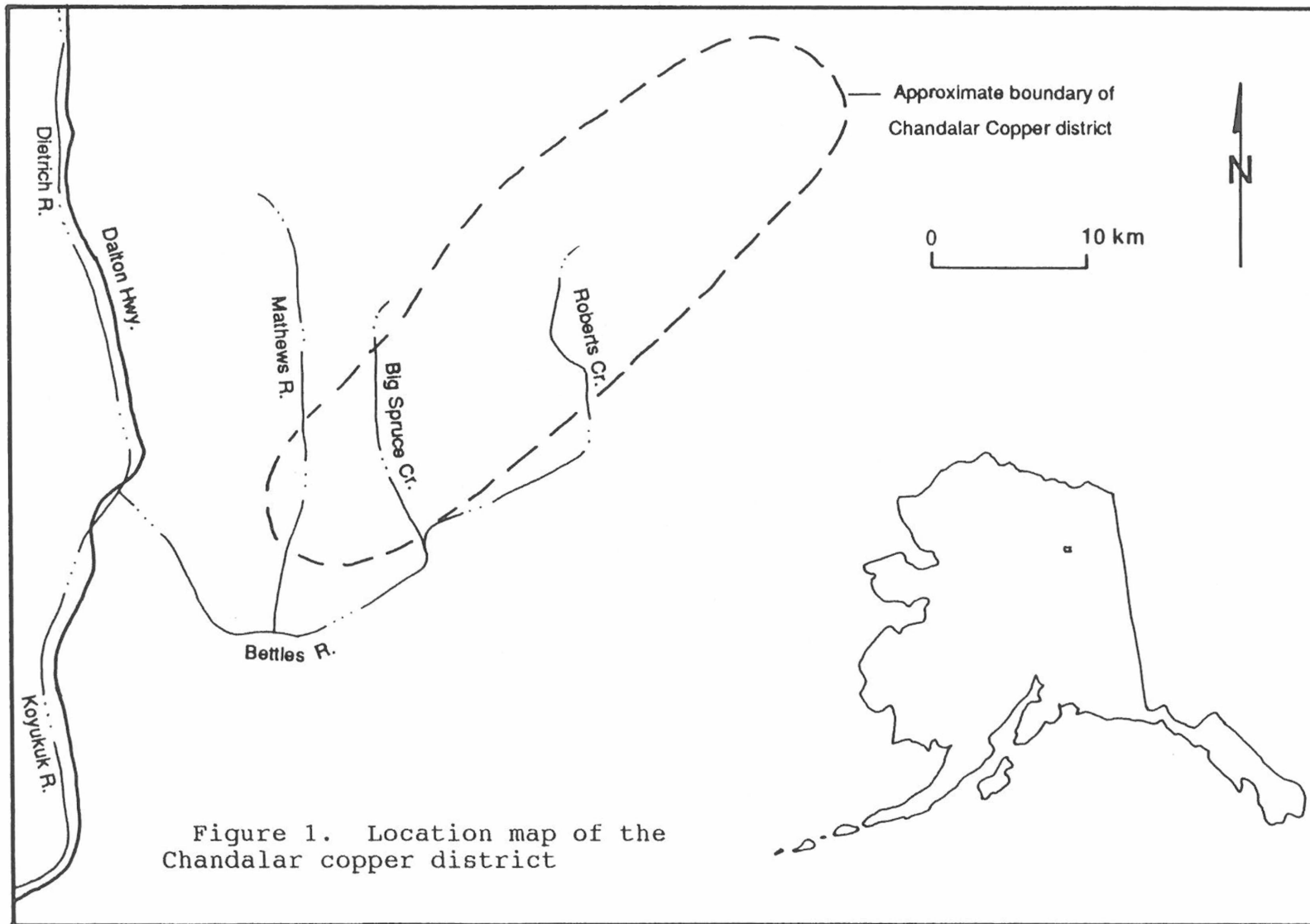
may contain further mineral reserves; however, exploration techniques and potential mineral wealth would vary, depending on which deposit types were actually present.

For example, the Yerington district in western Nevada is located within a belt of porphyry copper deposits, many with related copper skarns. This district, although of smaller areal extent than the Chandalar copper district, has been estimated to have reserves of more than 1000 m.t. (million tons) of ore with grades of 0.4% Cu (Einaudi, 1982a). On the other hand, prospects in the Ambler district of the western Brooks Range, which are approximately along strike with the Chandalar district, contain >100 m.t. of approximately 10% combined Cu, Zn and Pb (with appreciable Ag and Ba) in stratabound VMS deposits (Hitzman and others, 1986).

If the Chandalar area is analogous to either of the above districts, it could contain appreciable mineral resources. Assessment of whether additional exploration is warranted, given such economic constraints as metal prices, road building costs, etc., hinges on the types of mineralization that are likely to occur. This study was undertaken to clarify the deposit types present in the district.

I first present a brief description of the characteristics of metamorphosed porphyry copper, copper

skarn and VMS deposits, followed by a detailed description of the geology of study area and of 5 key prospects (Venus, Victor, Eva, Evelyn Lee, and Luna), with an emphasis on criteria used to distinguish between deposit types. These include composition and tectonic setting of the host rock; ore and gangue mineralogy, textures, and alteration types; gangue mineral compositions and zoning; and sulfur isotope ratios of sulfide minerals. These characteristics are then compared and contrasted with those of established ore deposit models. Finally, some general conclusions are drawn about the probable mineral resources in the area.

LOCATION AND ACCESS

The Big Spruce Creek area, which includes the Venus, Victor, Eva, and Evelyn Lee prospects, is located in the Chandalar C-5 quadrangle, approximately 15 kilometers east of the Dalton Highway and 10 kilometers north of the Bettles River. The Luna prospect is located in the southeast corner of the Chandalar D-5 quadrangle, just west of Roberts Creek. This portion of the central Brooks Range consists of gently rolling, tundra-covered hillsides and cliffs of exposed marble and igneous rock. Elevations in the study area range between 700 m (2300 ft) and 1606 m (5274 ft). The area was reached by helicopter from the Disaster Creek checkpoint along the Dalton Highway for this

study, but light aircraft can land in some of the larger drainages.

INVESTIGATIVE METHODS

Six weeks were spent in the Big Spruce Creek area: three weeks each during the summers of 1984 and 1985. Field work entailed geologic mapping (at 1:31,680 and larger) of granitic and metamorphic rocks in the area surrounding lower Big Spruce Creek. Detailed field descriptions were made of rock types, the nature of contacts, and textural and mineralogical variations on an outcrop scale. Samples were collected for petrologic analysis by transmitted and reflected light microscopy, for whole rock analysis, and for geochemical analysis. One thousand feet (300 m) of drill core from 4 drill holes at the Luna prospect (DDH-1, 2, 3, and 5) were logged and sampled for sulfur isotopic analysis, X-ray diffraction (XRD) analysis, and petrologic examination. Drill logs are included in Appendix 1.

ANALYTICAL METHODS

Sixty-two polished thin sections were examined to determine mineral paragenesis and textural relationships among the mineral phases. Microprobe analyses of selected mineral phases were performed using the Cameca electron microprobe at Washington State University, Pullman. A 15

kV filament voltage, a 13 nanoamp beam current, a 2 micron beam diameter, and a 10 second counting time were used. Well-characterized minerals were employed as standards. Microprobe results are given in Appendix 2. XRD analyses of garnets and sphalerite were performed on the Rigaku Miniflex X-ray diffractometer at the University of Alaska, Fairbanks. XRD results are given in Appendix 3. Chemical analyses for major, minor, and trace elements were performed on trimmed, fist-sized samples and sample aggregates by Bondar-Clegg, Inc, Vancouver, B.C.. Major oxides plus Ag, As, Bi, Co, Cr, Cu, Mn, Mo, Ni, Pb, Sb, Se, W, and Zn were determined using plasma emission spectrometry. Zr and Ba were determined using X-ray fluorescence. Hg content was determined using cold vapour atomic absorption, and Au content was determined by fire assay-atomic absorption. Major oxide and trace element analyses are given in Appendices 4 and 5, respectively.

Analyses of sulfur isotope ratios from sulfide samples were performed by Geochron Laboratories in Cambridge, Massachusetts, using standard techniques and a Canon Diablo troilite standard. Results are discussed in Chapter III.

PREVIOUS WORK

In 1964, the U. S. Geological Survey published the first 1:250,000 geological map and cross-section of the

Chandalar quadrangle (Brosge and Reiser, 1964). This map
included fossil and isotopic age determinations, and
concentrations of lead, copper, zinc, arsenic, and antimony
for 45 stream sediment samples from throughout the
quadrangle. DeYoung (1978) compiled a mineral resources
map which included brief descriptions of 86 hard rock and
placer mineral occurrences in the Chandalar quadrangle.

Croff and others (1979) and Croff and Bressler (1980)
described a number of Cu-, Zn-, and Pb-rich hard rock
occurrences in the Chandalar copper belt. They suggested
the possible occurrence of volcanogenic massive sulfide
deposits in the area, associated with rocks interpreted as
metamorphosed felsic and andesitic tuffs. They found
mineralization in calc-silicate rocks to be common, but
spatially associated meta-plutonic rocks were found only in
the southern prospects near Big Spruce Creek (Venus-Victor-
Evelyn Lee). They interpreted calc-silicate mineralization
in the northern prospects (e.g., Luna and Hurricane-Dianne)
to be formed by metamorphic remobilization of VMS-related
sulfides into metasomatized calcareous rock.

Dillon and others (1980) and Dillon and Tilton (1985)
gave evidence for Devonian magmatism in the southern Brooks
Range. Dillon also offered a detailed description of the
structure and stratigraphy of the Chandalar quadrangle in a
Dalton Highway field guide (Dillon, 1989). Newberry and

others (1986) described a number of regionally metamorphosed calc-silicate deposits and associated meta-plutonic rocks in the Brooks Range, which included Cu-Ag and Pb-Zn skarns near the Chandalar plutons.

REGIONAL GEOLOGY

The Chandalar copper district is situated within the Hammond subterrane of the Arctic Alaska tectonostratigraphic terrane described by Silberling and Jones (1984). A generalized geologic map of the area is shown in Figure 2. The terrane includes 1)Cambrian through Ordovician calc-schist, pelitic schist and marble (IPz), 2)lower Devonian siliciclastic and volcaniclastic rocks (IPz), 3)thick Devonian marble of the Skajit Formation (Ds), middle Devonian metavolcanic rock, metagraywacke, and carbonate of the Whiteface Mountains and Beaucoup Formations (north of map area), and 4)upper Devonian siliciclastic and calcareous rocks of the Hunt Fork Formation (Dh) (Dillon, 1989). Dillon suggested that the Whiteface Mountains metavolcanic rocks are coeval with the Devonian Ambler volcanic rocks, on the basis of their lithologies, age, and stratigraphic position. However, the thick carbonate packages of the Chandalar area do not occur in the Ambler district, and there are also other stratigraphic differences between the two areas. Also,
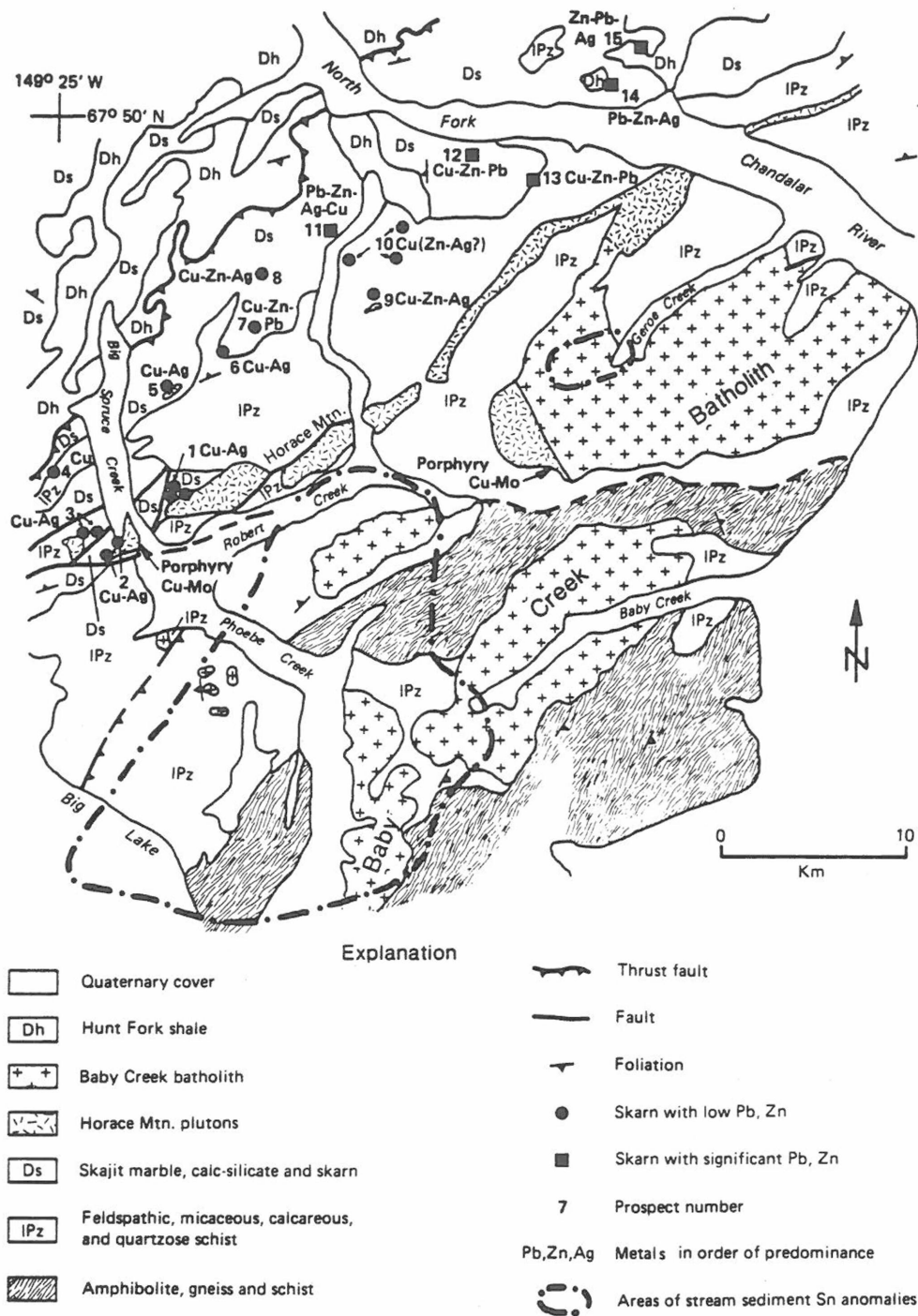
Figure 2. General geology and location of prospects in the Chandalar copper district. Prospects: 1 = Evelyn Lee, 2 = Venus, 3 = Victor, 4 = Eva, 5 = Ginger, 6 = Deimos, 7 = Hurricane-Diane, 8 = Luna, 9 = Pilgrim, 10 = Mike-Vicki-Cindy, 11 = Io, 12 = Jim-Montana, 13 = Mowgli, 14 = Gayle, 15 = Bob. Taken from Newberry and others (1986).

there are differences in U-Pb dates on rocks from the two districts (327-373 Ma for Ambler and >410 Ma for Chandalar) (Dillon and others, 1980; Dillon and Tilton, 1985). Hence, there is only a broad scale equivalence between the two areas.

The lower Paleozoic rocks mentioned above (those older than middle Devonian) have been intruded by early to middle Devonian granitic plutons. The plutons are separated into two categories by Newberry and others (1986) on the basis of their chemical and mineralogical characteristics. The Horace Mountain plutons are relatively small exposures of metaluminous, hornblende- and biotite-bearing, porphyritic granite and granodiorite. These rocks are thought by Newberry and others (1986) to represent I-type granites (Chappell and White, 1974). The Baby Creek batholith, on the other hand, consists of equigranular to porphyritic, peraluminous, biotite-muscovite granite which is thought (Newberry and others, 1986) to be an S-type granite.

Rb-Sr and U-Pb dates (Dillon and Tilton, 1985; Dillon, 1989) show ages for the Horace Mountain plutons of 402 ± 8 Ma and for the Baby Creek batholith of 380 ± 12 Ma. A potential chronology for Devonian events in the immediate Chandalar area is thus: (1) volcanism (>410 Ma) and carbonate sedimentation, (2) I-type plutonism (ca. 400 Ma), and finally (3) S-type plutonism (ca. 380 Ma). It should

be noted that this chronology may not apply to other portions of the Brooks Range.

The Ambler district (150 km west of the Chandalar district) is considered by Hitzman and others (1986) to have been part of a submerged continental platform which underwent extensional tectonics. They support this designation by the presence of bimodal volcanics and the presence of thick carbonate horst blocks which bound a graben filled with pelitic schist. Similar rock types are present in the Chandalar district, although volcanic rock protoliths have not been unambiguously identified.

The Paleozoic sedimentary and igneous rocks of the southern Brooks Range have been regionally metamorphosed, with greenschist facies mineral assemblages developed in the rocks of the Hammond subterrane (Dillon, 1989). Two penetrative schistosities and metamorphic mineral assemblages have been found by Dillon (1989). K-Ar cooling ages of the Chandalar plutons and stratigraphic relationships indicate that both events occurred between Jurassic and Cretaceous time (100-160 Ma) and affected both sedimentary and igneous rocks (Dillon, 1989). These metamorphic events are accompanied by large and small scale isoclinal folds and east-west trending thrust and strike-slip faults which generally parallel the metamorphic fabric. This deformation greatly complicates the

stratigraphic and structural relationships in the Chandalar copper district.

REGIONAL ORE OCCURRENCES

The Chandalar copper district is a northeast-trending belt which generally follows the trend of the Horace Mountain plutons. DeYoung (1978) noted this trend as a favorable area for skarn and porphyry copper occurrences. He also described a number of known occurrences within this belt. Locations of these mineral prospects are shown in Figure 2. Significant among these prospects is the Evelyn Lee prospect, which consists of copper-bearing calc-silicate rocks close to a metamorphosed hornblende granodiorite porphyry. This prospect is estimated to contain 1 million metric tons of 5 percent copper (DeYoung, 1978). The Venus, Victor and Eva prospects are believed by previous workers to contain porphyry copper-type disseminated chalcopyrite and pyrite mineralization with copper grades of 0.1 to 0.3 percent copper and small podiform masses of skarn (DeYoung, 1978). Mineralization at the Luna prospect was considered, in 1978, to be confined to skarn occurrences only. Further work by Croff and others (1979) suggested the possible presence of stratiform volcanogenic massive sulfide mineralization as well. The Evelyn Lee, Venus, Victor, Eva, and Luna

prospects are discussed further in the main body of this paper.

SUMMARY OF DEPOSIT TYPE COMPARISONS

Table 1 summarizes important characteristics of porphyry copper, copper skarn, and VMS deposits. There are additional diagnostic features which should be mentioned, involving relationships between porphyry copper and copper skarn deposits. In porphyry copper related skarns, retrograde alteration is often seen adjacent to sericitic alteration in the pluton. Conversely, prograde skarn is seen adjacent to potassic alteration in the pluton. A more detailed description of typical deposit features is included in Appendix 6. Although the characteristics described in Table 1 and Appendix 6 are diagnostic of certain deposit types, each one cannot be used alone in deposit identification (e.g., the presence of $del^{34}S$ values of 0 per mil, alone, does not indicate the presence of a porphyry copper deposit). All, or at least most, of these features must be present in order to characterize a deposit. These criteria have been considered in classifying the Chandalar occurrences.

TABLE 1

SUMMARY OF DEPOSIT CHARACTERISTICS

	PORPHYRY CU	COPPER SKARN	DEVONIAN VMS
HOST ROCK TYPE	intrusive rocks	carbonate rocks	volcanic and sedimentary rocks
ALTERATION	potassic sericitic propylitic	prograde retrograde	chloritic sericitic talc
CALC-SILICATES	none	high Fe^{3+}, low Mn^{2+}	high Mn^{2+}
ORE MINERAL CONCENTRATION	contact zone potassic-sericitic alteration	in retrograde assemblage or in marble	near chloritic or sericitic alteration
METAMORPHIC EFFECTS	foliated veins intact	none	sulfide deformation no primary textures
DEL^{34}S VALUES	zero	slightly negative	positive

CHAPTER II - DETAILED GEOLOGY OF THE STUDY AREA

INTRODUCTION

A 1:31,680 geologic map of the Big Spruce Creek area was made for this study during the 1984 and 1985 field seasons and is shown in Figure 3. Surface geology of the Luna prospect is taken from the map of Croff and others (1979) and is shown in Figure 4. Although the geology has not been continuously mapped between these two areas, geologic continuity has been suggested by Dillon (1989).

NON-MINERALIZED METASEDIMENTARY ROCKS

The meta-sedimentary and possibly metavolcanic rocks in the field area include a variety of schists consisting of various proportions of muscovite, quartz, chlorite, feldspar, biotite, and sphene. Thick resistant marble beds and less resistant argillaceous marbles are interbedded with the schist. Two types of hornfels are seen in the Big Spruce Creek prospects - calc-silicate hornfels and black hornfels. The above rock types are not mineralized and are not described in detail here. Instead, detailed descriptions are included in Appendix 7.

MINERALIZED ROCKS

The Big Spruce Creek prospects contain copper mineralization in Cu skarns and in chalcopyrite-bearing

15
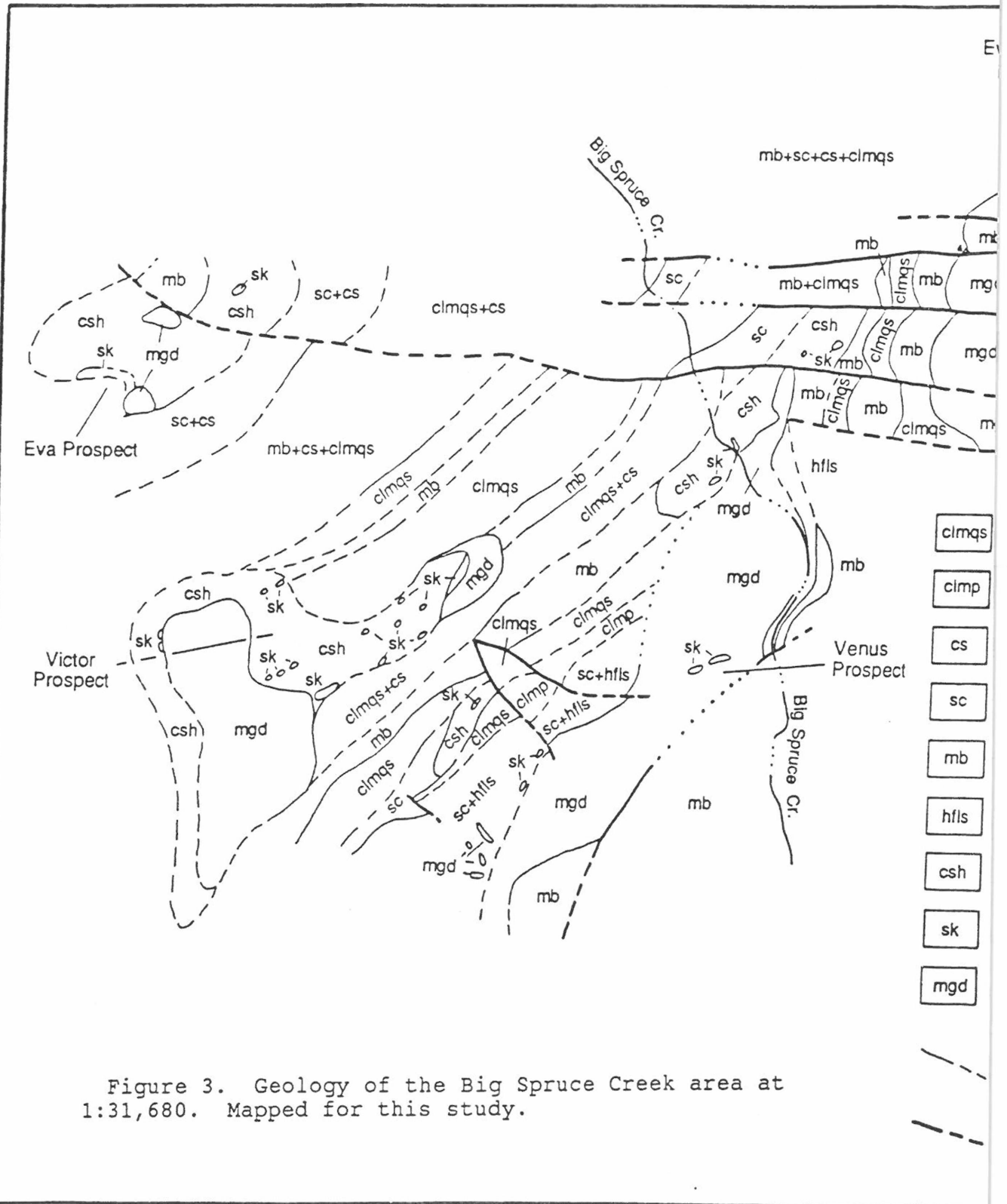
Figure 3. Geology of the Big Spruce Creek area at 1:31,680. Mapped for this study.
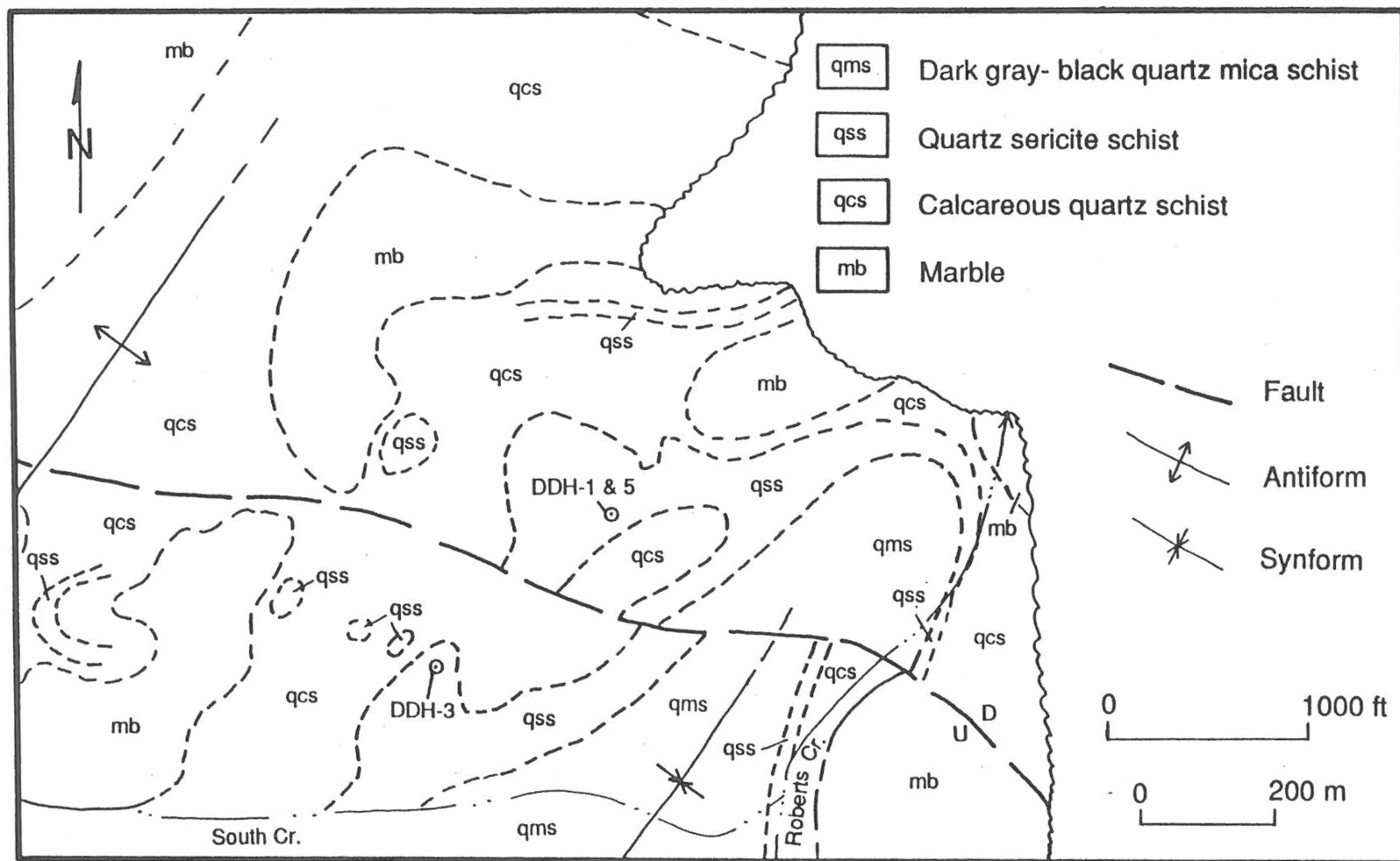
Figure 4. Generalized geology of the Luna prospect. Redrafted from Croff and Bressler, 1980.

metamorphosed porphyritic stocks. Cu skarns, Cu-Zn skarns
and Cu-Zn-Ag massive sulfide accumulations have been found
in 3 of the 4 logged drill holes at Luna (DDH-1, 3, and 5).
The northern drill holes (DDH-1 and 5) contain only Cu
mineralization, whereas DDH-3, in the southern portion of
the Luna prospect, contains Cu and Zn in both skarns and
massive sulfide occurrences. A detailed description
follows of mineralized meta-plutonic rocks, skarns, and
massive sulfide occurrences. These descriptions are based
on mapping and drill core logging from this study.

IGNEOUS PETROLOGY

Meta-igneous rocks in the Big Spruce Creek area
consist of three main bodies - the Venus stock, the Victor
stock, and the Horace Mountain pluton (Figure 5) - and a
number of associated small dikes and sills (0.5-3 m thick).
No major bodies of meta-igneous rocks have been identified
on the surface at the Luna prospect, but a number of dikes
and sills are present in the drill core.

Relict igneous textures are common but not ubiquitous.
In the interiors of the igneous bodies, the rocks are
medium-grained (1-3mm) with sub-equigranular textures.
Along the peripheries of the bodies, however, the textures
are often porphyritic with either a phaneritic or aphanitic
groundmass. Dikes and sills have a porphyritic-aphanitic
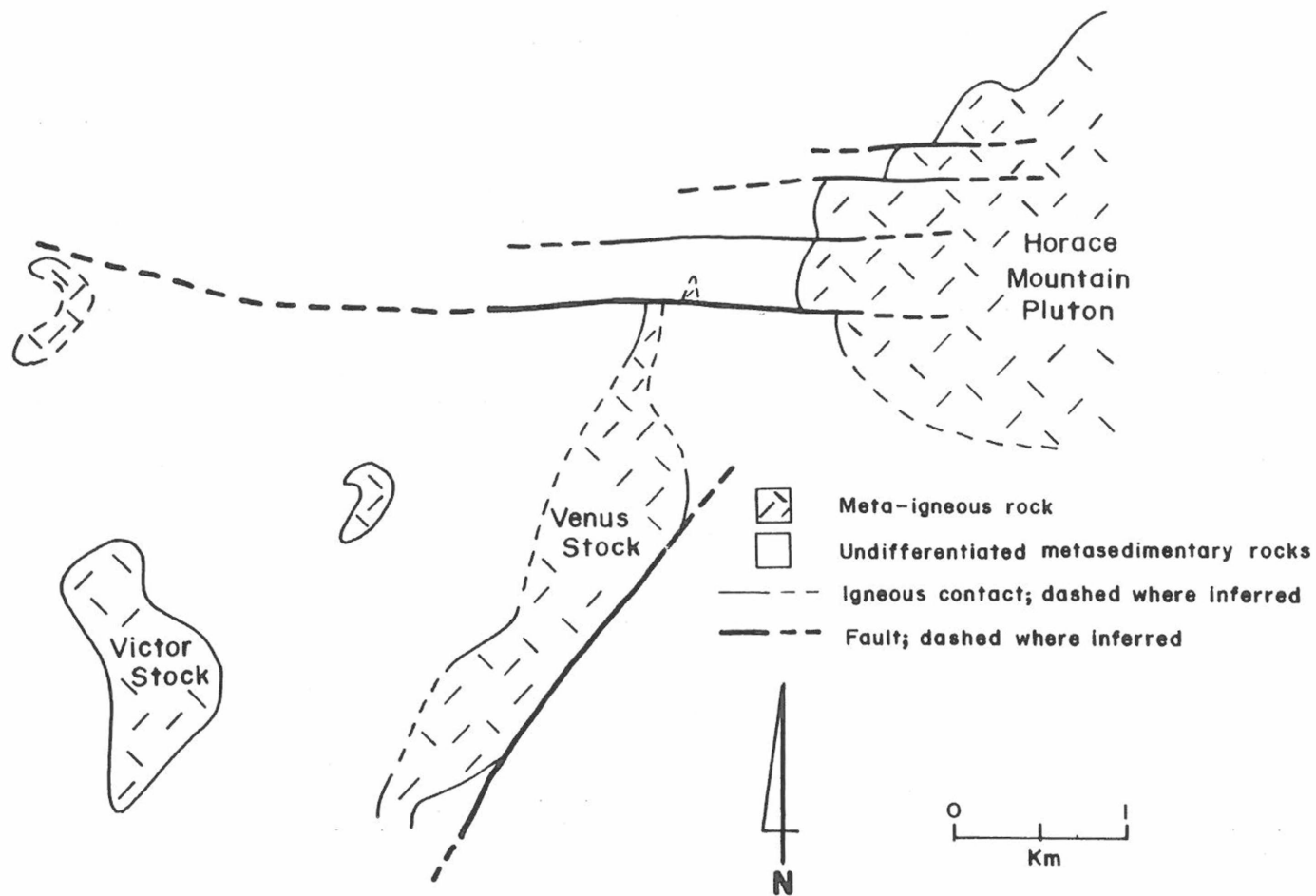
Figure 5. Location of meta-igneous bodies in the Big Spruce Creek area. Mapped for this study.

Meta-igneous rock

Undifferentiated metasedimentary rocks

Igneous contact; dashed where inferred

Fault; dashed where inferred

Horace Mountain Pluton

Venus Stock

Victor Stock

N

0   1
Km

19

texture. The large meta-igneous bodies are interpreted as metamorphosed high level plutons rather than meta-volcanic rocks on the basis of 1)their relict textures, 2)the lack of internal contacts, and 3) the lack of interbedded meta-sedimentary units. Grain sizes range from 0.05 mm to 5 mm. The groundmass makes up 55-75% of the rock and has grain sizes generally less than 0.05 mm. All meta-intrusive rocks are foliated to some extent, and foliation generally increases toward the contact with the country rock. Where they have a high platy mineral content, the rocks are highly foliated and lose their original igneous texture. This is especially apparent in sericitically altered rocks.

Modal mineralogies of relatively fresh samples (5-30% quartz, 10-25% plagioclase feldspar (10-35% An), 3-10% alkali feldspar, 0-20% hornblende +/- biotite) indicate that these meta-igneous rocks were originally hornblende granodiorites. Accessory minerals include zircon, apatite and sphene. In most samples, the feldspars and/or mafic minerals have been hydrothermally altered. This is especially true for dikes and sills. At the Luna prospect, no unaltered meta-igneous rocks were found. However, examination of relict phenocrysts within altered dikes and sills shows that their original composition was similar to the larger stocks in the Big Spruce Creek area.

Newberry and others (1986) give CIPW normative compositions for 11 relatively unaltered samples of Horace Mountain meta-intrusive rocks from within 10 km of the study area (see Figure 6). Thirteen additional CIPW compositions of Victor, Venus and Evelyn Lee meta-intrusive bodies from this study are also shown. Note that the majority of analyses plot within the granodiorite field.

Since most meta-igneous rocks in the Chandalar district are at least slightly altered, the meta-intrusive samples from this study were also analyzed for Zr. Winchester and Floyd (1977) show that certain immobile element ratios, such as Zr/Ti, can be used to help identify pre-alteration and pre-metamorphic volcanic rock types. By plotting SiO_2 vs Zr/TiO_2, Winchester and Floyd have outlined fields for fresh igneous rock types. Floyd and Winchester (1978) then show that the same diagram can be used to identify altered and metamorphosed high level intrusive and volcanic rocks. Figure 7 shows SiO_2 vs Zr/TiO_2 for Big Spruce Creek porphyry samples within Winchester and Floyd's delimited fields. Note that most of the samples fall within the granodiorite field within the diagram, as do the fresh samples on the CIPW normative plot.

A plot of alkali-silica variation for Chandalar plutonic rocks is shown in Figure 8. Fields for
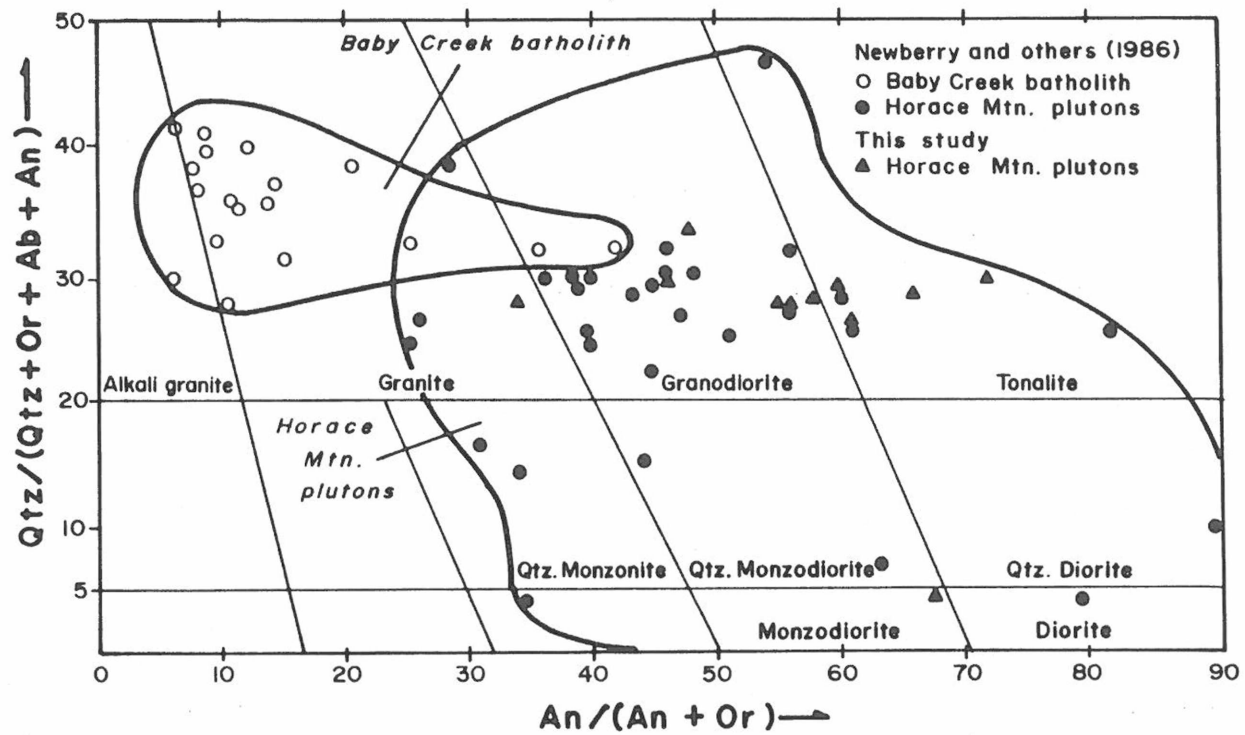
Figure 6. Normative quartz-feldspar ratio diagram, after
Streckeisen and LeMaitre (1979) for selected Horace Mountain plutonic
rocks. Data from Newberry and others (1986) and this study.
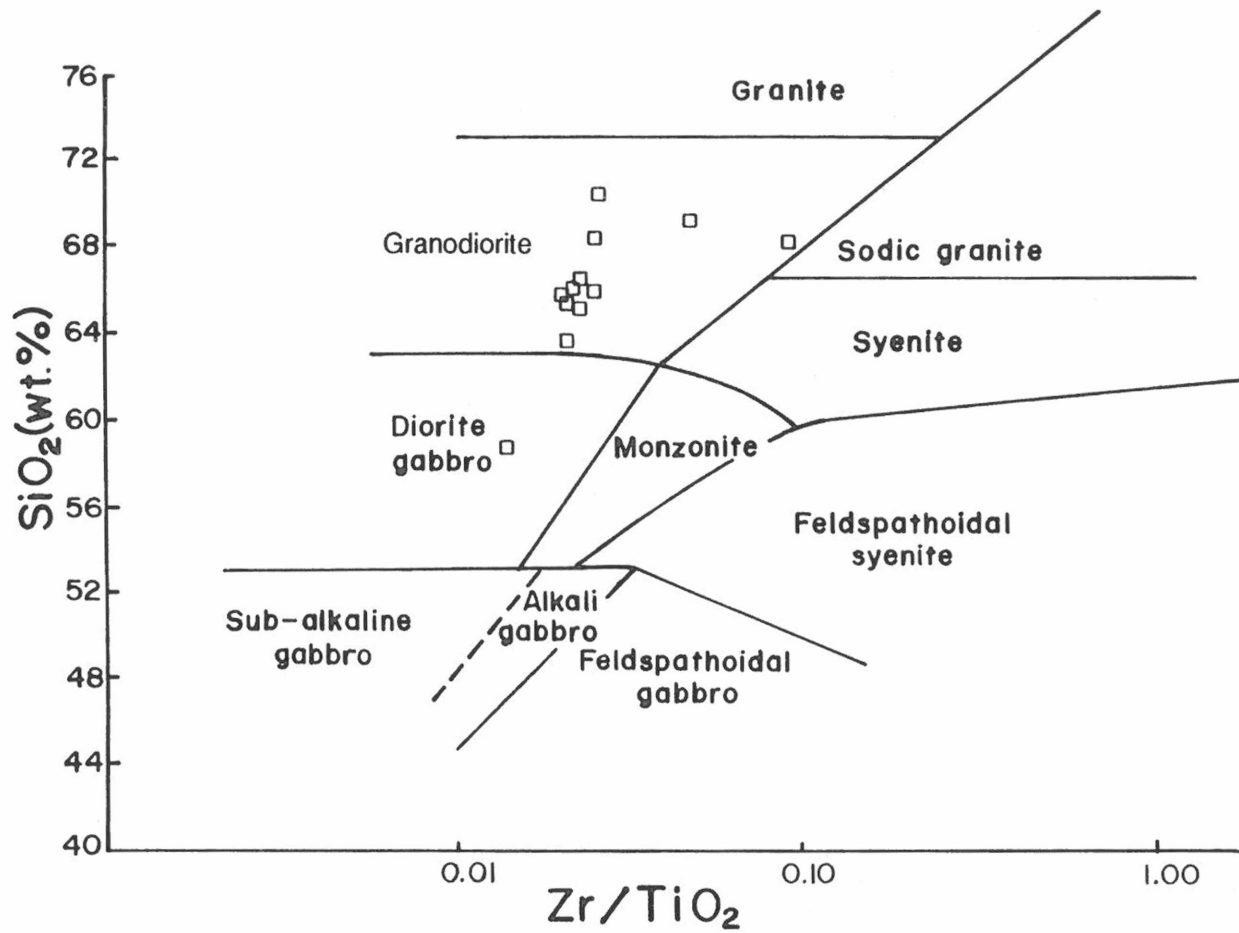
Figure 7. SiO2 - Zr/TiO2 diagram for Venus, Victor, and Evelyn Lee high-level intrusive rocks, showing the delimited fields for common plutonic rocks (after Winchester and Floyd, 1977). The data have been normalized to anhydrous totals of 100%.
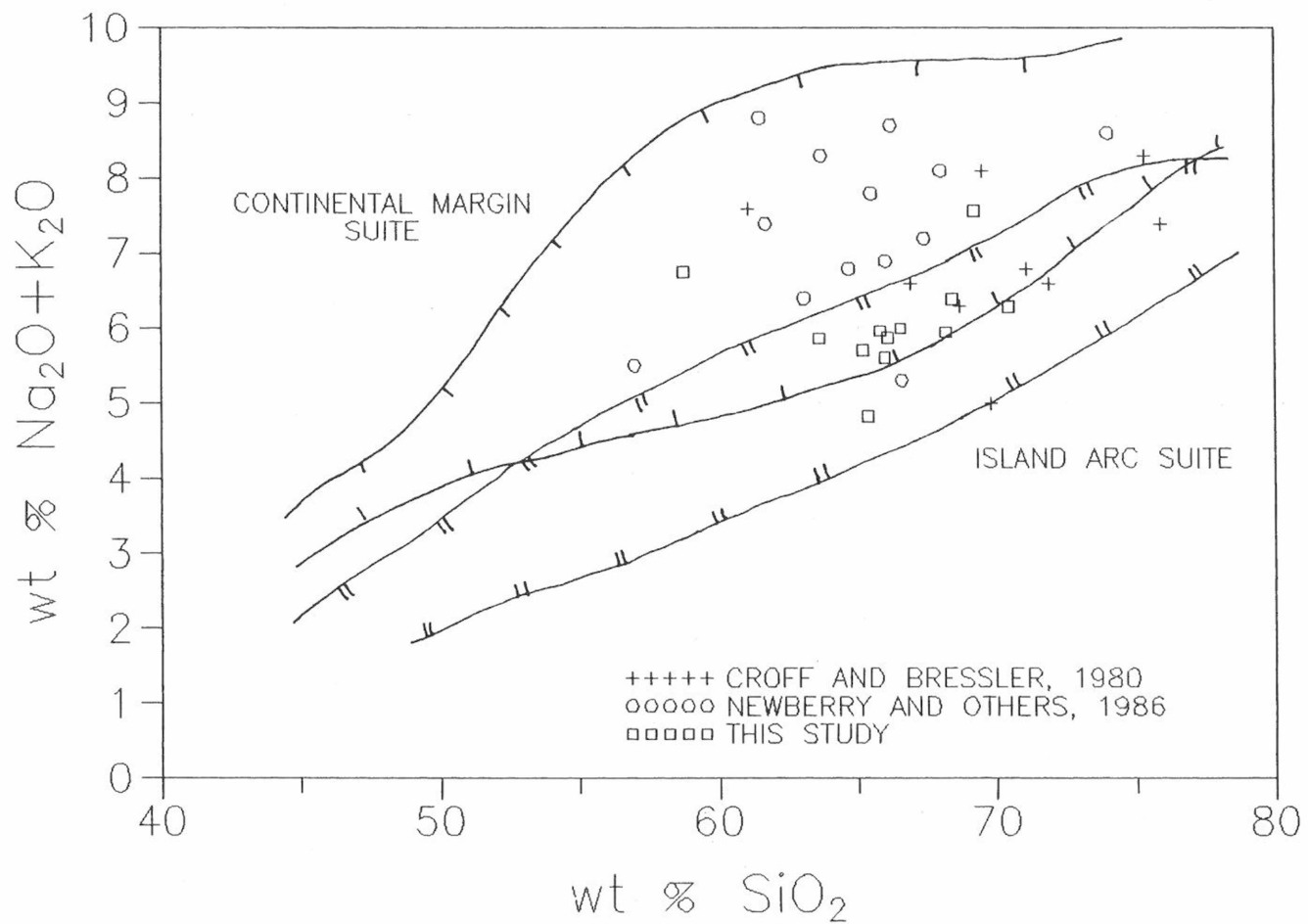
Figure 8. Alkali-silica variation diagram for meta-igneous rocks in the Chandalar copper district. Following standard petrologic practice, the data have been normalized to anydrous totals of 100%.

continental margin and island arc suites are taken from
Titley and Beane (1981). They outlined these fields using
data from known continental margin and island arc porphyry
copper-related intrusives. The data from Newberry and
others (1986) plot well within the continental margin
field; however, data from this study fall within the zone
of overlap between the two fields. It is likely that the
high alkali contents of Newberry and others' (1986) samples
are due to alteration rather than tectonic setting. When
their samples are disregarded, the remaining data are
compatible with either a continental margin or an island
arc setting.

ALTERATION

I have identified three hydrothermal alteration types
in intrusive rocks in the study area - propylitic,
potassic, and sericitic alteration. They are described
below and their distribution is shown in Figure 9. A more
detailed description of alteration occurrences in the
Chandalar area is included in Appendix 8.

PROPYLITIC ALTERATION

Propylitic alteration appears as an assemblage of
epidote, chlorite, calcite, pyrite, and sphene. In about
45% of propylitically altered rocks, this assemblage occurs
as a selective pervasive replacement of hornblende. In
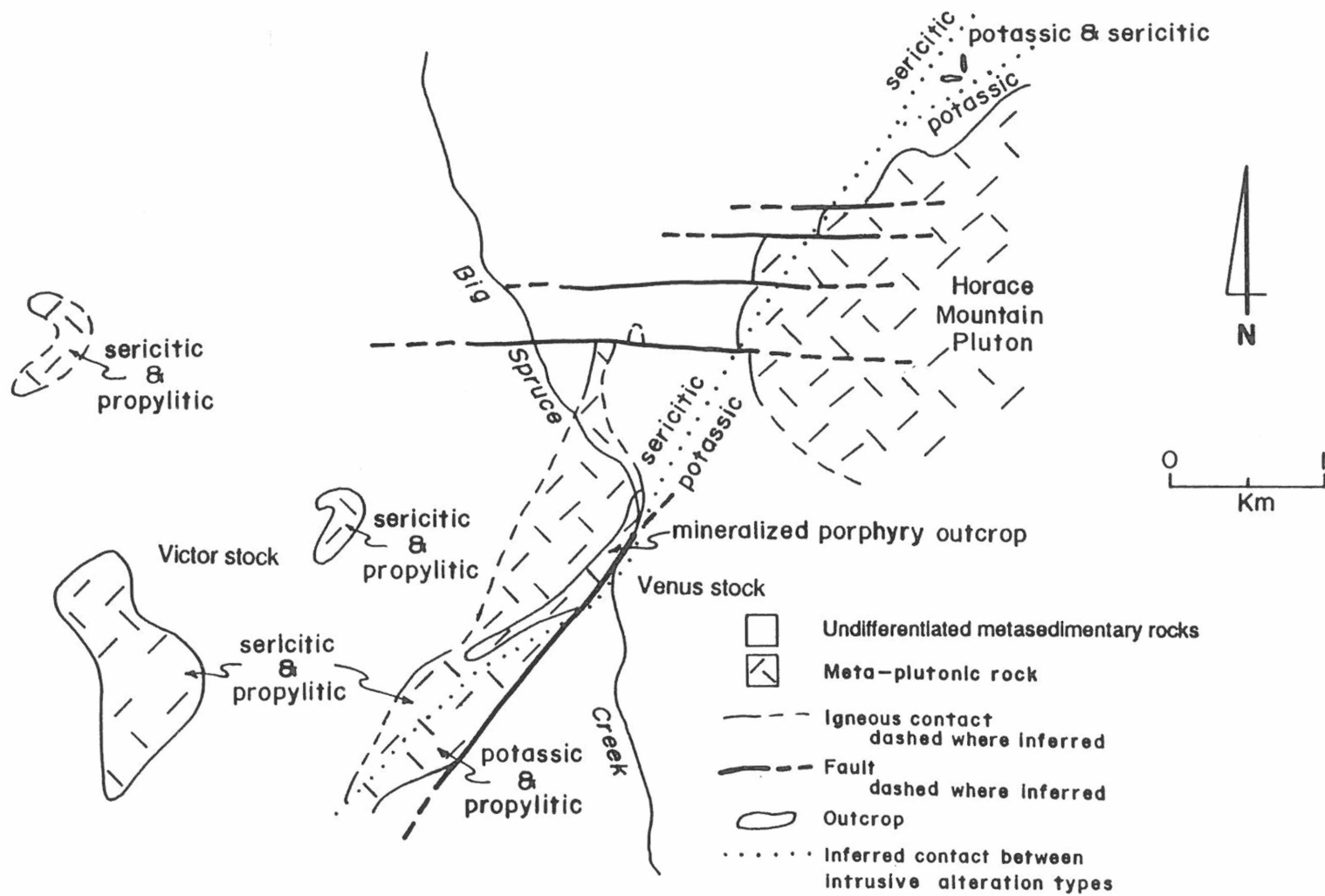
Figure 9. Inferred zonation of igneous alteration types in the Big Spruce Creek area.

another 45% of the cases, the assemblage occurs as veins of epidote, chlorite and calcite. In the remaining 10%, vein alteration and pervasive alteration occur together. This alteration type is restricted to the Venus and Victor stocks.

POTASSIC ALTERATION

Potassic alteration appears as selective replacement of hornblende by fine grained biotite $\pm$ rutile, as alkali feldspar veins, and as thin biotite veinlets. This alteration type is seen in the Venus stock and the Evelyn Lee stock.

SERICITIC ALTERATION

Sericitic alteration is difficult to recognize. Easily recognizable quartz-sericite-pyrite veins (see Figure 10) were seen in only two locations (the Venus and Luna prospects) where the intrusive rocks were little affected by metamorphic foliation. Elsewhere, masses of muscovite are present surrounding quartz veins. In most cases, because of the high percentage of muscovite in the rock, the veins have been stretched and recrystallized into lenses of quartz and muscovite with pyrite stringers. This alteration type is present in Venus Creek and the Victor stocks.

Sericitic Alteration
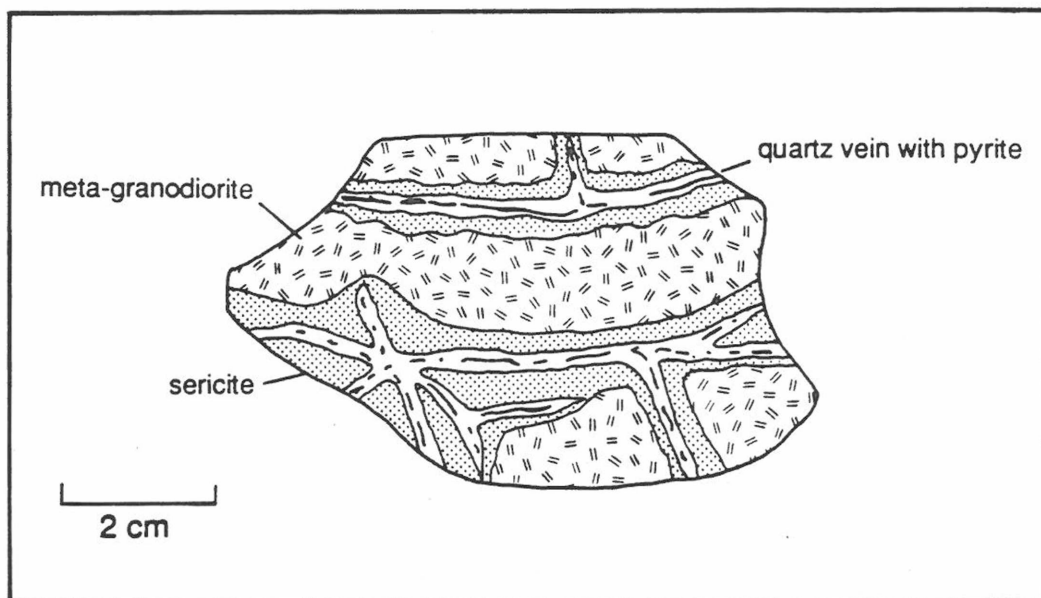
Figure 10. Sketch of quartz-sericite-pyrite veins in meta-intrusive rock from the Venus prospect.

The timing of these alteration events is determined by cross-cutting vein relationships. Secondary potassium feldspar veins which cut across epidote-chlorite veins provide evidence that potassic alteration locally occurred after propylitic alteration. This also indicates that at least some of the early epidote-chlorite veins are propylitic alteration assemblages and were not formed during the regional metamorphic episode.

MINERALIZATION

Disseminated chalcopyrite mineralization is present in propylitically altered rocks in the Venus stock. It is always associated with propylitic veins and masses of epidote, chlorite, and calcite. Chalcopyrite abundance is generally less than 0.5% , but locally as high as 1%.

Pyrite is present in abundances of between 1 and 15% in the Venus, Eva, and Evelyn Lee prospects and is associated with both propylitic and sericitic alteration assemblages. It occurs as fine to medium grained crystals and aggregates which are intergrown with veins and masses of epidote, chlorite and calcite. It also occurs as stringers in quartz and muscovite veins and as lenses associated with quartz-sericite-pyrite alteration of the intrusive.

ALTERATION AND MINERALIZATION ZONING

Figure 9 shows that propylitic alteration is present thoughout the western portion of the Big Spruce Creek field area. Potassic alteration, however, is restricted to the southern and eastern portions and sericitic alteration is restricted to the northern and western portions. An inferred contact between potassic and sericitic alteration zones is shown in Figure 9 by the dotted line. This contact zone roughly coincides with the locus of porphyry-type mineralization seen in the Venus prospect. Concentration of copper mineralization in the contact zone between potassic and sericitic alteration frequently occurs in porphyry copper deposits (Lowell and Guilbert,1970). The distribution of these alteration types suggests that the porphyry system has been tilted to the northwest, so that the deeper potassic alteration zone is now to the southeast of the shallower sericitic alteration zone.

SKARN PETROLOGY

Skarns in the study area occur as podlike masses within marble, argillaceous marble, and calc-schist and as xenoliths within meta-intrusive rocks. The skarns cut across and obliterate original bedding features. They are not foliated and show no metamorphic textures (i.e., annealing of grains). As mentioned earlier, in the Big

Spruce Creek prospects, the skarns are copper-rich and contain negligible zinc. The Luna prospect, however, contains both Cu and Cu-Zn skarns. Since there have been no major plutonic bodies found at the Luna prospect, either in the drill core or at the surface, the Luna skarns may be considered "distal skarns". Distal skarns (those formed away from the fluid source) often contain higher sphalerite contents (i.e., Groundhog Mine, N.M., Meinert,1987a; Tin Creek, AK, Szumigala, 1986).

Skarns from the study area may be classified further on the basis of their gangue mineral assemblages - garnet skarn and garnet-pyroxene skarn. Garnet-pyroxene skarn is found near the marble front. Garnet skarn may also be found at marble contacts when there is no garnet-pyroxene skarn present in the vicinity. However, when pyroxene skarn is present, garnet skarn is found away from marble or next to intrusive contacts. Garnet skarn is also the only type found in xenoliths.

SKARNOID

Partial metasomatic replacement of calc-silicate hornfels is fairly common in the Big Spruce Creek prospects. Such rocks show evidence for both metamorphic and metasomatic origins. The altered hornfels (skarnoid) consists of very fine grained epidote, pyroxene, quartz and calcite with small interpersed masses and veins of coarser

grained pyroxene (Hd_{22-47}) and birefringent garnet (Ad_{30-45}) and epidote-quartz-calcite veins. The calc-silicate compositions reflect an addition of Fe and Si to the metamorphic rock, probably through fluids, which is supported by the presence of veining. The rock, however, still retains much of its original bedding characteristics, as well as a fine-grained hornfels texture. Rocks such as these are neither completely metamorphic, nor completely metasomatic and, hence, are termed skarnoid (after Zharikov, 1970, and Einaudi and others, 1981).

GARNET SKARN

Garnet skarns are found in the Venus, Evelyn Lee, and Luna prospects and are the most abundant skarn type in the study area. They consist of 40-90% garnet, 0-25% chalcopyrite, 0-20% sphalerite, 0-45% epidote, 3-30% calcite, 2-20% quartz, and 0-3% pyrite. The higher (metal) grade skarns are non-retrograded garnet skarns occurring at marble contacts. Garnets are medium to coarse grained, ranging in grain size between 0.2 and 15 mm. They occur as subhedral dodecohedra and as veins, and range in color from colorless to green to brown under plane polarized light.

Several generations of garnet are present in the Big Spruce Creek skarns with the following paragenetic relationships between garnet generations. The earliest garnets formed are isotropic garnets with poikiloblastic

textures. These are probably metamorphic, based on the criteria of Williams and others (1982). These isotropic garnets are rimmed by birefringent garnets which are sometimes sector zoned. Birefringent unzoned and sector zoned garnets are rimmed by a later isotropic garnet generation. The late isotropic garnets are associated with higher grades of copper, since all lower grade samples lack this garnet type. A fourth type of garnet rims all of the earlier generations. These are concentrically banded birefringent garnets characterized by alternating layers of birefringent and isotropic garnet (Figure 11). They are designated as doubly banded birefringent (DBB) garnets. DBB garnets also occur as veins which cross-cut the earlier formed garnets. Luna skarns contain only the last two garnet generations (isotropic and DBB) which show the same paragenetic relationships as those in the Big Spruce Creek prospects.

Calcite, quartz and chalcopyrite are interstitial to garnet grains in garnet skarn. Isotropic and DBB garnets are embayed and rounded off by chalcopyrite. Some of the interstitial calcite occurs as fine-grained clusters which may be unreplaced carbonate host. In most cases, however, interstitial calcite is coarse grained, and single crystals may completely fill spaces between garnet grains. This

Banded Garnets
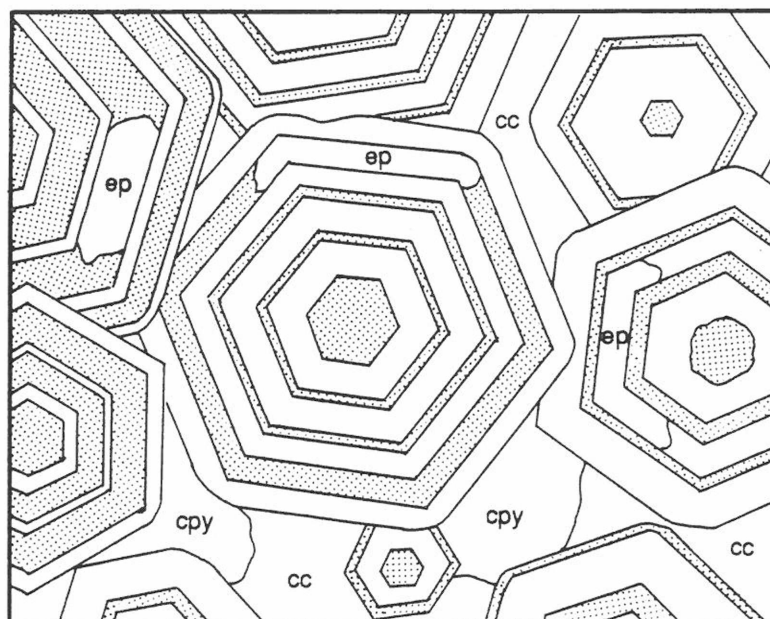
ep = Epidote   cc = Calcite   cpy = Chalcopyrite

1 mm

Figure 11.   Sketch of DBB garnets from skarn at the
Evelyn Lee prospect.

coarse grained calcite probably represents a late
recrystallization event.

Retrograde alteration of garnet skarn is characterized
by veins and clusters of epidote + calcite + quartz cutting
across garnet and chalcopyrite, or as islands of optically
continuous garnet and chalcopyrite within a matrix of these
minerals. In places, epidote and calcite have replaced
individual bands within DBB garnets (see Figure 11). At
the Luna prospect, actinolite and chlorite are also present
in the cross-cutting veins and masses.

GARNET-PYROXENE SKARN

Pyroxene is much less abundant than garnet in the
Chandalar skarns. Garnet-pyroxene skarn consists of 2-35%
clinopyroxene, 20-80% garnet, 4-15% actinolite, 1-30%
epidote, 3-10% calcite, 0-10% quartz, 0-3% chlorite, 0-10%
chalcopyrite, and 0-1% pyrite. This skarn type occurs in
the Victor, Evelyn Lee, and Luna prospects.

Pyroxenes occur as medium- to coarse-grained (0.3 - 5
mm) subhedral prisms which have been largely replaced by
fine- to medium-grained (0.05-0.4 mm) tremolite/actinolite,
quartz, calcite and, in places, chlorite. This retrograde
assemblage occurs as masses within relict pyroxene
crystals, surrounding irregular "islands" of original
pyroxene.

In garnet-pyroxene skarn, early, sector-zoned, birefringent garnet is rimmed by DBB garnet. Some small pyroxene grains are present completely within banded garnets. Others are present intersecting the bands of a DBB garnet. This suggests that pyroxene precipitated before, and possibly during, banded garnet formation. Retrograde epidote, calcite, quartz, actinolite $\pm$ sphene occur as veins and masses cross-cutting earlier calc-silicates. At the Victor and Luna prospects, veins which cross-cut only pyroxene skarn contain chalcopyrite. Hence, copper mineralization at both prospects is probably associated with the retrograde alteration of pyroxene. No copper minerals have been noted in garnet-pyroxene skarn at the Evelyn Lee prospect.

MARBLE FRONT REPLACEMENT

CU SKARN

Marble front skarn at the Evelyn Lee prospect consists of garnets with interstitial calcite or chalcopyrite and bornite. In some areas, the sulfides are intergrown with calcite alone and make up greater than 50% of the rock volume. This is considered massive sulfide replacement at the marble front.

At 151 feet in Luna drill hole 1, epidote-actinolite-magnetite skarn consists of fractured, fine-grained masses

of epidote, infilled with actinolite and chalcopyrite or
with magnetite. The skarn is in contact with massive
magnetite, containing lenses of calcite. These mineral
relationships suggest that massive magnetite first replaced
a thin marble bed. Epidote, actinolite and chalcopyrite
then partially replaced the massive magnetite. Replacement
of marble by magnetite at the marble front is fairly common
in porphyry copper-related skarns (Einaudi, 1982b).

CU-ZN SKARN

In Luna drill hole #3, along the contact between
marble and garnet skarn, intergrown sphalerite,
chalcopyrite and magnetite replace calcite and form a 5 cm
thick layer of massive sulfide. Within the drill
intercept, this massive layer contains 12% Zn and 3% Cu.
The entire skarn intercept averages 4% Zn and 1% Cu. This
is the only Zn-bearing skarn intercept in the drill core.
The nearest known intercept of meta-intrusive rock (a small
dike) is 200 m above this skarn.

CALC-SILICATE MINERAL COMPOSITIONS

Garnet and pyroxene compositions have been shown to
"fingerprint" skarn type (Zharikov, 1970; Einaudi and
others, 1981; Einaudi and Burt, 1982). Skarn garnet
compositions are usually expressed in terms of andradite
($Ca_3Fe_2Si_3O_{12}$), grossularite ($Ca_3Al_2Si_3O_{12}$) and

spessartine+almandine ($Mn_3Al_2Si_3O_{12} + Fe_3Al_2Si_3O_{12}$) end
members. Skarn pyroxenes are expressed in terms of
diopside ($CaMgSi_2O_6$), hedenbergite ($CaFeSi_2O_6$), and
johannsenite ($CaMnSi_2O_6$) end members. Figure 12 shows
generalized fields for garnet and pyroxene compositions
from typical porphyry copper related skarns. Garnets are
low in Mn content and have a wide range of grossularite-
andradite contents. Pyroxenes are low in Mn and are
diopside-rich.

Calc-silicates are also found in a number of
metamorphosed stratiform massive sulfide deposits
throughout the world, including the Gamsberg Zn deposit,
the Broken Hill Pb-Zn deposit, the Langban and Franklin
Furnace polymetallic deposits, the Virginia pyrite belt,
and the "gnurgle gneiss" of the Ambler district (Palache,
1929, 1935; Baker and Buddington, 1970; Both and Rutland,
1976; Rozendaal, 1978; Duke, 1983; Schmidt, 1986). The
calc-silicates are poorly zoned, Mn-rich, and are ascribed
to regional metamorphism of the Mn-rich host rocks.
Garnets are of the spessartine $\pm$ almandine variety, and
pyroxenes are rich in johannsenite (Figure 12). Franklin
Furnace and Langban also contain Mn-rich calcic amphiboles.
These Mn-rich varieties are significantly different from
calc-silicates found in Cu skarns, which are low in Mn^{2+}
and Fe^{2+}. These "non-skarn" calc-silicates also differ
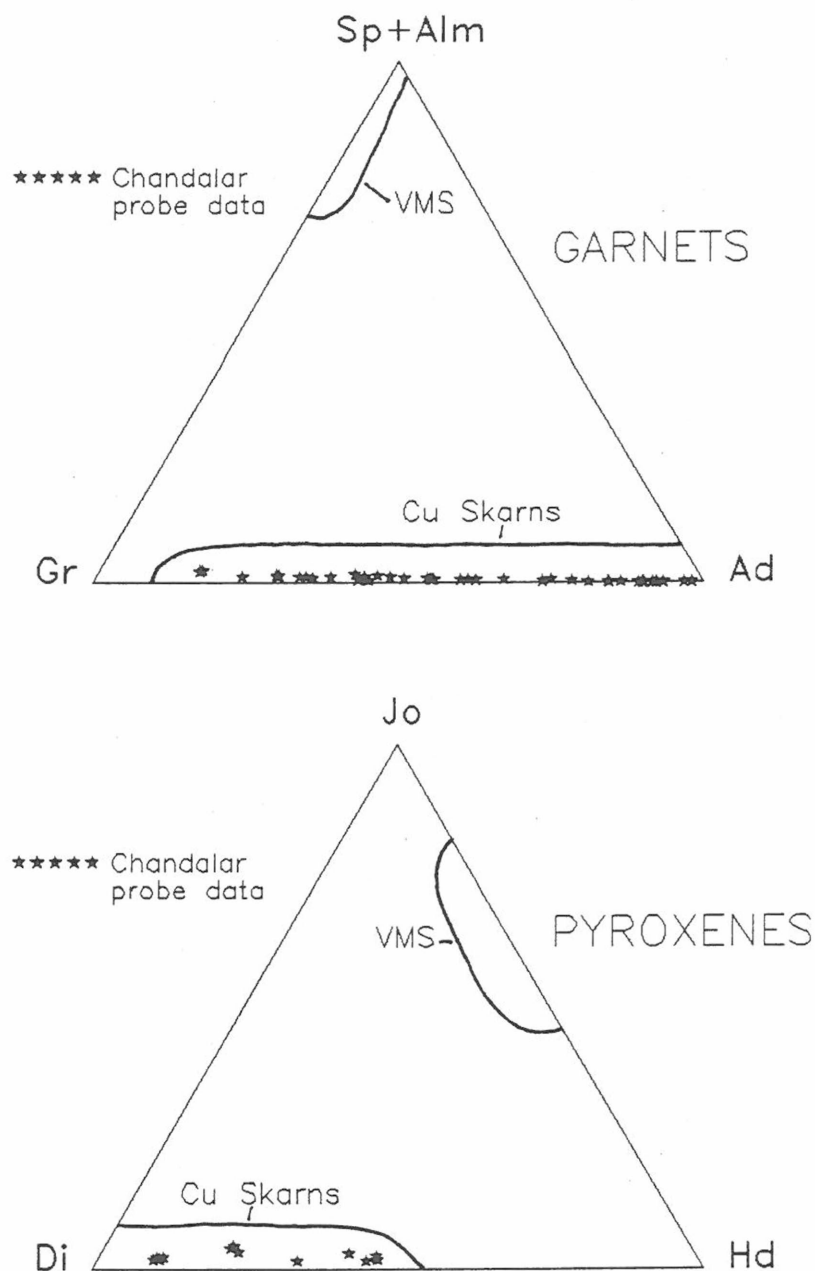
Figure 12. Comparison of Chandalar garnet and pyroxene compositions with those of other deposits. Compositions from porphyry copper related skarns (Einaudi and Burt, 1982; Meinert, 1982), metamorphosed VMS deposits (Palache, 1935; Baker and Buddington, 1970; Both and Rutland, 1976), and Chandalar skarns (this study). Pyroxene field for VMS deposits is estimated due to lack of reported analyses.

from skarns in that they are layered, parallel to foliation or original bedding.

Results of calc-silicate analyses from this study are given in Appendices 2 and 3, and in Figure 12. These analyses reveal that garnets fall along the andradite-grossularite solid solution series and contain less than 3% of the spessartine + almandine endmember. Similarly, pyroxenes fall along the diopside-hedenbergite solid solution series and contain 4% or less of the johannsenite endmember. These compositions correspond most closely with those of Cu skarns and are very different from those of metamorphosed VMS deposits.

GARNET

Metamorphic poikiloblastic garnets and sector zoned birefringent garnets from skarnoid, associated with Chandalar skarns, have compositions of Ad_{16-45}. Similar low Fe^{3+} skarnoid compositions are associated with Cu skarn deposits at Yerington, Cananea, and Darwin (Meinert, 1982; Harris and Einaudi, 1982; Newberry, 1987).

In areas where no skarnoid is seen, Chandalar skarn garnets are brown in hand specimen and isotropic in thin section. XRD and microprobe analyses of these garnets yield compositions of Ad_{80-100}.

Doubly banded birefringent (DBB) garnets from Big Spruce Creek skarns are similar to Meinert's (1982) 2BB

garnets. He found that consecutive bands of isotropic and anisotropic garnets alternated between ferric iron-poor and ferric iron-rich compositions (Ad_{30}-Ad_{99}). Similar compositions are seen in DBB garnets from Big Spruce Creek, where adjacent bands flip-flop between high iron and low iron contents (Ad_{30}-Ad_{93}; Figure 13). DBB vein garnets have average compositions of Ad_{34}. DBB garnets replace sector zoned skarnoid and poikiloblastic garnets during later skarn formation. They also form rims on isotropic skarn garnets, suggesting they are the latest garnets formed.

Big Spruce Creek skarn garnets generally show an increase in iron with time, from early metamorphic garnets to skarnoid garnets to isotropic skarn garnets. However, the latest formed DBB garnets have a lower mean Ad content and a much wider range in composition than the isotropic garnets, showing a late decrease in iron. A similar trend of increasing and then decreasing Fe^{3+} content in garnets is seen in the Cananea, Darwin and the Shinyama Cu skarns (Meinert, 1982; Newberry, 1987; Uchida and Iiyama, 1982)(Figure 14).

Other skarn types (e.g., Sn skarns, W skarns) show different patterns of garnet evolution (Figure 15). For example, the Lost River Sn skarn shows a change from early andraditic garnet to later grossularite-spessartine garnet.
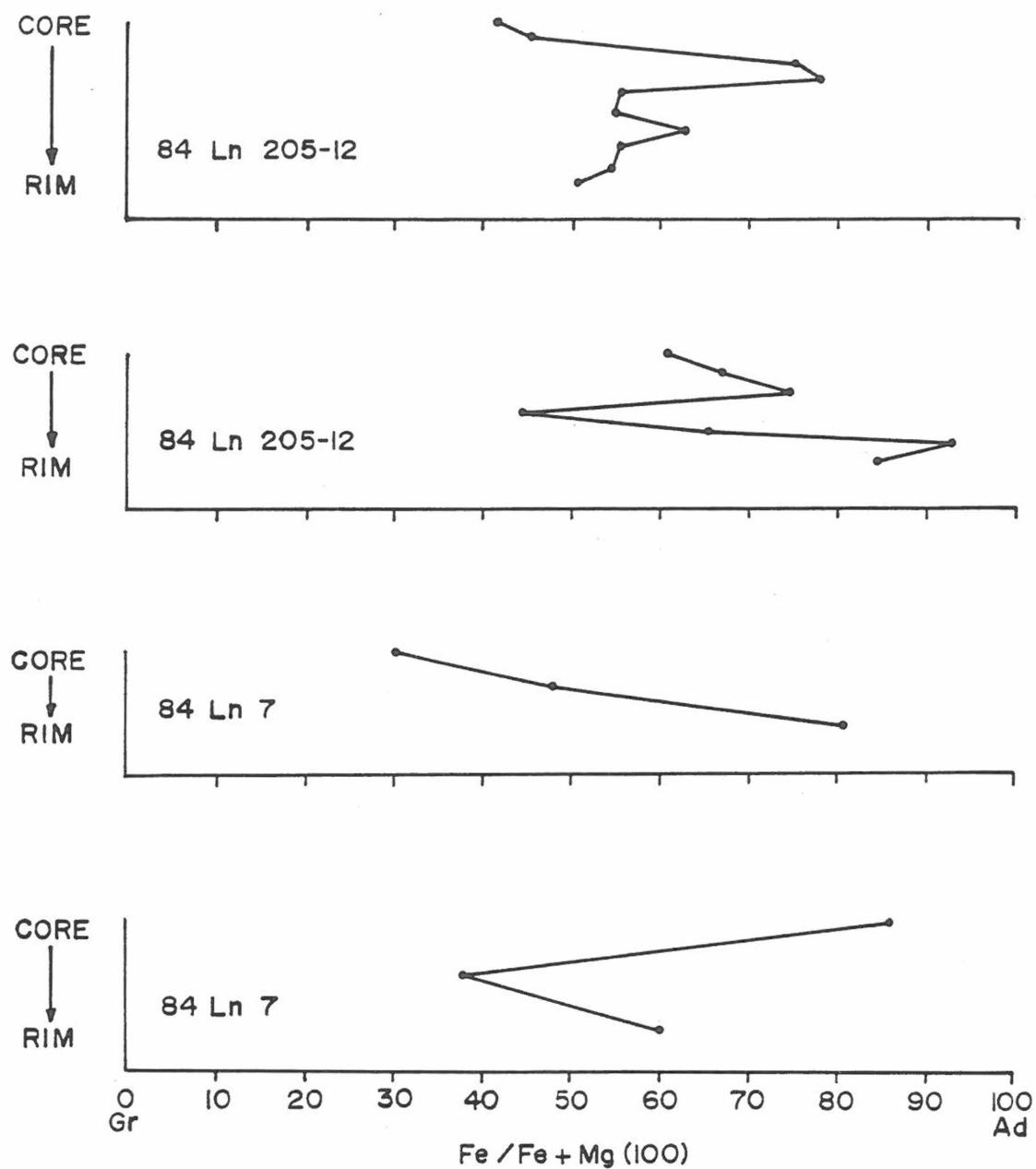
Figure 13. Core to rim garnet compositions for 4 doubly banded birefringent garnet grains from the Evelyn Lee and the Victor prospects. Microprobe data from this study.
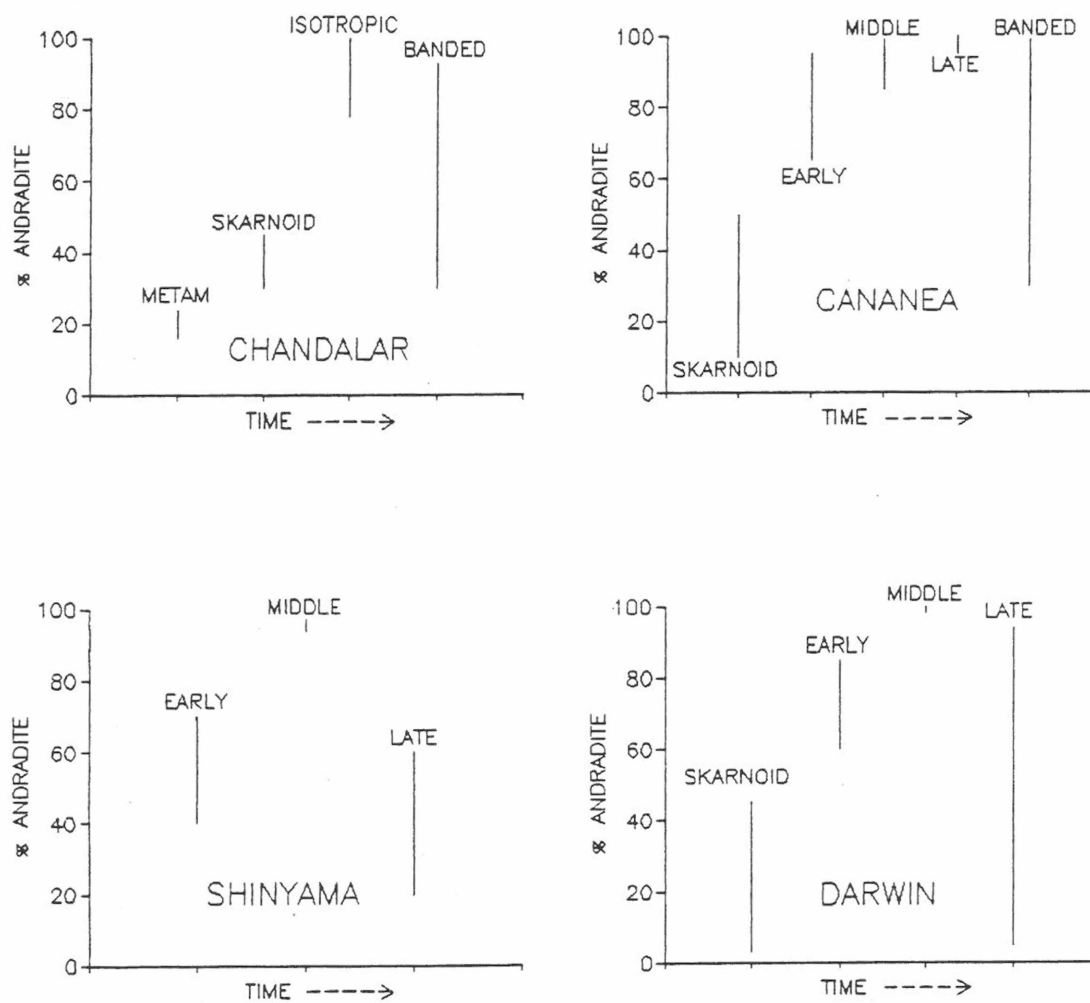
Figure 14. Garnet evolution for skarns from the
Chandalar prospects, Cananea, Shinyama, and Darwin. Data
from Meinert (1982), Uchida and Iiyama (1982), Newberry
(1987), and this study (microprobe data).
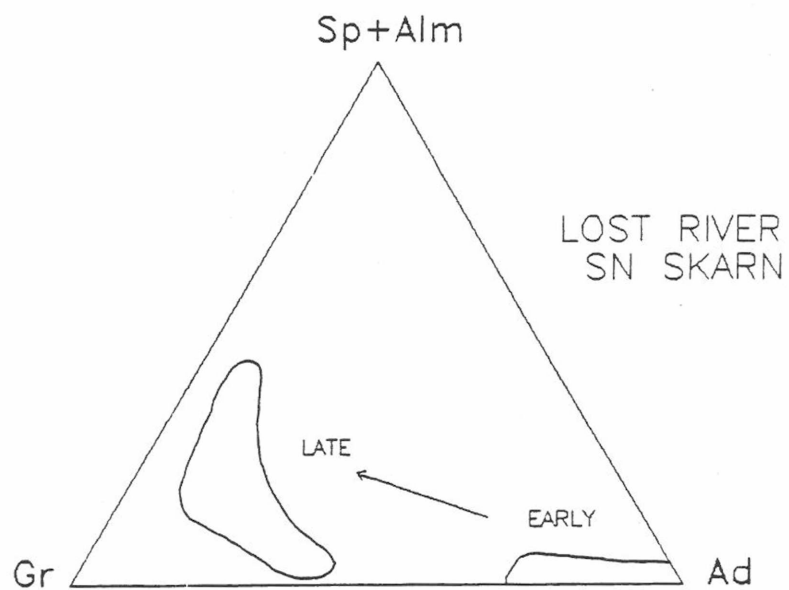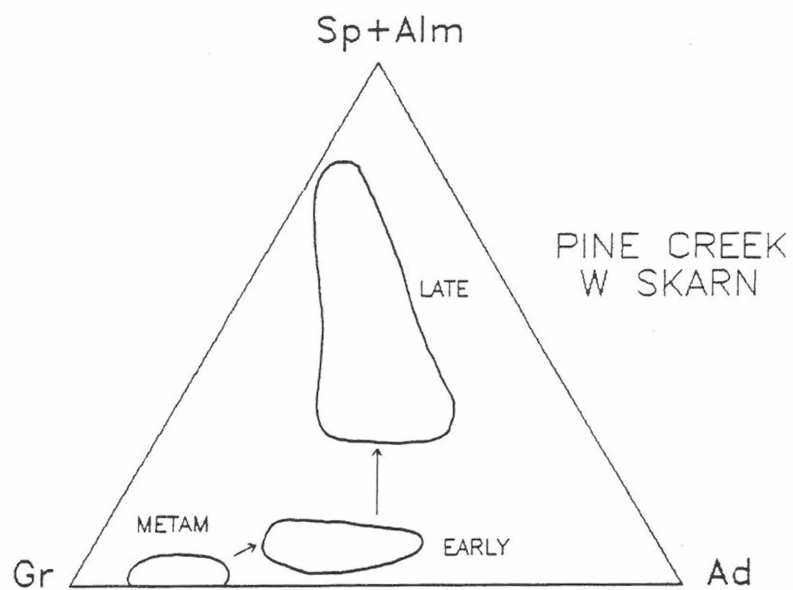
Figure 15. Garnet evolution for W and Sn skarns. Data from Dobson (1982) and Newberry (1982).

The Pine Creek W skarn shows an initial increase in andradite content of garnet between skarnoid and early skarn. Late skarn garnets, however, are almandine-spessartine rich and show no increase in the Fe^{3+} component. As mentioned above, "non-skarn" calc-silicates from Broken Hill, Franklin Furnace, etc., show little zoning and always have low grossularite and andradite components.

PYROXENE

As shown in Figure 12, pyroxenes are very low in Mn and their compositions range from Hd_9 to Hd_{46}. Core and rim analyses (205-12a and f) of one pyroxene crystal show an outward decrease in iron content.

AMPHIBOLE

Iron contents of Big Spruce Creek skarn amphiboles are shown in Figure 16; they show a Fe/Fe+Mg range of 40 to 53 percent. Amphiboles tend to have higher Fe/Fe+Mg ratios than clinopyroxenes. However, none of the analyses are from co-existing pyroxenes and amphiboles. The higher Fe/Fe+Mg ratios in amphiboles, in this case, may reflect the tendency for amphiboles to replace the most iron-rich pyroxenes present.
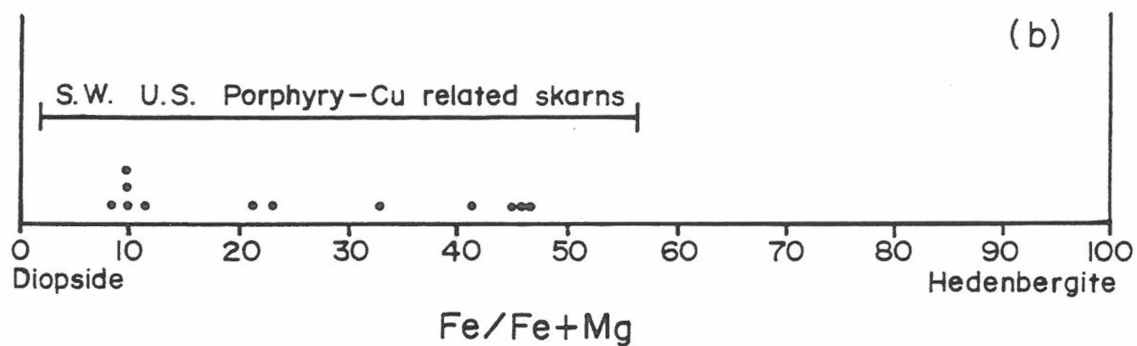
Figure 16.   Iron content of amphiboles from Chandalar
copper skarns and SW U.S. porphyry related copper skarn.
Data from Einaudi (1982b), Meinert (1982) and this study
(microprobe analyses).

MINERALIZATION

CU SKARN

Copper mineralization in skarns consists of chalcopyrite and occasional trace amounts of bornite. Chalcopyrite is interstitial to garnet in garnet skarn, replaces pyroxene in garnet-pyroxene skarn, and is intergrown with low temperature minerals in retrograde skarn. Bornite, when present, is intergrown with chalcopyrite. Copper grades in mineralized garnet skarn from Evelyn Lee, Venus and Luna range between 1.5% and 6%. Marble-front sulfide-replacement bodies from Evelyn Lee and Luna contain average grades of 10% Cu. Mineralized retrograded skarns from all prospects have copper grades of 1% to 2%. Garnet-pyroxene skarns generally have grades of less than 1% Cu.

CU-ZN SKARN

Zn-bearing skarn at the Luna prospect contains sphalerite ($4 \pm 4\%$ FeS - XRD analyses) which is intergrown with either retrograde assemblage minerals in interior skarns (1% Zn), or with chalcopyrite in marble front replacement bodies (up to 12% Zn).

METAL RATIOS

Figure 17 shows Cu/Cu+Zn ratios for skarns from all prospects. Data for the Big Spruce Creek prospects are
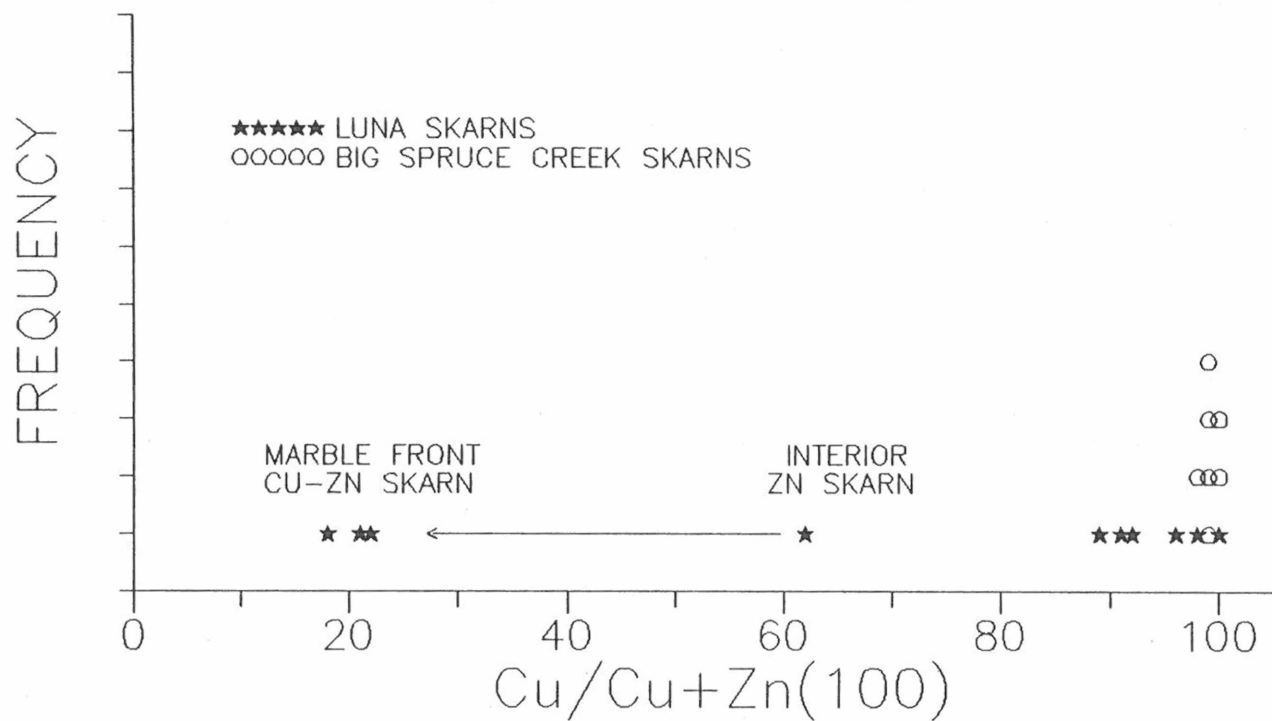
Figure 17. Cu:Zn ratios for Cu skarns and Cu-Zn skarns from the study area. Data from Croff and others (1979) and this study.

from this study, whereas Luna analyses are taken from Croff
and others (1979). Most samples plot above 0.89. These
points represent Cu skarns from Big Spruce Creek and Luna.
This high Cu:Zn ratio is typical of porphyry-related copper
skarns (Einaudi, 1982b). The four remaining data points
are from sphalerite-bearing skarn at Luna. Note that the
Cu/Cu+Zn ratio tends to decrease from the interior skarn
sample to those taken from marble front replacement bodies.
A parallel trend is seen in Luna DDH-5, where skarn
containing no Zn shows a decrease in Cu grades toward the
marble front and away from the meta-intrusive. This
general decrease in Cu (chalcopyrite and bornite) and
increase in Zn (sphalerite) away from intrusive contacts is
seen in many porphyry copper related skarns. Einaudi
(1982a) shows that, at the Carr Fork mine, the sulfide
assemblages are Cu-rich near the Bingham stock, and become
more Zn- and Pb-rich with increasing distance from the
stock. Einaudi and others (1981) show similar sulfide
zonations in other porphyry copper related skarns of the
southwestern U.S.

MINERAL ZONATION

There is no obvious calc-silicate zonation seen in the
Big Spruce Creek skarns. The typical Cu skarn zoning
(between intrusive and marble front) of garnet to pyroxene
to wollastonite, has not been observed. In fact,

wollastonite has not been observed at all. This lack of obvious zonation is most likely due to poor exposure, structural complications, or inappropriate conditions of metamorphism. In the Luna drill core, however, a zonation is seen between garnet skarn near porphyry dikes and garnet-pyroxene skarn at the marble front. A broader scale mineral zonation has been recognized area-wide. Cu-rich skarns predominate in the Big Spruce Creek prospects, surrounding the larger porphyry stocks. The Luna prospect, however, which contains only small dikes and sills, also contains both Cu and Zn skarns. The presence of Cu skarns near, and Zn skarns away from, a major fluid source has been widely observed (Meinert, 1982; 1987a).

SKARN DISTRIBUTION

Einaudi and others (1981) have suggested that prograde and retrograde skarns are spatially associated with specific alteration types in porphyry copper systems. Prograde skarn is usually associated with early hydrothermal alteration of the accompanying intrusive (potassic alteration). Retrograded skarn, on the other hand, is associated with - and presumably formed during - sericitic alteration of intrusive rocks.

Figures 18, 19, and 20 show the distribution of alteration in skarn relative to intrusive in the Big Spruce Creek prospects. For prospect locations, refer to Figures

VENUS PROSPECT
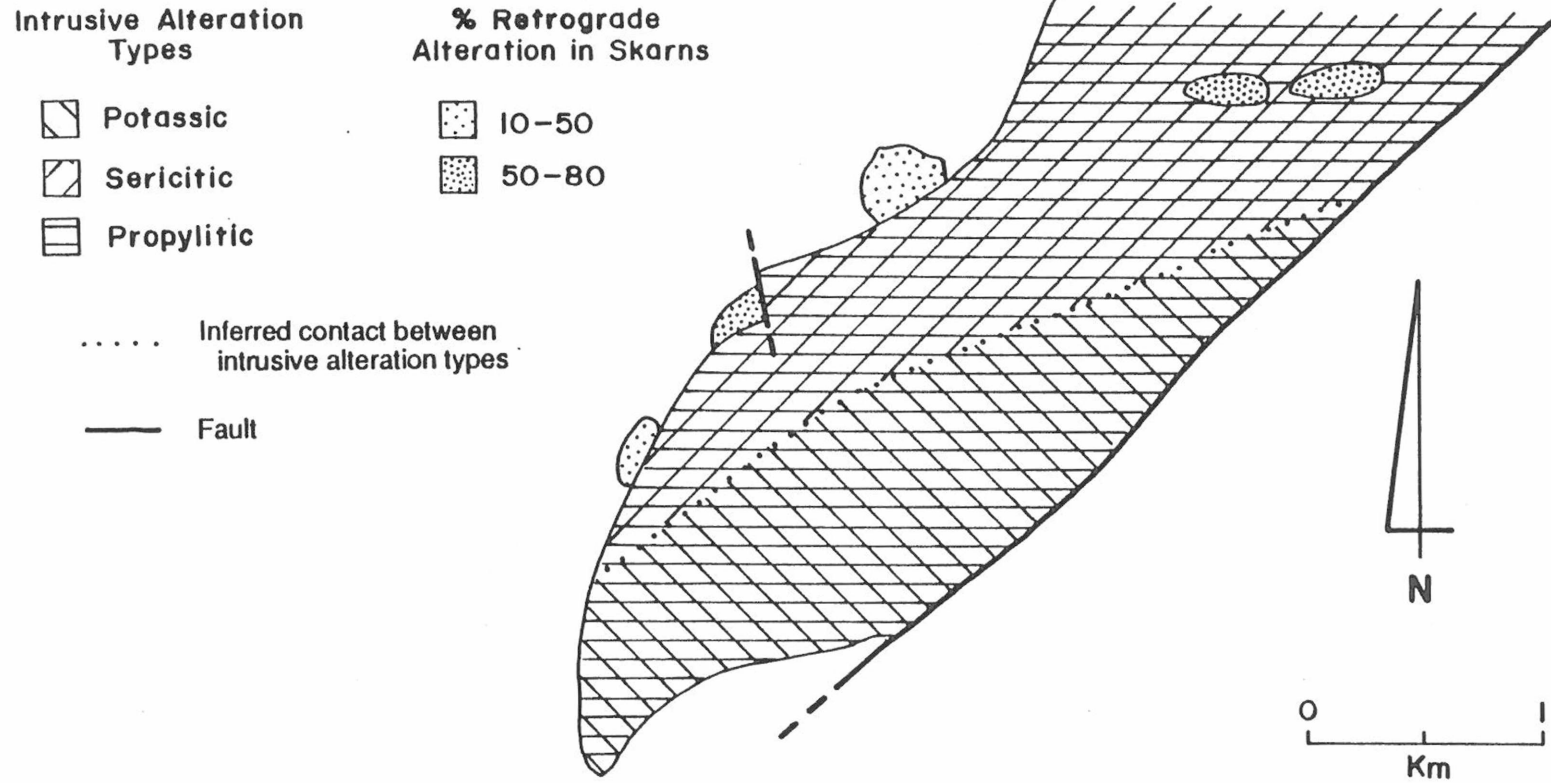
Figure 18. Spatial distribution of skarn and intrusive alteration types at the Venus prospect.

VICTOR PROSPECT
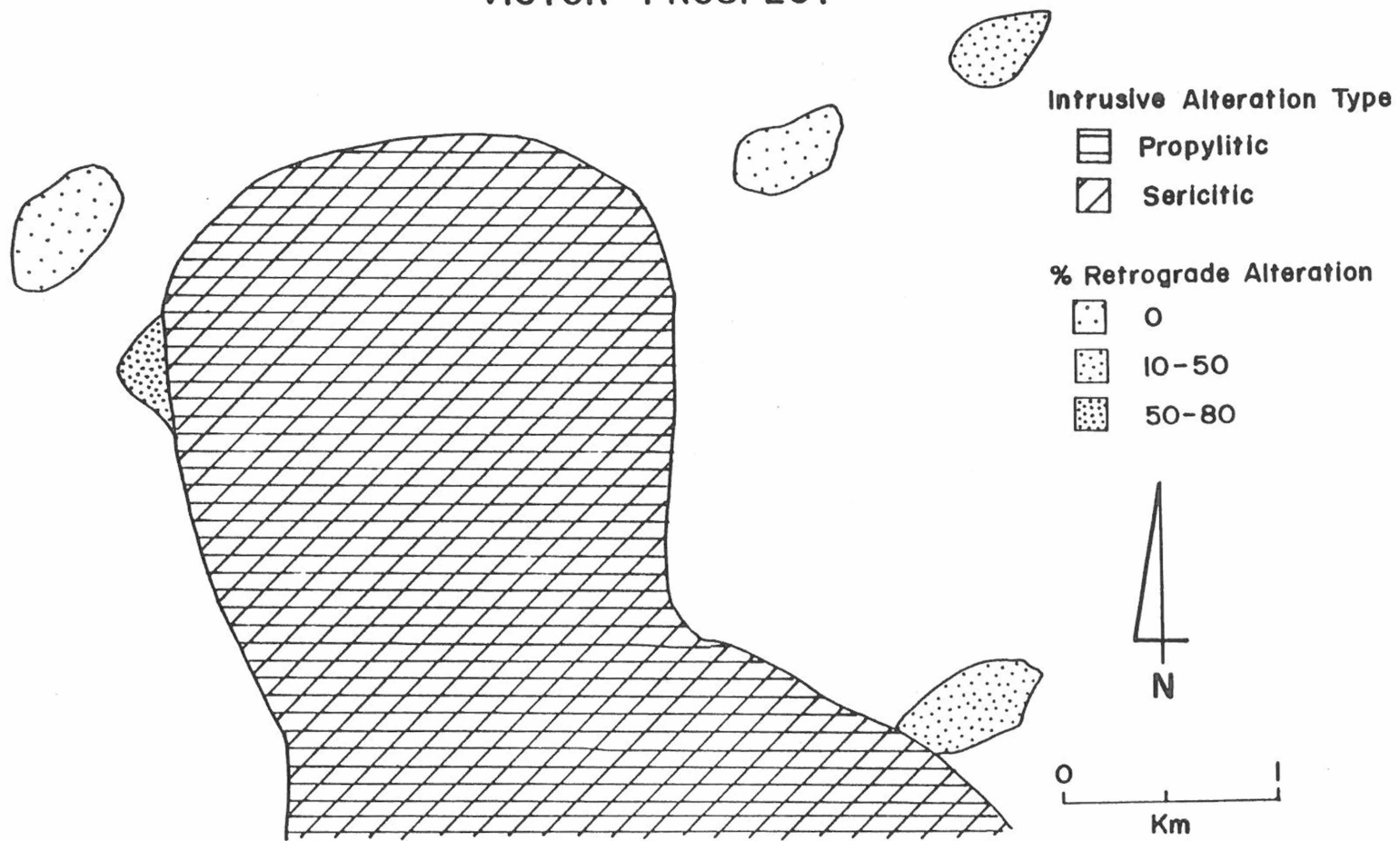
Figure 19. Spatial distribution of skarn and intrusive alteration types at the Victor prospect.
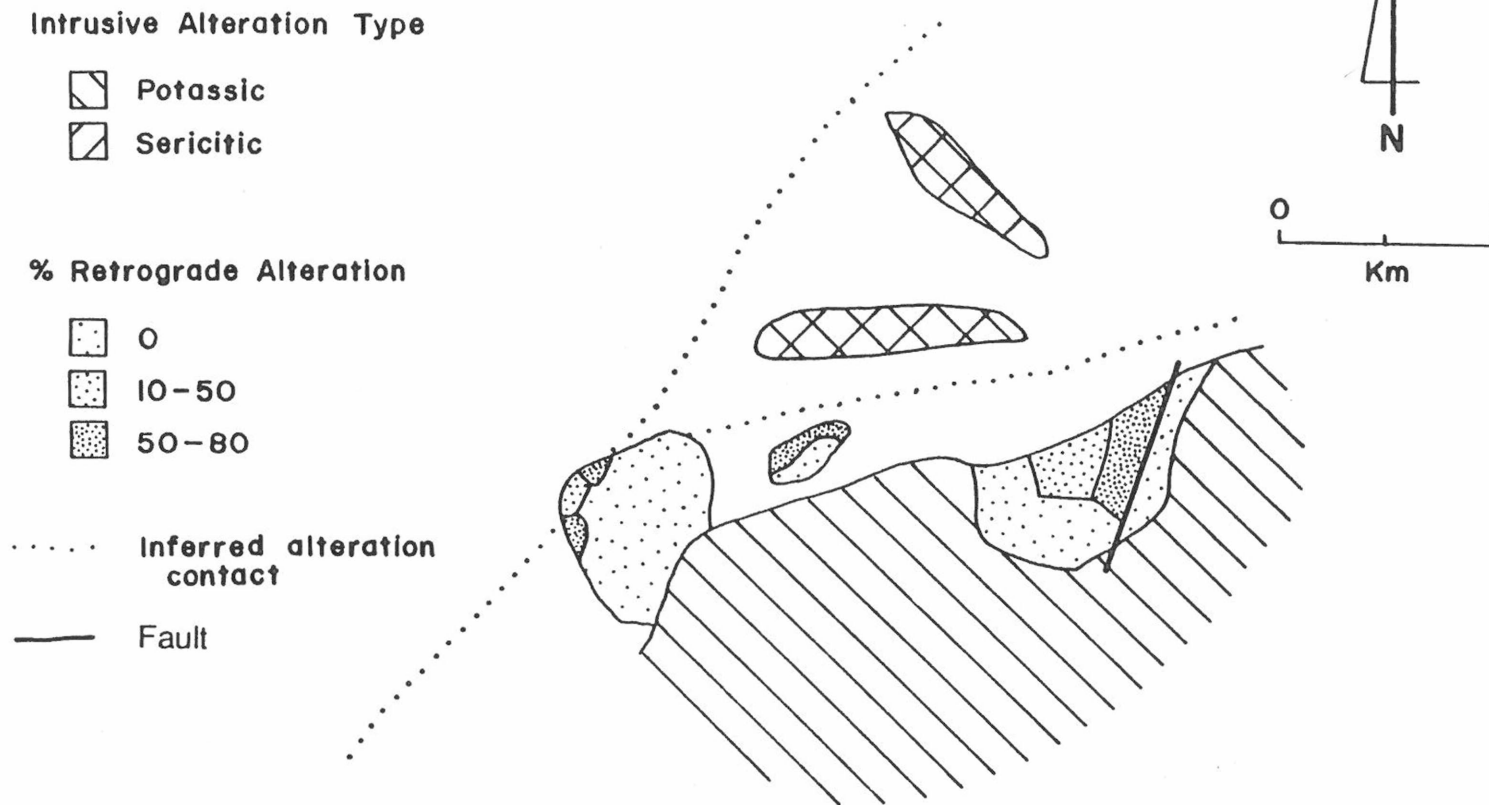
Figure 20. Spatial distribution of skarn and intrusive alteration types at the Evelyn Lee prospect.

2 and 3. At the Venus prospect, Figure 18, "islands" of
skarn within sericitically altered intrusive show a high
degree of retrograde alteration, as would be expected in
porphyry copper-related skarns. Skarn bodies along the
edge of the intrusion are slightly less retrograded, but
still contain >10% retrograde alteration.

The Victor prospect, in the western portion of the
study area, is shown in Figure 19. The main intrusive
stock and a small intrusive body in the northeastern corner
of the map area are sericitically altered. Highly
retrograded skarn is present on the western margin of the
stock, and slightly less retrograded skarn is present along
the eastern margin. Within 500 meters of the main
intrusive body, retrograde alteration drops to 0%. As the
smaller sericitically altered intrusive body is approached,
however, retrograde alteration of the skarn increases
again.

A map of the Evelyn Lee prospect (Figure 20) shows
fresh prograde skarn adjacent to potassic alteration in
intrusive rocks. Skarn shows a very general zonation from
prograde skarn near the potassically altered main intrusive
body to retrograde skarn as it approaches the sericitically
altered dikes to the north.

The above relationships between degree of retrograde
alteration and intrusive type in the Big Spruce Creek

prospects are consistent with the model proposed by Einaudi and others (1981) for porphyry related Cu skarns. This further suggests that the retrograde skarn assemblages, although similar in mineralogy to greenschist metamorphic assemblages, are a metasomatic phenomenon and are not caused by regional metamorphism.

VMS-RELATED SULFIDES

Massive sulfide layers, interpreted as VMS-related, are seen in the Luna drill core, but not in the Big Spruce Creek prospects. Three massive sulfide accumulations are contained within a 75-150 foot thick mineralized horizon intersected by drill holes 1, 3, and 5 (see drill logs in Appendix 1). Figure 21 shows a cross-section of DDH-3 and includes host rock types, massive sulfide zones, alteration zones, and skarns. The relationships seen in this drill hole are typical of those in the other two mineralized drill holes (DDH-1 and 5), but small and large scale folding and faulting makes correlation between the holes unrealistic.

Massive, stringer, and disseminated sulfides associated with VMS mineralization are approximately twice as abundant as skarn-related sulfides, and comprise approximately 10% of the Luna drill core. The intercepts contain an average of 1% Cu and 0.25% Zn. Massive sulfide

SW   NE

qs
sk
qs
cs+mbl
sk

qs

mbl
qs
sk
cs
cs
porph
mbl

cs

mbl

sk

mbl

qs

Chloritic alteration

Silicic alteration

Massive sulfide lens

qs - quartz schist

cs - calcareous schist

mbl - marble

sk - skarn

porph - porphyritic
        meta-intrusive

0

25 ft

0

10 m

Figure 21. Cross-section of
DDH-3 - Luna prospect. Taken
from drill core logs - this
study.
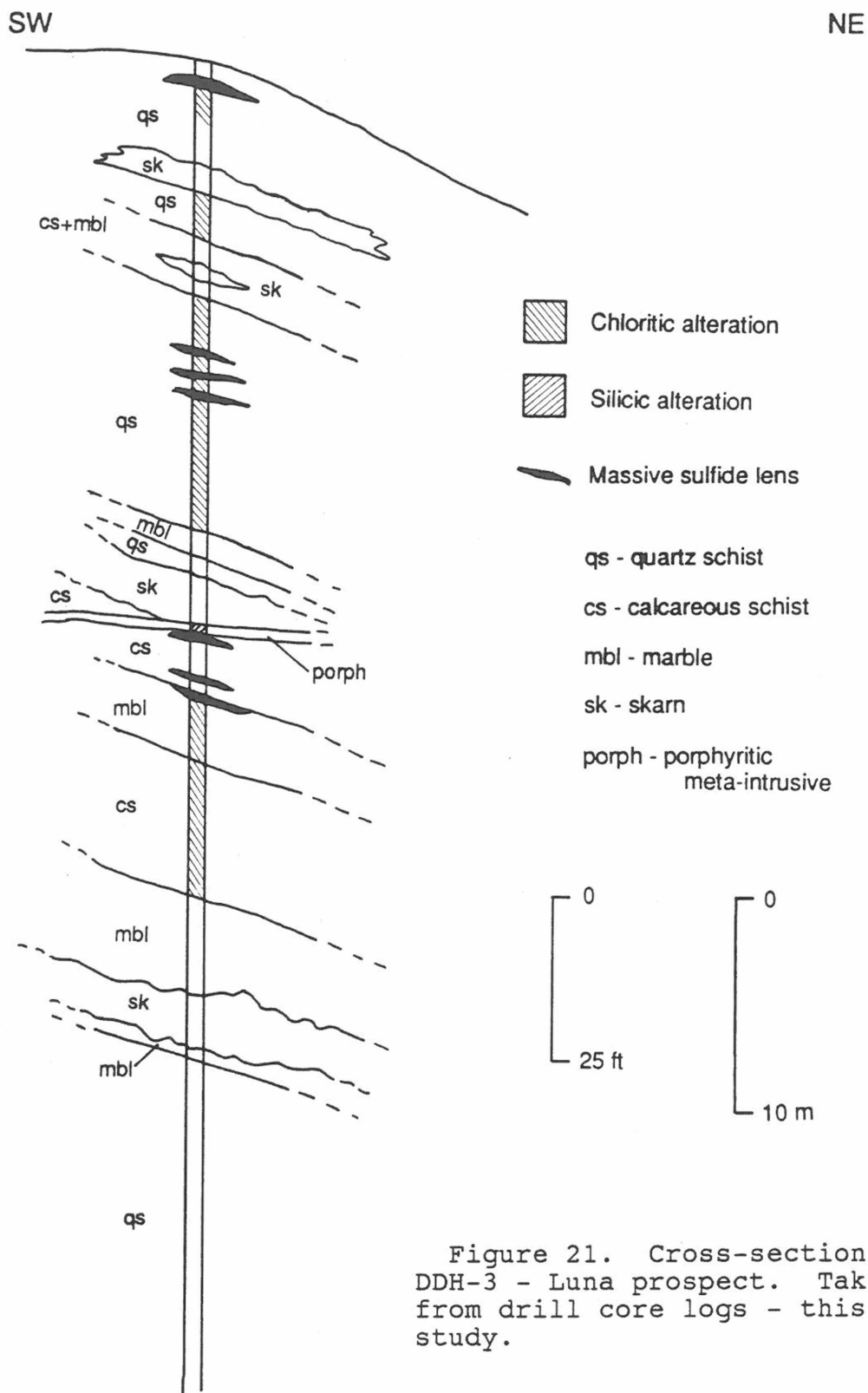
layers in drill core are generally thin (2-5 cm) and contain from 50-75% sulfides. Accumulations of these layers with interlayered schist may reach 75 cm in thickness. Sulfide-rich layers are composed of massive pyrite with subordinate chalcopyrite and sphalerite, massive chalcopyrite with subordinate pyrite and sphalerite, or of massive sphalerite with subordinate chalcopyrite, pyrite and arsenopyrite. Gangue minerals consist of white mica, chlorite, quartz, calcite, biotite, and plagioclase. There is a notable lack of obvious sulfate minerals in the Luna prospect. There are also no regional metamorphic calc-silicate minerals present at the Luna prospect (such as the Mn-rich garnets and pyroxenes shown in Figure 12).

In massive pyrite layers, pyrite occurs as massive aggregates of anhedral crystals concentrated in layers which parallel foliation of the surrounding schist. Fine-grained (0.5-2 mm) subhedral pyrite grains have recrystallized and consolidated into coarser grained aggregates (1-5 mm), containing inclusions of other sulfides and gangue minerals. Subordinate chalcopyrite +/- sphalerite occurs as 1-2 mm, randomly distributed, irregular grains.

Massive chalcopyrite layers consist of 40-70% interconnected, 1-5mm, irregular grains of chalcopyrite in

a matrix of silicate and/or carbonate gangue. Subordinate pyrite and sphalerite, when present, occur as fine-grained (0.5-1 mm), disseminated, euhedral crystals.

Massive sphalerite layers consist of 50-60% interconnected, elongate grains and masses of sphalerite (13$\pm$4% FeS - XRD analysis) with subordinate (10-20% each) disseminated, subhedral, 0.1-2 mm pyrite and anhedral 0.05-0.5 mm chalcopyrite. Arsenopyrite, where present, makes up less than a few percent of the rock volume and occurs as rims on pyrite grains. Gangue minerals consist of varying proportions of white mica, quartz, plagioclase, chlorite, biotite, and calcite.

Fine- to medium-grained pyrite, chalcopyrite, and magnetite occur as thin stringers and disseminations in the schists surrounding the massive sulfide layers. These stringer sulfides are much more abundant than the massive sulfide layers and, where present, comprise from 1-10% of the rock volume. Although skarn intercepts, massive sulfide layers, and stringer zones are closely spaced within the mineralized horizon (see Appendix 1), it is apparent that the stringer sulfides are spatially associated with massive sulfide layers, rather than skarn. These stringer zones may represent feeders for the massive sulfide layers.

ALTERATION

A number of different alteration types are possible in VMS deposits: chloritic alteration, sericitic alteration, and silicification (Franklin and others, 1981). Chloritic alteration at the Luna prospect occurs as extremely chlorite-rich schists (50-70% chlorite) and as massive chlorite layers and lenses in muscovite quartz schists. Figure 21 shows the location of chloritic alteration in the Luna drill holes. Note that the alteration is present either below or surrounding the massive sulfide zones. This spatial association between chloritic alteration and massive sulfides is also seen in the Ambler deposits where chloritic alteration is found in the footwall of the ore horizons (Schmidt, 1986).

Sericitic alteration (phengite-phlogopite-talc) surrounds the ore horizons at Ambler (Schmidt, 1986). This alteration type is not recognized at the Luna prospect. Many of the Luna schists are rich in white mica but, since most pelitic schists contain high percentages of muscovite, there is no compelling reason to assume the presence of sericitic alteration.

Silicic alteration affects the meta-intrusive dikes and sills of the Luna prospect and occasionally extends into the surrounding schists. In DDH-5, silicification, seen in a porphyritic granodiorite sill, extends one meter

into the overlying quartz-muscovite schist. This
alteration type is characterized by total removal of mafic
minerals from the rock. These silicified rocks contain
either no mineralization or disseminated and stringer
sulfides. The association between silicification and
stringer mineralization is common in VMS deposits (Franklin
and others, 1981).

METAL CONTENTS AND RATIOS

Metal values from VMS-related sulfides in DDH-1, 3 and
5, range from 0.2 to 3.2% Cu, 0.01 to 2.5% Zn, and 0.03 to
0.86 oz/ton (1 to 28 ppm) Ag, with average values of 1% Cu,
0.25% Zn, and 0.38 oz/ton (12 ppm) Ag (Croff and others,
1979). No values for Pb or Au were reported. DDH-1
intersects approximately 20 ft (6 m) of massive sulfide
accumulations in 4 zones and contains 24 ft-% Cu and 0.76
ft-% Zn.[1] DDH-3 intercepts 3 massive sulfide zones,
containing 30.6 ft-% Cu and 16.0 ft-% Zn. DDH-5 intercepts
3 massive sulfide zones with 8.7 ft-% Cu and 2.7 ft-% Zn.

Cu/Cu+Zn ratios for VMS-related mineralization are
given in Appendix 1 and shown in Figure 22. Note that most
data points cluster near the Cu-rich end. The lower values
are from sphalerite-bearing layers. The two lowest values
come from massive chalcopyrite-sphalerite layers in DDH-3.

---

[1]Ft-% is the length of an assay interval multiplied by the
metal grade over that interval.

Figure 22. Cu:Zn ratios for Luna VMS occurrences. Data from Croff and others (1979) and this study.

Cu/Cu+Zn ratios are generally higher in the northern drill holes (DDH-1 and 5) than in the southern drill hole (DDH-3). In accordance with the general model that Cu/Zn ratios decrease away from a feeder vent in VMS deposits (Franklin and others, 1981), it is likely that DDH-1 and 5 are more proximal and DDH-3 is more distal to the original fluid source. Because of isoclinal folding seen in the drill core and the larger scale folds and faults mapped by Croff and others (1979), the presence and location of a feeder zone is difficult to pinpoint.

CHAPTER III - SULFUR ISOTOPIC INVESTIGATIONS

Under favorable conditions, isotopic compositions of sulfides and sulfates can be used to determine the source of sulfur in an ore deposit. Sulfur isotope compositions are expressed as $del^{34}S$, which is defined as the per mil (per 1000) relative difference between the $^{34}S/^{32}S$ ratio of the sample and that of the Cañon Diablo meteorite standard. Igneous sulfides have average $del^{34}S$ values close to that of meteorites (0 per mil) (Ohmoto and Rye, 1979). Seawater sulfates are enriched in ^{34}S and have values ranging between +10 and +30 per mil, depending on the age of the sulfate (Ohmoto and Rye, 1979). Sedimentary sulfides have a wide range in $del^{34}S$ values, but are typically depleted

in ^{34}S relative to the meteorite standard (Ohmoto and Rye, 1979) (see Figure 23).

Del^{34}S values of sulfides from porphyry copper deposits typically fall between -4 and +3 per mil (Ohmoto and Rye, 1979) (Figure 24) and reflect an igneous source for the sulfur. Sulfur isotopic ratios for skarns have a wider range, but are commonly between -5 and +2 per mil (Rye and others, 1974; Chukrov and others, 1977; Shimazaki and Yamamoto, 1979; Sato and others, 1981; Figure 24). Sasaki and Ishihara (1980) have shown that the sulfur isotopic ratios of hydrothermal ore deposits commonly correlate with those of the associated granitic rocks.

Del^{34}S values of sulfides from some Devonian VMS deposits are also shown in Figure 24 and range between +2 and +11 per mil (Ayres and others, 1979; South and Taylor, 1985; Schmidt, 1983). Sangster (1968) showed that the average del^{34}S value for VMS sulfides is approximately 17 per mil less than that of contemporaneous seawater. Ohmoto and Rye (1979) suggested that in VMS deposits, seawater sulfate is reduced by reaction with hot Fe^{2+}-bearing volcanic rocks. They also pointed out that the sulfur isotopic variation in VMS deposits is larger than that in porphyry copper deposits. Franklin and others (1981) showed that, at the Millenbach VMS deposit, there is a systematic variation in isotopic ratios between copper- and
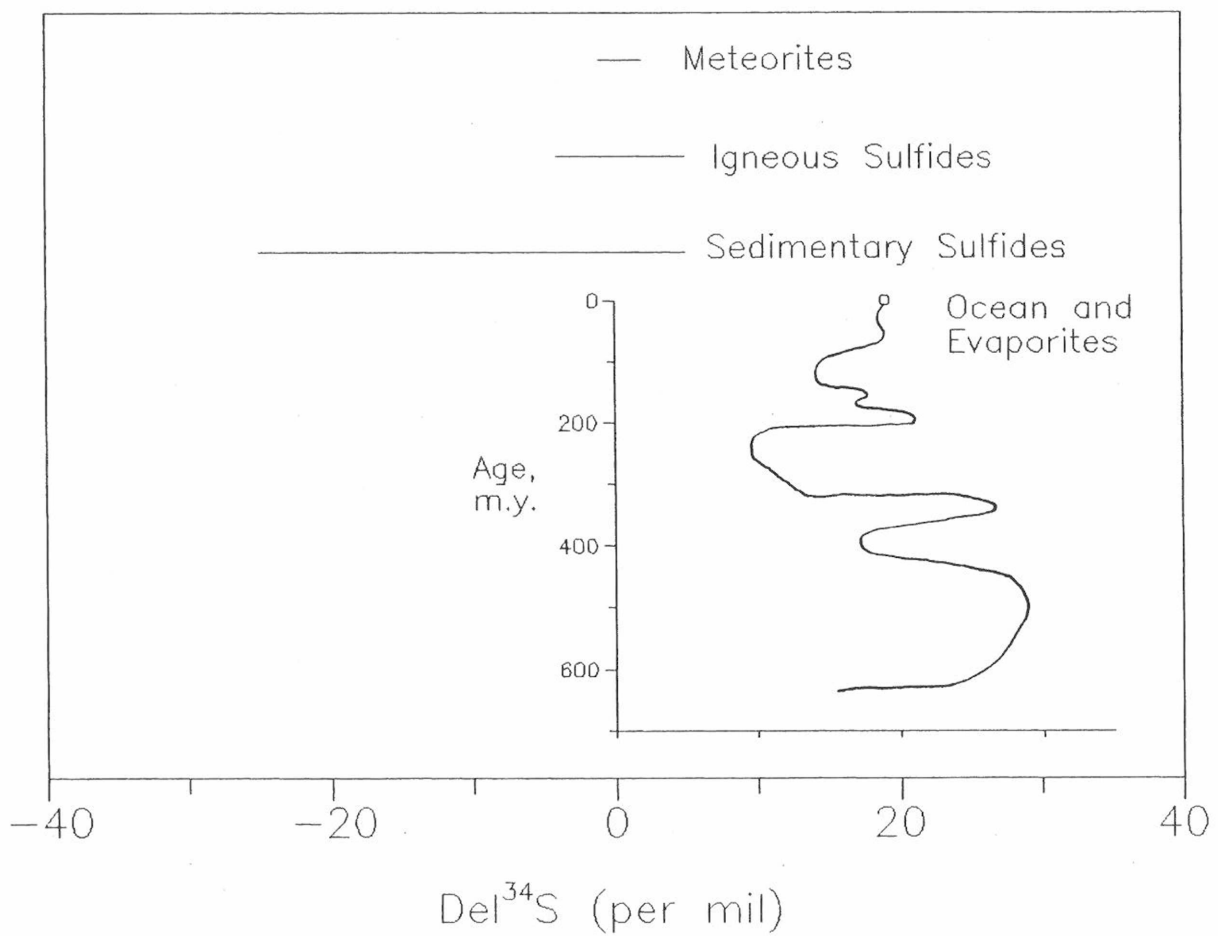
Figure 23. Sulfur isotopic variation in nature. Modified from Ohmoto and Rye (1979).
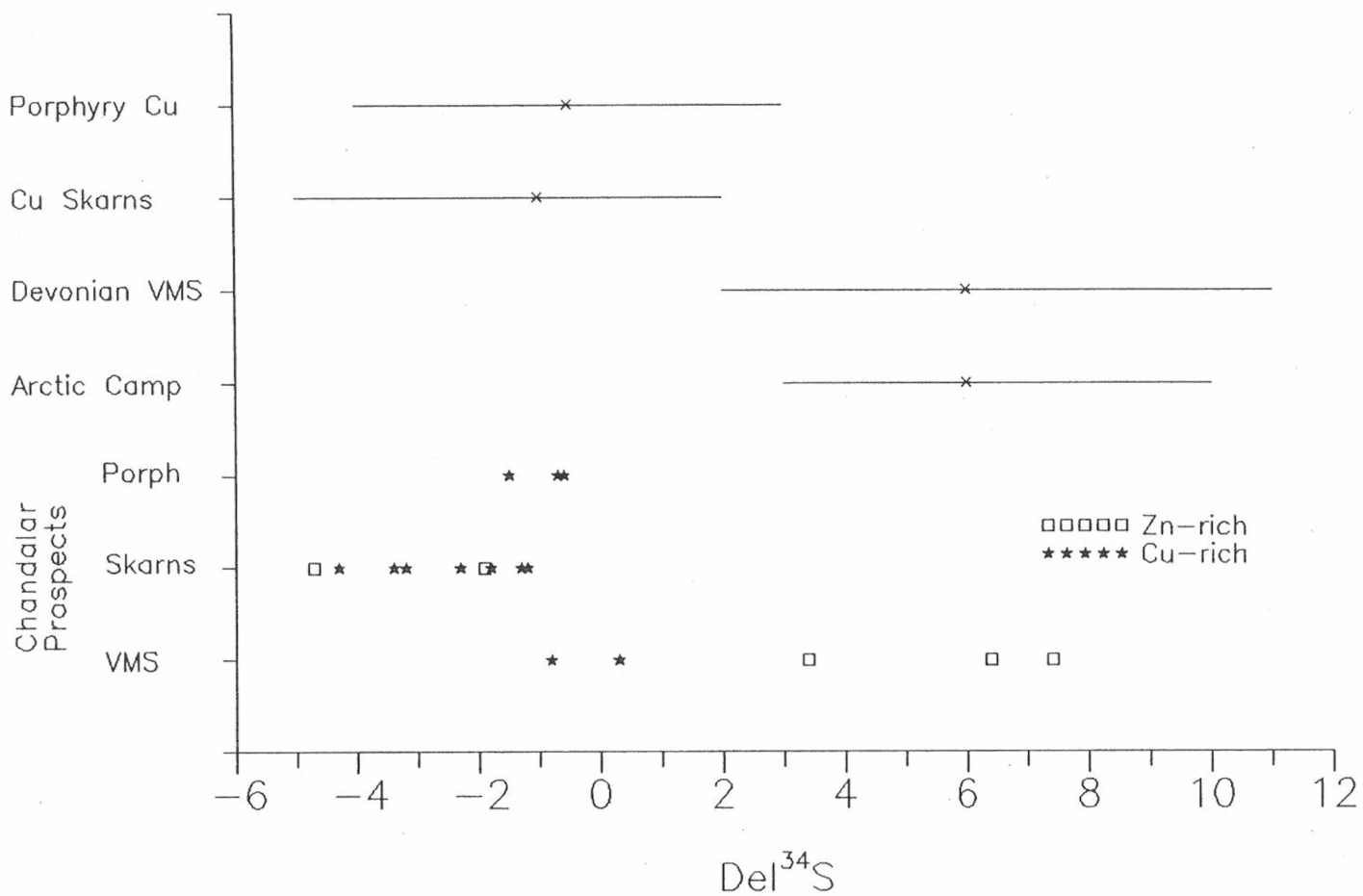
Figure 24. Del^{34}S values for porphyry, skarn and VMS samples from study area prospects compared to typical ranges for porphyry Cu deposits, Cu skarn deposits, Devonian VMS deposits, and the Arctic Camp prospect (Rye and others, 1974; Ayres and others, 1979; Ohmoto and Rye, 1979, Shimazaki and Yamamoto, 1979, Sato and others, 1981; Schmidt, 1983; South and Taylor, 1985; and this study).

zinc-rich ore horizons. The zinc-rich massive ores contain
more positive $del^{34}S$ values than the copper-rich stringer
ores.

Three sulfur isotope samples of pyrite were taken from
quartz-sericite-pyrite veins within the Venus Creek
porphyry. The $del^{34}S$ values for these samples are shown in
Figure 24. Note that these values fall within the range of
typical porphyry copper deposits and cluster around -1.

Sulfur isotope values for nine skarn samples from the
study area are also shown in Figure 24. Seven of these are
from chalcopyrite-bearing "Cu-rich" skarns and two are from
sphalerite-bearing "Zn-rich" skarns. Note that these
values are generally more negative than values from the
porphyry samples, and all are less than -1 per mil.

Ohmoto (1972) showed that the $del^{34}S$ of a sulfur
species is a function of the $del^{34}S$ of the sulfur in the
depositing fluid, temperature (T), oxygen fugacity (fO_2),
pH, and ionic strength (I). He showed that at constant T,
I, and $del^{34}S_{fluid}$, an increase in pH or fO_2 will be
accompanied by a decrease in the $del^{34}S$ value of the
sulfide species. Rye and others (1974) and Rye and Ohmoto
(1974) further showed that as hydrothermal fluids move from
an intrusive into a carbonate host rock, the pH could
increase by appproximately 2 units through reactions with
the host rock minerals. Figure 25(a) shows 1) the pH

fields for intrusive (K-feldspar+muscovite+quartz) and carbonate host rock (calcite+wollastonite+feldspar); 2) mineral stability fields for pyrite, pyrrhotite, magnetite, chalcopyrite and bornite; 3) contours for %FeS in sphalerite, and; 4)del^{34}S contours for pyrite. When sulfur isotope samples from this study are plotted in Figure 25(a), taking mineral assemblages and sphalerite compositions into account, a projected path can be drawn from pyrite-chalcopyrite bearing porphyry samples through sphalerite-magnetite-pyrite-chalcopyrite-bearing marble front skarn samples. Figure 25(b) shows the location of key samples along this path, and the overlapping fields for porphyry, "proximal" Cu-skarn and "distal" Cu-Zn skarn samples. This projected path shows an increase in pH and decrease in fO$_2$ of the skarn-forming fluids, which would be expected for fluids reacting with a graphitic carbonate.

Sulfur isotope values from massive sulfide layers at Luna are also shown in Figure 24. The values for the five samples range between -0.8 and +7.4. Early Devonian (380-400 m.y.) seawater sulfates have del^{34}S values of approximately +20 per mil (see Figure 23). The mean value for Luna sulfur isotope ratios (3.3 per mil) is approximately 17 per mil lower than the value for early Devonian seawater, consistent with Sangster's (1968) observations of typical VMS-related sulfides. The sulfides
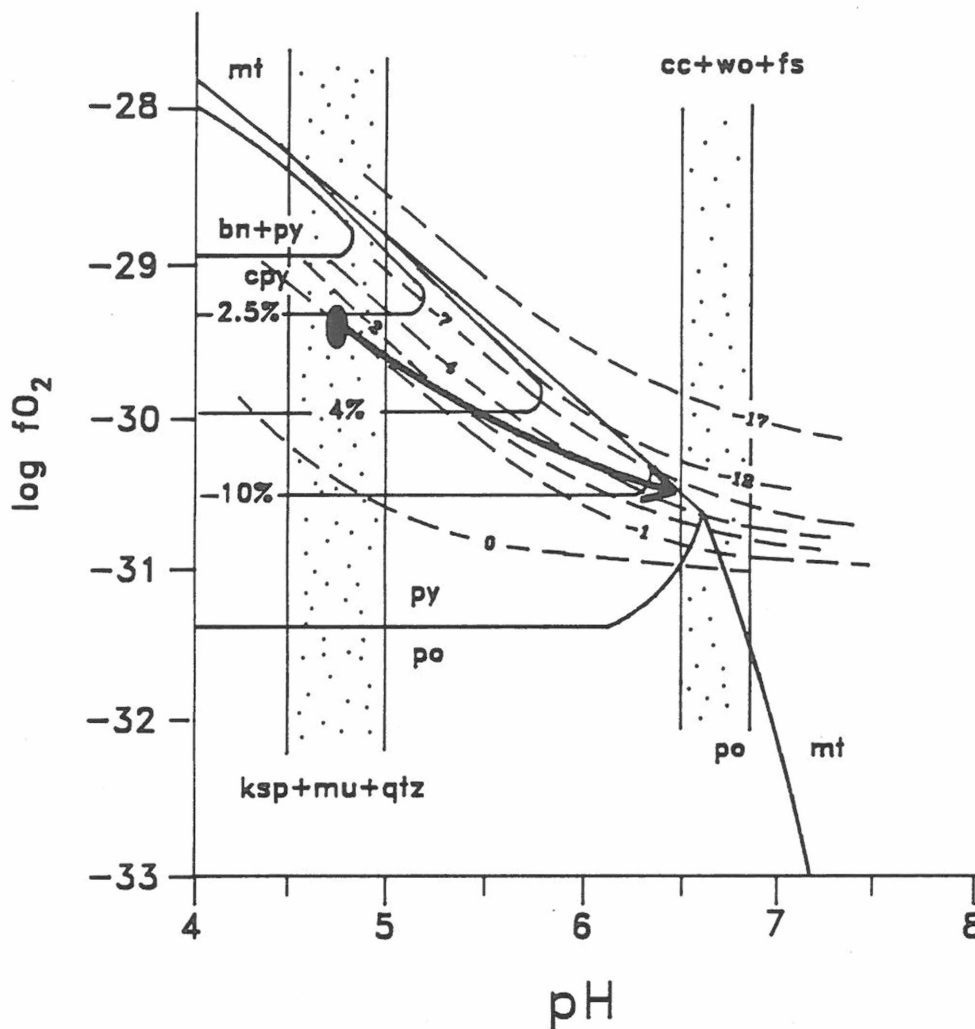
Figure 25(a). Log fO_2 vs. pH diagram for hydrothermal
fluids in a porphyry copper/copper skarn system. Diagram
shows (1) pH fields for a mineral assemblage compatible
with a granitic composition intrusive (ksp+mu+qtz) and
shaly marble (ca+wo+qtz); (2) mineral stability fields; (3)
del^{34}S contours for pyrite precipitated from a fluid at 350
^{O}C, with del^{34}Sfluid = 0 per mil and S$_{total}$ = 0.01M, (4)
contours for %FeS in sphalerite,and (5) the projected path
for fluids moving from porphyry into skarn (after Rye and
Ohmoto, 1974). Ksp=K-feldspar, mu=muscovite, qtz=quartz,
cc=calcite, wo=wollastonite, fs=feldspar, py=pyrite,
po=pyrrhotite, mt=magnetite, cpy=chalcopyrite, bn=bornite.
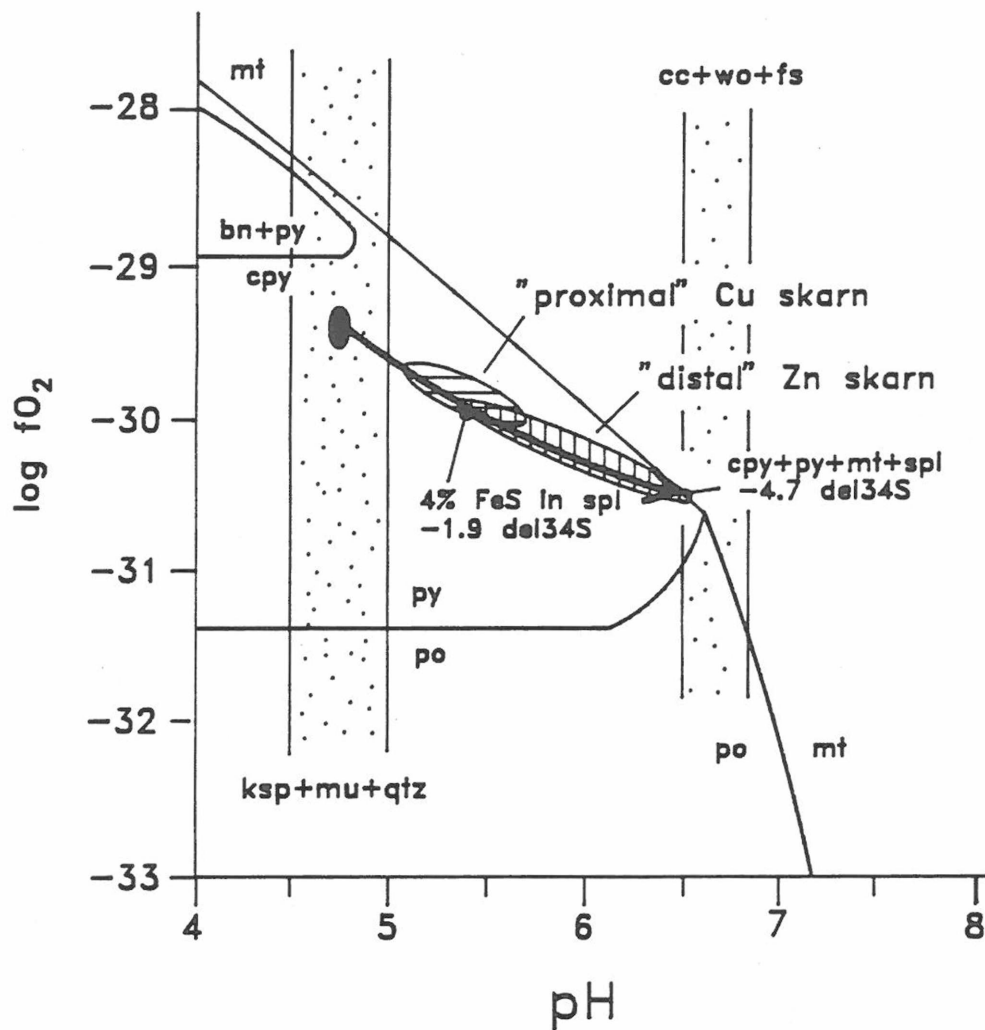
Figure 25(b). Data from this study plotted with respect to figure 25(a). Ksp=K-feldspar, mu=muscovite, qtz=quartz, cc=calcite, wo=wollastonite, fs=feldspar, py=pyrite, po=pyrrhotite, mt=magnetite, cpy=chalcopyrite, bn=bornite.

interpreted as VMS-related also show a systematic increase in del^{34}S from the Cu-rich to the Zn-rich ores, similar to the pattern seen in other VMS systems (Franklin and others, 1981) and different from the pattern seen in skarns (Rye and others, 1974; Rye and Ohmoto, 1974). Finally, the Luna values overlap those of the Arctic camp VMS sulfides in the Ambler district, but have a slightly more depleted mean value. This difference may be due to the younger age of the Arctic Camp deposit (327-373 Ma; Schmidt, 1983). Seawater sulfates from this time period have slightly more enriched values (+20 to +27 per mil) than do those from earlier Devonian (380-400 m.y.) time (+18-+23 per mil) (see Figure 23).

In summary, the Chandalar porphyry and skarn samples have del^{34}S values typical of other porphyry copper/skarn systems. Skarn samples are depleted in ^{34}S with respect to porphyry (magmatic) sulfides. These values cannot be produced by reaction between magmatic fluids (0 to -1 per mil) and early Devonian seawater (+18 to +23 per mil), as in a VMS system. Instead, the depletion in ^{34}S in skarns is explained by an increase in pH and slight decrease in fO_2 through reaction of magmatic hydrothermal fluids with graphitic carbonate host rocks.

Layered massive sulfides from the Luna prospect have del^{34}S values and a Cu to Zn trend typical of early

Devonian VMS deposits and show little overlap with the values for granitic rocks and skarns. They are enriched in ^{34}S with respect to the porphyry sulfides. There is no currently accepted mechanism to generate these values by precipitation from magmatic hydrothermal fluids alone or through sedimentary processes. These positive del^{34}S values can be explained through a process involving sulfate reduction of Devonian seawater.

It is apparent that there has been no mixing between VMS-related sulfur and magmatic sulfur during skarn formation. Luna VMS-sulfides have positive values consistent with a seawater source for sulfur. Luna skarn sulfides, however, have negative del^{34}S values similar to those from Big Spruce Creek skarns and are consistent with a magmatic sulfur source. If mixing had occurred between VMS-related sulfur and magmatic sulfur during skarn formation at Luna, skarn sulfides would have del^{34}S values intermediate between those of the massive sulfides and the porphyry sulfides.

CHAPTER IV - DEPOSIT COMPARISONS

COMPARISONS OF CHANDALAR PROSPECTS TO TYPICAL PORPHYRY COPPER AND COPPER SKARN SYSTEMS

The Evelyn Lee, Venus, Victor, Eva, and Luna prospects share many features with typical porphyry copper deposits and related skarn deposits. The following observations summarize the evidence for porphyry copper related mineralization in the study area:

1)   There are three hydrothermal alteration types present - potassic, sericitic, and propylitic - which are common to porphyry copper deposits (Titley, 1982; Beane, 1982).

2)   There is a general pattern of alteration zoning across the Big Spruce Creek area from potassic alteration in the southeast to sericitic alteration in the northwest (Figure 9), which indicates that these alteration types do not represent a metamorphic overprint.

3)   Mineralization in meta-porphyritic rocks is concentrated in the zone of overlap between potassic and sericitic alteration (Figure 9), as seen in many porphyry copper deposits (Lowell and Guilbert, 1970).

4)   Sulfur isotopic ratios for mineralized meta-
intrusive rocks (-1.5 to -0.7 per mil) are
similar to those for porphyry copper deposits
worldwide (Ohmoto and Rye, 1979) and reflect an
igneous source for the sulfur (Figure 24).

The following points summarize the evidence for
porphyry related skarn mineralization in the study area.

1)   The skarns are Cu-bearing and contain andraditic
garnets and diopsidic pyroxenes with low
manganese contents. These mineral compositions
are similar to porphyry copper related skarns
(Einaudi and Burt, 1982) and are quite different
from those of mineralized metamorphic calc-
silicate-bearing VMS deposits (Palache, 1929,
1935; Baker and Buddington, 1970; Both and
Rutland, 1976; Rozendaal, 1978; Duke, 1983;
Schmidt, 1986) (Figure 12).

2)   Garnets and pyroxenes are compositionally zoned.
Mineralogical evolution of garnets reflects an
initial increase, followed by a decrease, in
Fe^{3+}. This pattern is similar to that seen in
some porphyry-related Cu and Cu-Zn skarns and
different from garnet evolution in other skarn
types (Meinert, 1982; Newberry, 1982; Uchida and

Iiyama, 1982; Dobson, 1982; Newberry, 1987)
(Figures 14 and 15).

3) Skarns cross-cut layering and obliterate original
sedimentary textures. This differs from
mineralized metamorphic calc-silicate deposits
which parallel foliation or retain original
bedding features (Both and Rutland, 1976;
Rozendaal, 1978; Duke, 1983; Schmidt, 1986).

4) Skarns at the Luna prospect show a calc-silicate
zonation from garnet skarn to garnet pyroxene
skarn as marble is approached, as typically seen
in skarn deposits (Einaudi and others, 1981).

5) There is a spatial association between retrograde
altered skarn and sericitically altered meta-
intrusive and between fresh skarn and
potassically altered intrusive (see Figures 18-
20). This feature is seen in many porphyry
copper related skarns (Einaudi and others, 1981).

6) Cu skarns are adjacent to meta-plutonic stocks in
the Big Spruce Creek area, whereas Cu-Zn skarns
at the Luna prospect are not associated with any
major plutonic bodies. The presence of Cu skarns
near, and Zn skarns distal to, the hydrothermal
fluid source is found in many porphyry systems
(Einaudi and others, 1981; Einaudi, 1982a).

7) Sulfur isotopic ratios for skarn reflect a
    magmatic source of sulfur, but are slightly more
    negative than those for the meta-intrusive rocks
    (Figure 24). These ratios reflect a depletion in
    ^{34}S possibly explained by a change in pH and fO_2
    through reaction of magmatic fluids with
    graphitic carbonate rocks.

COMPARISONS OF THE LUNA PROSPECT WITH VMS DEPOSITS

Because they lie approximately along strike with the
VMS deposits of the Ambler district, it has been suggested
that the Chandalar copper prospects may contain VMS-type
mineralization. Of the five prospects studied, Luna is the
only one which contains any layered massive sulfide
concentrations. Sulfides in the other four prospects are
related to either porphyries or skarns.

The following observations summarize the evidence for
the presence of VMS-type mineralization at Luna.

1) Sulfur isotopic ratios from massive sulfide
    layers range between -0.8 and +7.4 per mil. The
    high del^{34}S values argue against a magmatic
    source for the sulfur. These values are
    approximately 17 per mil lower than the value for
    early Devonian seawater (+18 to +23 per mil) and
    can be explained by the reduction of seawater

sulfates by hot Fe^{2+}-bearing rocks (presumably mafic volcanic rocks). The values are consistent with those of other Devonian massive sulfide deposits (Ayres and others, 1979; South and Taylor, 1985; Schmidt, 1986) (Figure 24).

2) Chloritic alteration in the form of massive chlorite layers and lenses occurs both below and surrounding massive sulfide zones. The association between chloritic alteration and massive sulfides is seen in many VMS deposits (Franklin and others, 1981) and is also seen in the Ambler deposits (Schmidt, 1986).

3) Silicification, a common type of alteration in VMS deposits (Franklin and others, 1981), is spatially associated with sulfide stringers in Luna drill holes.

4) Stringer and disseminated sulfide mineralization is spatially associated with massive sulfide layers, a pattern common to VMS deposits (Franklin and others, 1981).

Barite gangue, abundant in the Ambler deposits, is absent at Luna. The massive sulfide layers at Luna represent a low fO_2 environment, as evidenced by the presence of arsenopyrite and high-Fe sphalerite. This low

oxidation state precludes the formation of sulfates and, therefore, the lack of barite at Luna is not surprising.

Although it is suggested above that the stringer and disseminated ores could be related to feeder zones, they are not concentrated below or "central" to the massive sulfide layers. This may be a result of deformation, or the present exposure of the Luna area may be an intergradational zone between stringer and massive sulfides, as in the Furutobe deposit in Japan (Kuroda, 1983).

In summary, the presence of stratiform massive sulfide layers, high sulfur isotopic ratios, and the spatial association between chloritic alteration and massive sulfide layers and between silicic alteration and stringer mineralization all support the identification of some of the mineralization in the Luna prospect as VMS type. The zoning from Cu-rich to Cu+Zn-rich sulfide mineralization between DDH-1 and DDH-3 suggests that a feeder zone, if present, is located in the northern part of the prospect.

CHAPTER V - ESTIMATED MINERAL POTENTIAL

Grades and tonnages for VMS mineralization at the Luna prospect can be roughly estimated using assay data from drill core intercepts (DDH-1, 3, and 5), location of massive sulfide outcrops, and bedding attitudes taken from

77

the map of Croff and others (1979). There are at least two possible tonnage models. The first assumes continuity of massive sulfide mineralization between DDH-1 and DDH-3. The second assumes that mineralization in each of the drill holes represents smaller, disconnected ore bodies.

Tonnage estimation using Model 1 is made with the following assumptions -

1)   Depth extent is 1/2 the strike length (Peters, 1978).

2)   Strike length of the ore body parallels the strike of the surrounding rocks, which approximately parallels a line connecting DDH-1 and DDH-3.

3)   Mineralization is continuous between the two drill holes.

Total thickness of combined VMS-related assay intervals within each hole averages 10 m. 30 m north of DDH-1, in DDH-5, this thickness drops to 2 m. DDH-1 is therefore considered the northern extent of mineralization. Since no massive sulfide outcrops are found south of DDH-3 within the Luna prospect, this drill hole is considered the southern extent. Strike length between the two equals 350 m. Depth (= 1/2 strike length) equals 175 m. Total volume, therefore, equals approximately 600,000 m^3. Assuming that 1 m^3 of rock weighs approximately 3 metric tons (average density of 3 gm/cm^3), this represents a tonnage of 1.8 million tons. Average grades over this

interval are 0.93% Cu, 0.35% Zn, and 0.19 oz/ton (6 ppm) Ag. This tonnage is comparable to average Kuroko-type VMS deposits. However, Cu and Ag grades are slightly lower and Zn grades are much lower than average grades for typical Kuroko deposits (Cox and Singer, 1986).

Estimates for Model 2 use the same assumptions as those for Model 1 but also account for rapid pinch out of massive sulfide between DDH-1 and DDH-5. They also assume no continuity of mineralization between drill holes and that the two ore bodies are of the same size. An ore body surrounding DDH-1 with a strike length of 100 m, a depth extent of 50 m, and a thickness of 10 m which pinches out rapidly to all sides would contain approximately 70,000 tons of 0.94% Cu, 0.03% Zn, and 0.3 oz/ton (10 ppm) Ag. A similar size body surrounding DDH-3 would have average grades of 0.92% Cu, 0.67% Zn, and 0.07 oz/ton (2 ppm) Ag.

The two grade and tonnage models described above only account for mineralization in the vicinity of the drill holes. Surface exposures of massive sulfide found in other portions of the prospect have not been drilled. Additional tonnages of VMS mineralization may surround these outcrops. Croff and others (1979) suggest that the mineralized horizon seen at Luna may extend 10 km to the southwest, toward the Hurricane-Diane, Deimos, and Ginger prospects

(shown in Figure 2). Evidence for massive sulfide mineralization has been found in all of these prospects.

Grades and tonnages for skarn mineralization at the Luna prospect can be calculated in much the same way as VMS mineralization using 2 similar models. The first assumes continuous mineralization between the two drill hole collars and a depth of approximately 1/2 that of the strike length. A continuous skarn body 350 m X 175 m X 3 m would give a tonnage of approximately 550,000 tons of 1.95% Cu, 1.45% Zn, and 0.65 oz/ton (21 ppm) Ag. Model 2 assumes two separate pods of skarn each extending 100 m (= 1/2 distance to DDH-2) around drill holes 1 and 3 and with a thickness of 3 m. These two bodies would give 280,000 tons of 3.1% Cu, 0.30% Zn, 1 oz/ton (32 ppm) Ag, and 280,000 tons of 0.8% Cu, 2.6% Zn and 0.3 oz/ton (10 ppm) Ag, respectively.

If both VMS and skarn mineralization are taken together in a continuous mineralized horizon averaging 35 m in thickness, a total grade and tonnage estimate gives 2.1 million tons, averaging 0.54% Cu, 0.17% Zn and 0.01 oz/ton (0.32 ppm) Ag.

Grade and tonnage estimates for skarn mineralization in the Big Spruce Creek prospects are based on areal exposure of surface outcrops and estimates of depth equal to 1/2 the strike length of mineralized skarn. At the Evelyn Lee prospect, exposure of mineralized skarn

containing 5% Cu covers an area of roughly 5500 m^2.
Assuming a depth of 50 m (approximately 1/2 the strike
length) this gives 1 million tons of 5% Cu. An additional
2300 m^2 of skarn containing 2% Cu is exposed in the area.
Assuming a 15 m depth for each outcrop, this translates to
an additional 140,000 tons of 2% Cu. Exposure of skarn
pods at the Victor and Eva prospects reveals a possible
50,000 tons of 2% Cu. The scattered skarn pods at the
Venus prospect give a combined tonnage of 80,000 tons of 3%
Cu. These tonnage estimates are close to the median
tonnage for non-porphyry-related copper skarns, but much
less than the average size of porphyry-related skarns (Cox
and Singer, 1986). This relatively small size for the
estimated deposit and the abundance of carbonate in the
area may indicate an appreciable amount of undiscovered
skarn resources in the area.

Mineralized surface exposure of the Venus stock
(porphyry copper mineralization) has a length of
approximately 1000 feet and a width of approximately 40
feet, where it is exposed in Venus Creek. Croff and others
(1979) report average grades of 0.3% Cu and 0.015% Mo over
17 feet of drill core for this intrusive. Two other holes
they drilled assayed 13 feet of 0.52% Cu and 57 feet of
0.2% Cu, respectively. No drill hole locations are
available for the Venus holes, which makes estimation of

grades and tonnages difficult. However, if copper mineralization is continuous along Venus and Big Spruce Creek, following the inferred contact between sericitic and potassic alteration zones, then a conservative grade and tonnage estimate for porphyry-related mineralization would be 300,000 tons of 0.3% Cu. The meta-intrusive at the Evelyn Lee prospect is only weakly mineralized. A 512 foot hole drilled by Croff and others (1979) encountered grades of less than 0.1% Cu. The Victor, Eva, and Luna prospect contain no mineralization in meta-intrusive rocks.

UNDISCOVERED GOLD POTENTIAL

A number of porphyry-related skarn deposits throughout North America contain significant levels of precious metals, including the Bingham, Ely, and Fortitude deposits (James, 1976; Atkinson and Einaudi, 1978; Wotruba and others, 1986). At Bingham, the highest gold grades are found in pyritized and silicified skarn (Atkinson and Einaudi, 1978). At the Fortitude Au-Ag skarn deposit, Au mineralization is associated with pyrrhotite-dominant sulfide replacement bodies and with chloritic retrograde alteration. Cu skarns associated with barren stocks, such as those in the Whitehorse District, Yukon Territory, contain significant by-product Au in sulfide-rich skarn with abundant retrograde alteration (Meinert, 1987b). Pb-Zn skarns, such as the skarns of the Groundhog Mine, N.M.

(Meinert, 1987a), contain byproduct Ag but little Au mineralization.

As yet, no significant Au mineralization has been found in the study area. Croff and others (1979) analyzed for Au in some surface and drill core samples, but no Au values were reported. Since only "significant" metal values were reported, these samples must have contained very low Au levels. No mention was made of which rock types or drill core intervals were analyzed for Au. Skarn samples from the Big Spruce Creek prospects contain ≤ 0.01 oz/ton (0.32 ppm) Au. The higher Au values (0.01 oz/ton - 0.32 ppm) are found in marble front, sulfide-rich skarn. Interior skarns generally have <0.005 oz/ton (0.16 ppm) Au. There is some potential for undiscovered gold in the field area, but more systematic sampling of the skarns is required. Analyses of pyrite-rich and chlorite retrograde altered skarn may show elevated gold levels. As yet, no pyrrhotite or silicified skarn have been found in the field area, but if further exploration reveals these features, samples should be analyzed for Au.

FURTHER EXPLORATION

Much of the data on the Chandalar copper district is based on surface mapping. Exploration for VMS-type mineralization to the southwest of the Luna prospect is suggested by the continuity of the mineralized quartz-

muscovite and calcareous schist package along this trend. The presence of extensive intrusive bodies emplaced into carbonate rocks also suggests the possibility for further undiscovered skarn mineralization. Further exploration in the study area should involve ground based geophysics, including magnetic and electromagnetic (VLF) surveys. Magnetic surveys should be useful in detecting buried ore bodies, especially in the Big Spruce Creek prospects, where the skarns are podiform and discontinuous. VLF surveys may help in locating unexposed faults which may dislocate ore bodies. Further drilling at the Luna prospect, where indicated by geophysical studies, is required to determine the continuity of VMS layers and mineralized horizons. Shallow drilling at the Evelyn Lee prospect by Croff and others (1979) collared and bottomed in mineralized skarn. Deeper drilling is needed to estimate reserves at this prospect. Trenching or drilling might be indicated by geophysical surveys in other prospects also.

CHAPTER VI - CONCLUSIONS

The existence of VMS mineralization at the Luna prospect is strongly supported by sulfur isotopic ratios consistent with those of known Devonian VMS deposits. Chloritic and silicic alteration are spatially associated with massive sulfide and stringer sulfide mineralization,

respectively. Metal zoning from Cu-rich in the northern part of the prospect to Cu+Zn-rich in the southern part of the prospect suggests that a feeder zone may be present to the north of drill holes 1 and 5. No VMS mineralization has been observed in the Big Spruce Creek prospects.

Mineralization at the Big Spruce Creek prospects resembles that of known porphyry copper and related skarn deposits. Evidence includes intrusive composition and alteration types, alteration and mineralization zoning, calc-silicate compositions and zoning, and sulfur isotopic ratios. No major meta-plutonic bodies and hence no porphyry mineralization are present at the Luna prospect. Skarns at this prospect have essentially the same features as those in Big Spruce Creek but have higher Zn contents. On an area-wide, basis the Big Spruce Creek prospects represent "proximal" porphyry copper and related skarn mineralization, whereas the Luna prospect contains "distal" Cu-Zn skarn mineralization.

Although the presence of two unrelated mineralization events (VMS and porphyry/skarn) may seem unlikely, this juxtaposition of ore deposit types is seen in a number of locations throughout the world. A similar relationship is seen in the the Rosebery mine in Tasmania, where both Cambrian massive sulfide and Devonian metasomatic rocks occur together (Burrett and Martin, 1989). The Bathurst-

Newcastle area in New Brunswick, also contains massive
sulfide deposits and porphyry-related "fissure" deposits
which occur within 15 km of each other (Tupper, 1960).
Like the Chandalar prospects, the sulfur isotopic ratios of
the two sets of deposits in the area fall into two distinct
groups. The mean del^{34}S values for the massive sulfide and
"fissure" deposits are 11.2 per mil and 0.9 per mil,
respectively (Tupper, 1960). In addition, in the Fiji
islands, a number of late Miocene porphyry and skarn
deposits occur within 8 km of early Miocene VMS deposits
(Colley and Greenbaum, 1980). Figure 26 shows an idealized
tectonic setting where the three deposit types may occur.
Colley and Greenbaum (1980) suggest that a change in the
plate tectonic regime brings about a change from
predominantly volcanogenic-exhalative deposits to orogenic
deposits, such as porphyry copper and skarn deposits.
Within the Chandalar study area, a change from an
extensional environment (hypothesized for the Ambler
deposits; Hitzman and others, 1986) to a subduction
(convergent) environment could explain the juxtapositioning
of the two deposit types.

Sulfur isotopic values suggest that little or no
mixing has occurred between VMS-related sulfides and
porphyry-related sulfides, indicating little remobilization
of VMS sulfides into skarn.
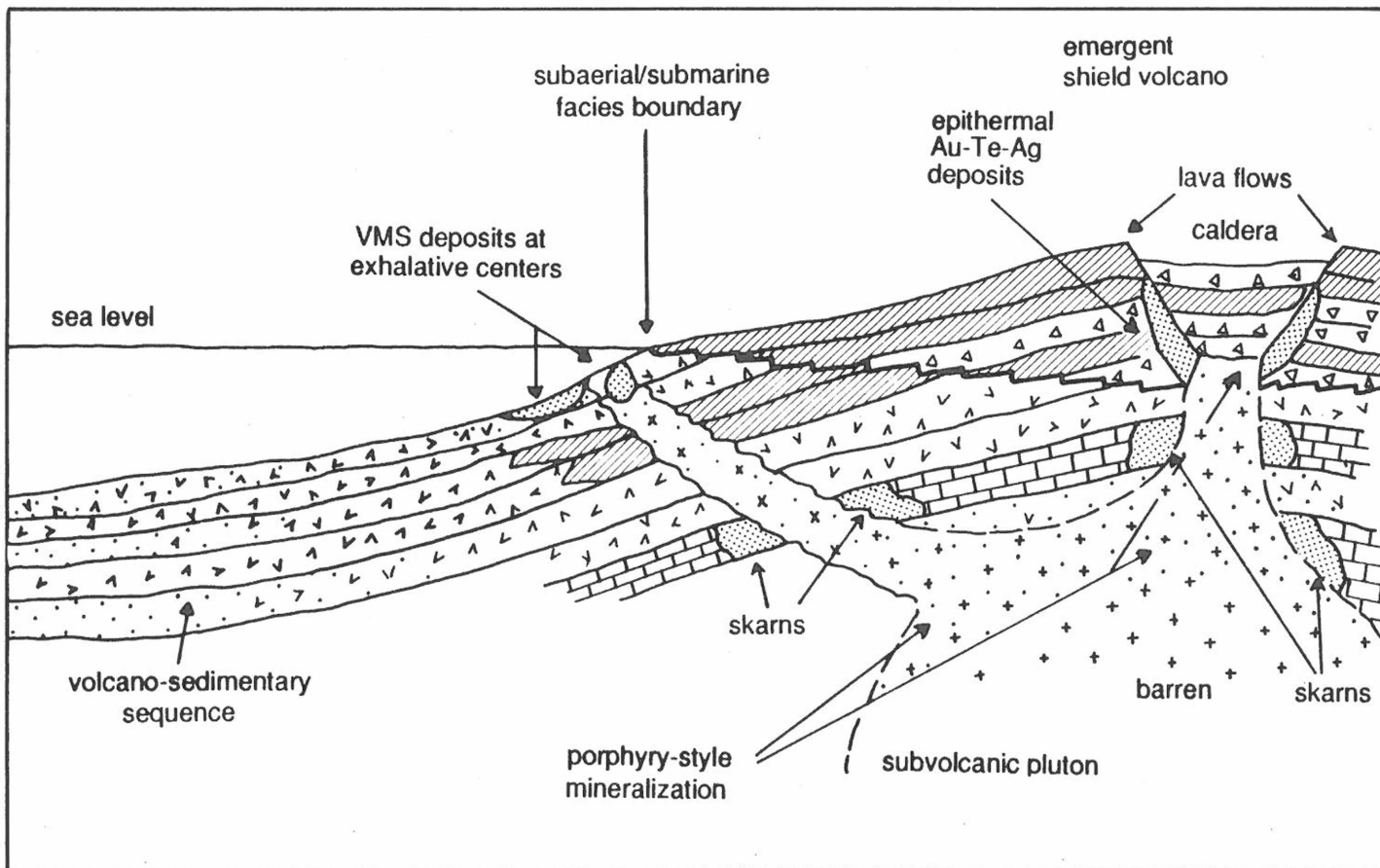
Figure 26. Schematic diagram illustrating a geologic environment
containing porphyry copper, copper skarn, and VMS mineralization.
Modified from Colley and Greenbaum, 1980.

FURTHER WORK

Detailed surface mapping accompanied by systematic sampling of both surface exposures and drill core are needed at the Luna prospect. Thin section examination of quartz, muscovite, and chlorite schists should be undertaken to look for relict volcanic textures. Examination of porphyritic meta-intrusives in thin section should help to identify the presence or absence of additional porphyry-related alteration types.

Electron microprobe analyses of minerals are also needed at Luna. Microprobe analyses of skarn pyroxenes will be necessary to determine their compositions, since the scarcity and fine grain size of this mineral make XRD analysis difficult. Microprobe analysis of banded garnets from Luna would help to determine the evolution of skarn-forming fluids with time.

Additional sulfur isotopic analyses of a larger number of samples from the Chandalar prospects would aid in differentiating between VMS and porphyry copper-related mineralization. This would be especially helpful in areas where skarn occurs as massive replacement bodies which resemble stratiform sulfide layers.

REFERENCES CITED

Adams, D. D., 1983, Geology of the northern contact area of the Arrigetch Peaks pluton, Brooks Range, Alaska: Unpub. M.S. thesis, Univ. Alaska-Fairbanks, 86 p.

Ayres, D. E., Burns, M. S., and Smith, J. W., 1979, Sulphur-isotope study of the massive sulphide orebody at Woodlawn, New South Wales: Jour. Geol. Soc. Australia, v. 26, p. 197-201.

Atkinson, W. W. and Einaudi, M. T., 1978, Skarn formation and mineralization in the contact aureole at Carr Fork, Bingham, Utah: Econ. Geol., v. 73, p. 1326-1365.

Baker, D. R. and Buddington, A. F., 1970, Geology and magnetite deposits of the Franklin quadrangle and part of the Hamburg quadrangle, New Jersey: U.S. Geol. Survey Prof. Paper 638, 73 p.

Barton, P. B., Jr., and Toulmin, P., III, 1966, Phase relation involving sphalerite in the Fe-Zn-S system: Econ. Geol., v. 61, p. 815-849.

Beane, R. E., 1982, Hydrothermal alteration in silicate rocks, in Titley, S. R., ed., Advances in geology of the porphyry copper deposits, southwestern North America: Tucson, Univ. Ariz. Press, p. 117-137.

Both, R. A. and Rutland, R. W. R., 1976, The problem of identifying and interpreting stratiform ore bodies in highly metamorphosed terrains: the Broken Hill example, in, Wolf ed., Handbook of stratabound and stratiform ore deposits: Amsterdam, Elsevier, v. 4, p. 261-325.

Brosge, W. P., and Reiser H. N., 1964, Geologic map and section of the Chandalar quadrangle, Alaska: U.S. Geol. Survey Misc. Geol. Inv. Map I-375.

Burnham, C. W., 1979, Magmas and hydrothermal fluids, in, Barnes, H. L., ed., Geochemistry of hydrothermal ore deposits: New York, John Wiley and Sons, p. 71-13.

Burrett, C. F. and Martin E. L., eds., 1989, Geology and mineral resources of Tasmania: Geol. Soc. of Australia, Spec. Publ. 15, 385 p.

Chappell, B. W., and White, A. J. R., 1974, Two contrasting granite types: Pacific Geol., v. 8, p. 173-174.

Chukhrov, F. V., Ermilova, L. P. and Nosik, L. P., 1977, Isotopic composition of sulphur and the genesis of hydrothermal sulphates, in, Klemm, D. D. and Schneider, H. J., eds., Time- and strata-bound ore deposits, p. 384-395.

Colley, H. and Greenbaum, D., 1980, The mineral deposits and metallogenesis of the Fiji platform: Econ. Geol., v. 75, p. 807-829.

Cox, D. P. and Singer, D. A., 1986, Mineral deposit models: U.S. Geol. Survey Bull. 1693, 379 p.

Croff, C., Andrews, T., Sherwonit, B., 1979, Luna volcanogenic massive sulfide and associated base-metal deposits and anomalies of the Chandalar copper belt: Doyon Annual Progress Report - 1978, courtesy of Doyon Ltd., Fairbanks, AK, 23 p.

Croff, C. and Bressler, J., 1980, Chandalar copper belt: Doyon Annual Progress Report - 1978, courtesy of Doyon Ltd., Fairbanks, AK, 27 p.

DeYoung, J.H., 1978, Mineral resources map of the Chandalar quadrangle, Alaska: U.S. Geol. Survey Misc. Field Studies Map MF-878-B.

Dillon, J. T., 1989, Structure and stratigraphy of the southern Brooks Range and northern Koyukuk basin near the Dalton highway, in, Mull, C. G. and Adams, K. E., eds., Dalton highway, Yukon river to Prudhoe bay, Alaska, bedrock geology of the easter Koyukuk basin, central Brooks range, and eastcentral arctic slope: Alaska Div. Geol. Geophys. Surveys, Guidebook 7, v. 2, p. 157-187.

Dillon, J. T., and Tilton, G. R., 1985, Devonian magmatism in the Brooks Range, Alaska [abs.]: Am. Assoc. Petroleum Geologists, Pacific Sec., 60th Ann. mtg., Program and Abstracts, p. 35.

Dillon, J. T., Pessel, G. H., Chen J. H., and Veach, N. C., 1980, Middle Paleozoic magmatism and orogenesis in the Brooks Range, Alaska: Geology, v. 7, p. 338-342.

Dobson, D. C., 1982, Geology and alteration of the Lost
    River tin-tungsten-fluorine deposit, Alaska: Econ.
    Geol., v. 77, p. 1033-1052.

Drummond, A. D., Tennant, S. J. and Young, R. J., 1973, The
    interrelationship of regional metamorphism,
    hydrothermal alteration and mineralization at the
    Gibraltar mines copper deposit in B.C.: CIM Bull., v.
    66, p. 48-55.

Duke, N. A., 1983, A metallogenic study of the central
    Virginia gold-pyrite belt: Unpub. Ph.D. dissert.,
    Univ. Manitoba, 197 p.

Einaudi, M. T., 1982a, Description of skarns associated
    with porphyry copper plutons, southwestern North
    America, in, Titley, S. R., ed., Advances in geology
    of the porphyry copper deposits, southwestern North
    America: Tucson, Univ. Ariz. Press, p. 139-184.

Einaudi, M. T., 1982b, General features and origin of
    skarns associated with porphyry copper plutons,
    southwestern North America, in, Titley, S. R., ed.,
    Advances in geology of the porphyry copper deposits,
    soutwestern North America: Tucson, Univ. Ariz. Press,
    p. 185-209.

Einaudi, M. T., Meinert, L. D., and Newberry, R.J., 1981,
    Skarn deposits: Econ. Geol., 75th Anniv. Vol., p. 317-
    391.

Einaudi, M.T. and Burt, D.M., 1982, Introduction-
    Terminology, classification, and composition of skarn
    deposits: Econ. Geol., v. 77, p. 745-754.

Floyd, P. A., and Winchester, J. A., 1978, Identification
    and discrimination of altered and metamorphosed
    volcanic rocks using immobile elements: Chem. Geol.,
    v. 21, p. 291-306.

Franklin, J. M., Sangster, D. M., and Lydon, J. W., 1981,
    Volcanic-associated massive sulfide deposits: Econ.
    Geol., 75th Anniv. Vol., p. 485-627.

Gilmour, P., 1982, Grades and tonnages of porphyry copper
    deposits, in, Titley, S. R. ed., Advances in geology
    of the porphyry copper deposits, southwestern North
    America: Tucson, Univ. Ariz. Press, p. 7-35.

Guilbert, J. M. and Park, C. F., 1986, The geology of ore deposits, W.H. Freeman and Company, p. 837-854.

Gustafson, L. B., and Hunt, J. P., 1975, The porphyry copper deposit at El Salvador, Chile: Econ. Geol., v. 70, p. 857-912.

Harris, N. B. and Einaudi, M. T., 1982, Skarn deposits in the Yerington district, Nevada: Metasomatic skarn evolution near Ludwig: Econ. Geol., v. 77, p. 877-898.

Hitzman, M. W., Proffett, J. M., Schmidt, J. M., and Smith, T. E., 1986, Geology and mineralization of the Ambler district, northwestern Alaska: Econ. Geol., v. 81, p. 1592-1618.

James, L. P., 1976, Zoned alteration in limestone at porphyry copper deposits, Ely, Nevada: Econ. Geol., v. 71, p. 488-512.

Kuroda, H., 1983, Geologic characteristics and formation environments of the Furutobe and Matsuki Kuroko deposits, Akita prefecture, northeast Japan: Econ. Geol. Monograph 5, p 149-166.

Lowell J. D., and Guilbert J. M., 1970, Lateral and vertical alteration-mineralization zoning in porphyry ore deposits: Econ. Geol., v.65, p. 373-408.

Meinert, L. D., 1982, Skarn, manto, and breccia pipe formation in sedimentary rocks of the Cananea mining district, Sonora, Mexico: Econ. Geol., v. 77, p. 919-949.

Meinert, L. D., 1987a, Skarn zonation and fluid evolution in the Groundhog mine, Central mining district, New Mexico: Econ. Geol., v. 82, p. 523-545.

Meinert, L. D., 1987b, Gold in skarn deposits - a preliminary overview: Proc. 7th Quadrennial IAGOD Symposium, p. 363-374

Mookherjee, A., 1976, Ores and metamorphism: Temporal and genetic relationships, in, Wolf K. H., ed., Handbook of stratabound and stratiform ore deposits: Amsterdam, Elsevier, v. 4, p. 203-260.

Newberry, R. J., 1982, Tungsten-bearing skarns of the Sierra Nevada. I. The Pine Creek mine, California: Econ. Geol., v. 77, p. 823-845.

Newberry, R. J., 1987, Use of intrusive and calc-silicate compositional data to distinguish contrasting skarn types in the Darwin polymetallic skarn district, California, USA: Mineral. Deposita, v. 22, p. 207-215.

Newberry, R.J., Dillon, J.T., and Adams, D.D., 1986, Regionally metamorphosed, calc-silicate-hosted deposits of the Brooks Range, northern Alaska: Econ. Geol., v. 81, p. 146-170.

Ohmoto, H., 1972, Systematics of sulfur and carbon isotopes in hydrothermal ore deposits: Econ. Geol., v. 67, p. 551-578.

Ohmoto, H., and Rye, R. O., 1979, Isotopes of sulfur and carbon, in, Barnes, H. L., ed., Geochemistry of hydrothermal ore deposits: New york, John Wiley and Sons, p.509-567.

Palache, C., 1929, A comparison of the ore deposits of Langban, Sweden, with those of Franklin, New Jersey: Amer. Mineral., v. 14, p. 43-47.

Palache, C., 1935, The minerals of Franklin and Sterling Hill, Sussex county, New Jersey: U.S. Geol. Survey Prof. Paper 180, 135 p.

Peters, W. C., 1978, Exploration and mining geology: New York, John Wiley and Sons, 696 p.

Rockingham, C. J. and Hutchinson, R. W., 1980, Metamorphic textures in Archean copper-zinc massive sulphide deposits: CIM Bull., v. 73, p.104-112.

Rozendaal, A., 1978, The Gamsberg zinc deposit, Namaqualand, in, Verwoerd, W. G., ed., Mineralization in metamorphic terranes, Geological Society of S. Africa Special Pub. 4, p. 235-265.

Rye, R. O. and Ohmoto, H., 1974, Sulfur and carbon isotopes and ore genesis: a review: Econ. Geol., v. 69, 0. 826-842.

Rye, R. O., Hall, W. E., and Ohmoto, H., 1974, Carbon, hydrogen, oxygen, and sulfur isotope study of the Darwin lead-silver-zinc deposit, southern California: Econ. Geol., v. 69, p. 468-481.

Sangster, D. G., 1968, Relative sulfur isotope abundance of ancient seas and stratabound sulphide deposits: Proc. Geol. Assoc. Can., v. 19, p. 79-86.

Sangster, D. F. and Scott, S. D., 1976, Precambrian, stratabound, massive Cu-Zn-Pb sulfide ores of north America, in, Wolf, K. H., ed., Handbook of stratabound and stratiform ore deposits, v. 6, Elsevier, p. 129-222.

Sasaki, A. and Ishihara, S., 1980, Sulfur isotopic characteristics of granitoids and related mineral deposits in Japan: Proc. 5th IAGOD Symp., Snowbird, Utah, 1978, E. Schweizerbart'sche Verlagsbuchhandlung, Germany, Stuttgart, p. 325-335.

Sato, K., Shimazaki, H., and Chon, H. T., 1981, Sulfur isotopes of the ore deposits related to felsic magmagism in the southern Korean peninsula: Min. Geol., v. 31, p. 321-326.

Schmidt, J. M., 1983, Geology and geochemistry of the Arctic prospect, Ambler district, Alaska: Unpub. Ph.D. dissert., Stanford Univ., 253 p.

Schmidt, J. M., 1986, Stratigraphic setting and mineralogy of the Arctic volcanogenic massive sulfide prospect, Ambler district, Alaska: Econ. Geol., v. 81, p. 1619-1643.

Shimazaki, H. and Yamamoto, M., 1979, Sulfur isotope ratios of some Japanese skarn deposits: Geochem. Jour., v. 13, p. 261-268.

Silberling, N. J. and Jones, D. L., 1984, Lithotectonic terrane maps of the North American cordillera: U.S. Geol. Survey Open-File Rept. 84-523, 102 p.

Sinclair, A. J., Drummond, A. D., Carter, N. C., and Dawson, K. M., 1982, A preliminary analysis of gold and silver grades of porpyry-type deposits in western Canada: in, Levinson, A. A., ed., Precious metals in thee northern Cordillera, Assoc. of Exploration Geochemists, Special Publication 10, p. 157-172.

South, B. C. and Taylor, B. E., 1985, Stable isotope geochemistry and metal zonation at the Iron Mountain mine, west Shasta district, California: Econ. Geol., v. 80, p. 2177-2195.

Streckeisen, A. L., and LeMaitre, R. W., 1979, A chemical approximation to the model QAPF classification of the igneous rocks: Neues Jahrb. Mineralogie Abh., v. 136, p. 169-206.

Szumigala, D. J., 1986, Geology and geochemistry of the Tin Creek zinc-lead-silver skarn prospects, Farewell mineral belt, southern Alaska Range, Alaska: Unpub. M.S. thesis, Univ. Alaska-Fairbanks, 144 p.

Titley, S. R., 1982, The style and progress of mineralization and alteration in porphyry copper systems, in, Titley, S. R., ed., Advances in geology of the porphyry copper deposits, southwestern North America: Tucson, Univ. Ariz. Press, p. 93-116.

Titley, S. R., and Beane, R. E., 1981, Porphyry copper deposits, Part I: Geologic settings, petrology, and tectogenesis: Econ. Geol., 75th Anniv. Vol., p. 214-235.

Tupper, W. M., 1960, Sulfur isotopes and the origin of the sulfide deposits of the Bathurst-Newcastle area of northern New Brunswick: Econ. Geol., v. 55, p. 1676-1707.

Uchida, E. and Iiyama, J. T., 1982, Physiochemical study of skarn formation in the Shinyama iron-copper ore deposit of the Kamaishi mine, northeastern Japan: Econ. Geol., v. 77, p. 809-822.

Vokes, F. M., 1969, A review of the metamorphism of sulphide deposits: Earth Sci. Rev., v. 5, p. 99-143.

Williams, H., Turner, F. J., and Gilbert, C. M., 1982, Petrography - An introduction to the study of rocks in thin section, 2nd edition: San Francisco, W. H. Freeman and Co., 626 p.

Winchell, H., 1958, The composition and physical properties of garnet: Amer. Min., v. 43, p. 595.

Winchester, J. A., and Floyd, P. A., 1977, Geochemical discrimination of different magma series and their differentiation products using immobile elements: Chem. Geol., v. 20, p. 325-343.

Wotruba, P. R., Benson, R. G., and Schmidt, K. W., 1986, Geology of the Fortitude gold-silver skarn deposit,

Copper Canyon, Lander county, Nevada: Bulk Mining Symposium, 17 p.

Zharikov, V. A., 1970, Skarns: Internat. Geology Rev., v. 12, p. 541-559, 619-647, 760-775.

APPENDIX 1 - LUNA DRILL CORE LOGS

EXPLANATION

▨	Denotes presence of indicated mineral assemblage
▨	Chloritic alteration
▨	Silicic alteration
▵▵▵	Breccia
╱	Quartz veins
⳾	Calcite veins
·.·.·	Disseminated minerals
╱	Veins or veinlets
⌐	Patches, lenses, or blebs

ABBREVIATIONS

G = graphite	py = pyrite	mtx = matrix
C = calcite	cpy = chalcopyrite	x-cut = cross cut
CL = chlorite	spl = sphalerite	conc = concentrated
M = muscovite	mt = magnetite	dissem = disseminated
Q = quartz	dk = dark	grad = gradational
S = schist	gry = gray	SK = skarn
mbl = marble	wh = white	V = VMS
intr = intrusive	blk = black	minzn = mineralization
qtz = quartz	mass = massive	retro = retrograde
fsp = feldspar	porph = porphyry	
calc = calcite	eqgr = equigranular	
musc = muscovite	phenos = phenocrysts	

97

DEPTH	TEXTURES	DESCRIPTION	MINZ TYPE	VEINS	ALTERATION	SKARNS			OPAQUES				AMOUNTS				CU/CU+ZN
						GARNET	PYROXENE	RETRO	CPY	PY	SPL	MT	% CPY	% PY	% SPL	% MT	

QMS

— — grad contact — — —

-10

-20 CLQMS

-30 fsp phenos - 1-2 mm

-40

-50

qtz veins x-cut foliation and each other

py along vein-schist contacts

-60

-70

% PY values: <1, 3, 0, 2, 3, 4, <1

DDH-1   p. 1

DEPTH	TEXTURES	DESCRIPTION	MINZ TYPE	VEINS	ALTERATION	SKARNS			OPAQUES				AMOUNTS				CU/CU+ZN
						GARNET	PYROXENE	RETRO	CPY	PY	SPL	MT	% CPY	% PY	% SPL	% MT	
		qtz veins cut foliation												2			
														3			
-80		py dissem along foliation												<1			
		CLQMS												2			
														5			
-90														0			
														3			
-100		calcite breccia											1	2			
		massive cpy layers and blebs - locally 50% cpy	VMS										2	0			99
-110		CLCS											10				98
		mt follows foliation												5		10	99
														3			
-120		massive py blebs - locally 50% py															98
		CLCS												5			
-130		META-PORPH DIKE												1			
		CCLS															96
-140		massive py at sill contact												25			

DDH-1   p.2

DEPTH	TEXTURES	DESCRIPTION	MINZ TYPE	VEINS	ALTERATION	SKARNS			OPAQUES				AMOUNTS				CU/CU+ZN
						GARNET	PYROXENE	RETRO	CPY	PY	SPL	MT	% CPY	% PY	% SPL	% MT	
		META-PORPH SILL											0	25			89
		massive py at sill contact											4	3			
		CCLS											1	1			98
150		SCALE CHANGE											1	1			
		1 in = 5 ft											<1	<1			
		SKARN - mass mbl front magnetite															
155		CCLS											2	3			
		GRAY MARBLE															
		GARNET SKARN															
160		GRAY MARBLE															
		CCLS	V										30				
165														2			98
		GRAY MARBLE											2				95
170		CCLS												<1			
		CCLQS															
		massive cpy bleb 40% cpy - 1.5" thick															94
175			V										10	5			
														30			
													10				
														5			
		SKARN - mass mbl front	SK										40				91
180		CCLQS											0	2			

DDH-1   p.3

DEPTH	TEXTURES	DESCRIPTION	MINZ TYPE	VEINS	ALTERATION	SKARNS			OPAQUES				AMOUNTS				CU/CU+ZN
						GARNET	PYROXENE	RETRO	CPY	PY	SPL	MT	% CPY	% PY	% SPL	% MT	
		CCLQS												2			
		CLGQS												3		0	30
185																	
190		2" mt-rich zone CLMQS											0	<1		20	
195														4		0	
200		EQGR SILL + SKARN meta-intr w/ pods of skarn	SK										1	3			
		CLMQS - crenulated											0	5			
														1			
205		END OF HOLE															

DDH-1   p. 4

DEPTH	TEXTURES	DESCRIPTION	MINZ TYPE	VEINS	ALTERATION	SKARNS			OPAQUES				AMOUNTS				CU/CU+ZN
						GARNET	PYROXENE	RETRO	CPY	PY	SPL	MT	% CPY	% PY	% SPL	% MT	
-10		CLCS												0		<1	
														<1			
-20		CLMQS - dk gry												0			
		CLMQS + CLCS												<1			
-30		--- grad contact ---												1			
														3			
-40		CLMQS												1			
-50														<1			0
-60																	
		--- grad contact ---												1			
-70		CLMS															

DDH-2   p. 1

DEPTH	TEXTURES	DESCRIPTION	MINZ TYPE	VEINS	ALTERATION	SKARNS			OPAQUES				AMOUNTS				CU/CU+ZN
						GARNET	PYROXENE	RETRO	CPY	PY	SPL	MT	% CPY	% PY	% SPL	% MT	
		CLMS - banded												1			
-80		thinner banding in clms												2			
														0			
-90		QCLMS												2			
-100		WHITE MARBLE												<1			
		CLMS - banded															
-110		WHITE MARBLE												0			
														3			
-120		MCCLS												2			
-130		WHITE MARBLE												<1			
-140																	
						DDH-2	p. 2										

wh mbl

gry mbl

DEPTH	TEXTURES	DESCRIPTION	MINZ TYPE	VEINS	ALTERATION	SKARNS			OPAQUES				AMOUNTS				CU/CU+ZN
						GARNET	PYROXENE	RETRO	CPY	PY	SPL	MT	% CPY	% PY	% SPL	% MT	
-150		WHITE MARBLE 3" long pyrite vein (1/16 - 3/4 ") in calcite mtx												10			
														<1			
-160		CLMS - 6"															
		WHITE MARBLE												1			
		CLMCS															
-170		- - - grad contact - - - -												<1			
		CLMQS															
-180		WHITE MARBLE - streaked															
		CLMQS															
		- - - grad contact - - - -															
-190		CMCLS deep blue green												0			
-200		End of Hole															

DDH-2   p. 3

DEPTH	TEXTURES	DESCRIPTION	MINZ TYPE	VEINS	ALTERATION	SKARNS			OPAQUES				AMOUNTS				CU/CU+ZN
						GARNET	PYROXENE	RETRO	CPY	PY	SPL	MT	% CPY	% PY	% SPL	% MT	
		QMS											0	<1			
		CCLQS	V										5	5			96
		CCLMQS											3	3			75
-10																	
		CLS											0	<1			
		SKARN	SK														
-20															0		
		CCLMS											1				
-30			V										2	<1			
		GRY MBL + SKARN	SK										0				
		MCCLS											3				
-40		MQCLS											0				91
		CCLS											5	2	50		4
		CQMCLS	V														95
-50		MASS SPL + CPY LAYER															93
		6 cm thick											2	5	0		
-60		CQMCLS															
-70													0	0			
		GRY MBL - Fe rich				DDH-3	p. 1										

DEPTH	TEXTURES	DESCRIPTION	MINZ TYPE	VEINS	ALTERATION	SKARNS			OPAQUES				AMOUNTS				CU/CU+ZN
						GARNET	PYROXENE	RETRO	CPY	PY	SPL	MT	% CPY	% PY	% SPL	% MT	
		CQMCLS															
		GRY MBL - Fe rich												0			
		CQMCLS															
-80		SKARN - barren	SK										0		0		
		META-PORPH DIKE												10			
		CCLQS															
-90		MCCLS + CLMCS											5		3		88
															0		26
																	95
-100		BLK MBL+ MCCLS													3		
													0				
-110		MCCLS											0				
-120															0		
		py conc. in qtz lenses												3			
		GRAY MARBLE banded & micaceous															
-130		CLMS												0			
		GRAY MARBLE															18
-140													10	3	25	2	22
		SKARN	SK														21
													1	2	tr		62

DDH-3   p. 2

DEPTH	TEXTURES	DESCRIPTION	MINZ TYPE	VEINS	ALTERATION	SKARNS			OPAQUES				AMOUNTS				CU/CU+ZN
						GARNET	PYROXENE	RETRO	CPY	PY	SPL	MT	% CPY	% PY	% SPL	% MT	
		SKARN	SK										1	2	tr		21 / 62
150		CLQS												3			
		CLS													0		
		CLQS												<1			
160																	
		QMS w/ high musc content												20	tr		
170													0				
		QMS												<1			
180															0		
		stringers and blebs of pyrite parallel to foliation												5			
190																	
		QMS												0			
200		End of Hole															
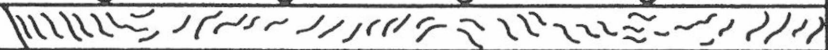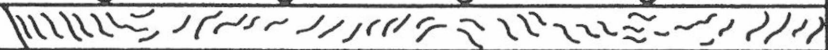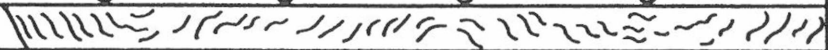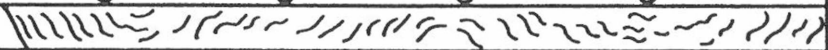
DDH-3   p. 3

DEPTH	TEXTURES	DESCRIPTION	MINZ TYPE	VEINS	ALTERATION	SKARNS			OPAQUES				AMOUNTS				CU/CU+ZN
						GARNET	PYROXENE	RETRO	CPY	PY	SPL	MT	% CPY	% PY	% SPL	% MT	
-10		QMS												3			
-20														2			
-30		META-PORPH SILL															
-40		CLMQS												3			
-50		qtz veins and lenses												2			
														4			
		CLCS												3			
-60		CLMQS															98
-70		CLCS dissem mt & py												2			

DDH-5   p. 1

DDH-5   p.2

DEPTH	TEXTURES	DESCRIPTION	MINZ TYPE	VEINS	ALTERATION	SKARNS			OPAQUES				AMOUNTS				CU/CU+ZN
						GARNET	PYROXENE	RETRO	CPY	PY	SPL	MT	% CPY	% PY	% SPL	% MT	
		CLMQS											0	2			
-150													10	25			65
		CCLQS qtz-calc vein with sulfide stringers	VMS											0			91
														25			
		GRAY MARBLE												0			
-160		CMCLQS qtz-calc lens parallel to foliation											0	<1			
-170													1	0			
		GRY MBL - streaked															
		QTZ-CALC LAYER												<1			
-180		GRAY MARBLE streaked															
-190		CLCS streaked											0	20			
														4			
-200		MCLQS												1			
-210																	

DDH-5   p.3

DEPTH	TEXTURES	DESCRIPTION	MINZ TYPE	VEINS	ALTERATION	SKARNS			OPAQUES				AMOUNTS				CU/CU+ZN
						GARNET	PYROXENE	RETRO	CPY	PY	SPL	MT	% CPY	% PY	% SPL	% MT	
		MCLQS												1			
−220		− − − grad contact − − − −															
		QCLMS													0		
−230		CLMQS - qtz-rich															
		CLQMS															
−240																	
		qtz-calc lenses - 6" thick													tr		
−250													<1				
		qtz lenses															
−260		CLQMS													0		
		qtz lenses															
−270																	
−280		qtz lens															

DDH-5   p. 4

DEPTH	TEXTURES	DESCRIPTION	MINZ TYPE	VEINS	ALTERATION	SKARNS			OPAQUES				AMOUNTS				CU/CU+ZN
						GARNET	PYROXENE	RETRO	CPY	PY	SPL	MT	% CPY	% PY	% SPL	% MT	
		qtz-calc lens												<1			
290																	
		CLQMS												0		0	
300																	
310		CLCS												3			
																3	
320		SKARN												0			
																0	
		CLCS - banded												2			
330																1	
		dissem mt & py in calcite bands																
340														<1			
		CCLMS w/ qtz and calc lenses															0	
350																	

DDH-5   p. 5

DDH-5 p. 6

Field	Content
DEPTH	400 — 390 — 380 — 370 — 360
TEXTURES	(wavy texture pattern)
DESCRIPTION	End of Hole · MCLS · CLQMS · grad contact · CCLMS
MINZ TYPE	
VEINS	(vein symbol)
ALTERATION	(hatched box)
SKARNS — GARNET	
SKARNS — PYROXENE	
SKARNS — RETRO	
OPAQUES — CPY	
OPAQUES — PY	(dotted pattern)
OPAQUES — SPL	
OPAQUES — MT	
AMOUNTS — % CPY	
AMOUNTS — % PY	<1
AMOUNTS — % SPL	
AMOUNTS — % MT	
CU/CU+ZN	

APPENDIX 2 - MICROPROBE ANALYSES

Microprobe analyses were performed on polished thin-sections by Rainer Newberry using a Cameca MBX electron microprobe at Washington State University, Pullman. A 15 kV filament voltage, a 13 nanoamp beam current, a 2 micron beam diameter, and a 10 second counting time were used. Well characterized minerals were employed as standards.

Garnet compositions were calculated based on the distribution of Ca^{2+}, Al^{3+}, Si^{4+}, Mg^{2+}, Mn^{2+}, Fe^{2+}, and Fe^{3+} ions per 12 oxygen atoms. Distribution of total Fe between Fe^{2+} and Fe^{3+} was determined using ideal stoichiometry, based on the fact that atomic Fe^{2+} in garnet should equal atomic $Si^{4+}-(Ca^{2+}+Mg^{2+}+Mn^{2+})$. Any remaining Fe will fill the trivalent site as Fe^{3+}. Proportions of endmember compositions were calculated as follows:

% Andradite (Ad) = $Fe^{3+}/(Fe^{3+}+Al^{3+})$

% Grossularite (Gr) =
$(Al^{3+}/(Fe^{3+}+Al^{3+}))(Ca^{2+}/(Ca^{2+}+Mn^{2+}+Fe^{2+}+Mg^{2+}))$

% Spessartine+Almandine (Sp+Alm) = 100-(Ad+Gr)

Pyroxene compositions were calculated based on the distribution of atomic Ca^{2+}, Fe^{2+}, Mg^{2+}, and Mn^{2+} per 6 oxygen atoms. Proportions of endmember compositions were calculated as follows:

% Hedenbergite (Hd) = $Fe^{2+}/(Fe^{2+}+Mg^{2+}+Mn^{2+})$

% Diopside (Di) = $Mg^{2+}/(Fe^{2+}+Mg^{2+}+Mn^{2+})$

% Johannsenite (Jo) = $Mn^{2+}/(Fe^{2+}+Mg^{2+}+Mn^{2+})$

Amphibole compositions were calculated based on the distribution of atomic Ca^{2+}, Mg^{2+}, Fe^{2+}, Mn^{2+}, Al^{3+}, and Si^{4+} per 23 oxygens (anhydrous method).

Abbreviations used for garnet type in the table are as follows:

metam = metamorphic garnet

isot = isotropic skarn garnet

banded = doubly banded birefringent garnet.

Ad = andradite garnet

Gr = grossularite garnet

Sp+Alm = spessartine+almandine garnet

GARNET MICROPROBE DATA

Sample	124a	124b	124c	7-1a	7-1b	7-1c
Garnet type	metam	metam	metam	skarnoid	skarnoid	skarnoid
Weight fraction						
Na2O	0.0000	0.0002	0.0002	0.0000	0.0000	0.0004
Fe2O3	0.0892	0.0575	0.0556	0.1479	0.1045	0.1233
K2O	0.0000	0.0000	0.0000	0.0000	0.0000	0.0000
SiO2	0.3881	0.3860	0.3865	0.3792	0.3877	0.3843
CaO	0.3540	0.3574	0.3557	0.3518	0.3612	0.3555
Al2O3	0.1735	0.1793	0.1801	0.1247	0.1574	0.1425
TiO2	0.0017	0.0156	0.0145	0.0004	0.0000	0.0000
MgO	0.0004	0.0026	0.0023	0.0000	0.0003	0.0001
MnO	0.0066	0.0084	0.0081	0.0040	0.0073	0.0059
total	1.0135	1.0070	1.0030	1.0080	1.0184	1.0120
Cations per 12 oxygens						
Na2+	0.0000	0.0000	0.0000	0.0000	0.0000	0.0000
Fe2+	0.0199	0.0000	0.0000	0.0000	0.0000	0.0000
Fe3+	0.4929	0.3304	0.3204	0.8745	0.6026	0.7202
K+	0.0000	0.0000	0.0000	0.0000	0.0000	0.0000
Si4+	2.9631	2.9475	2.9586	2.9805	2.9723	2.9825
Ca2+	2.8960	2.9242	2.9175	2.9629	2.9671	2.9563
Al3+	1.5613	1.6138	1.6250	1.1553	1.4223	1.3036
Ti2+	0.0098	0.0896	0.0835	0.0024	0.0000	0.0000
Mg2+	0.0046	0.0296	0.0262	0.0000	0.0034	0.0012
Mn2+	0.0427	0.0543	0.0525	0.0266	0.0474	0.0388
total	7.9901	7.9894	7.9837	8.0022	8.0152	8.0026
% Ad	24.0	17.0	16.5	43.1	29.8	35.6
% Gr	74.3	80.7	81.3	56.4	69.1	63.6
% Sp+Alm	1.7	2.3	2.2	0.5	1.2	0.9

GARNET MICROPROBE DATA

Sample	5a	5b	7a	7b	EVE-2a	EVE-2b
Garnet type	skarnoid	skarnoid	skarnoid	skarnoid	isot	isot
Weight fraction						
Na_2O	0.0002	0.0003	0.0001	0.0013	0.0001	0.0003
Fe_2O_3	0.1199	0.1159	0.1051	0.1453	0.2885	0.2872
K_2O	0.0000	0.0003	0.0002	0.0011	0.0001	0.0000
SiO_2	0.3836	0.3868	0.3857	0.3586	0.3632	0.3622
CaO	0.3539	0.3563	0.3522	0.3590	0.3364	0.3376
Al_2O_3	0.1459	0.1472	0.1543	0.1136	0.0219	0.0199
TiO_2	0.0003	0.0009	0.0017	0.0002	0.0011	0.0006
MgO	0.0005	0.0004	0.0005	0.0000	0.0000	0.0016
MnO	0.0070	0.0068	0.0072	0.0041	0.0016	0.0011
total	1.0113	1.0149	1.0070	0.9832	1.0129	1.0105
Cations per 12 oxygens						
Na^{2+}	0.0000	0.0000	0.0000	0.0000	0.0000	0.0000
Fe^{2+}	0.0000	0.0000	0.0114	0.0000	0.0115	0.0000
Fe^{3+}	0.6998	0.6731	0.6011	0.8911	1.7798	1.7884
K^+	0.0000	0.0030	0.0020	0.0114	0.0011	0.0000
Si^{4+}	2.9756	2.9857	2.9863	2.9224	2.9967	2.9976
Ca^{2+}	2.9415	2.9469	2.9219	3.1349	2.9741	2.9938
Al^{3+}	1.3340	1.3393	1.4082	1.0912	0.2130	0.1941
Ti^{2+}	0.0018	0.0052	0.0099	0.0012	0.0068	0.0037
Mg^{2+}	0.0058	0.0046	0.0058	0.0000	0.0000	0.0197
Mn^{2+}	0.0460	0.0445	0.0472	0.0283	0.0112	0.0077
total	8.0043	8.0022	7.9937	8.0806	7.9941	8.0050
% Ad	34.4	33.4	29.9	45.0	89.3	90.2
% Gr	64.5	65.5	68.6	54.6	10.6	9.7
% Sp+Alm	1.1	1.1	1.5	0.5	0.1	0.1

GARNET MICROPROBE DATA

Sample	EVE-2c	EVE-2d	EVE-2e	EVE-2f	EVE-2g	EVE-2h
Garnet type	isot	isot	isot	isot	isot rim	isot rim
Weight fraction						
Na_2O	0.0004	0.0005	0.0004	0.0002	0.0008	0.0000
Fe_2O_3	0.2849	0.2897	0.2950	0.2651	0.3055	0.2986
K_2O	0.0000	0.0001	0.0001	0.0000	0.0000	0.0000
SiO_2	0.3651	0.3612	0.3648	0.3667	0.3604	0.3626
CaO	0.3326	0.3351	0.3368	0.3391	0.3358	0.3375
Al_2O_3	0.0195	0.0166	0.0156	0.0307	0.0040	0.0063
TiO_2	0.0006	0.0001	0.0029	0.0007	0.0000	0.0000
MgO	0.0004	0.0005	0.0000	0.0006	0.0016	0.0016
MnO	0.0021	0.0019	0.0021	0.0014	0.0018	0.0017
total	1.0056	1.0057	1.0177	1.0045	1.0099	1.0083
Cations per 12 oxygens						
Na^{2+}	0.0000	0.0000	0.0000	0.0000	0.0000	0.0000
Fe^{2+}	0.0526	0.0000	0.0176	0.0105	0.0000	0.0000
Fe^{3+}	1.7264	1.8157	1.8102	1.6363	1.9194	1.8740
K^+	0.0000	0.0011	0.0011	0.0000	0.0000	0.0000
Si^{4+}	3.0291	3.0081	3.0031	3.0273	3.0092	3.0241
Ca^{2+}	2.9568	2.9903	2.9708	2.9996	3.0043	3.0160
Al^{3+}	0.1907	0.1630	0.1514	0.2987	0.0394	0.0619
Ti^{2+}	0.0037	0.0006	0.0180	0.0043	0.0000	0.0000
Mg^{2+}	0.0049	0.0062	0.0000	0.0074	0.0199	0.0199
Mn^{2+}	0.0148	0.0134	0.0146	0.0098	0.0127	0.0120
total	7.9791	7.9984	7.9867	7.9940	8.0049	8.0079
% Ad	90.1	91.8	92.3	84.6	98.0	96.8
% Gr	9.7	8.2	7.6	15.3	2.0	3.2
% Sp+Alm	0.2	0.1	0.1	0.1	0.0	0.0

GARNET MICROPROBE DATA

Sample	7c	7d	7e	7f	7g	7h
Garnet type	banded	banded	banded	banded	banded	banded
Weight fraction						
Na_2O	0.0007	0.0018	0.0007	0.0002	0.0002	0.0004
Fe_2O_3	0.1517	0.0944	0.2536	0.1798	0.1234	0.2654
K_2O	0.0000	0.0002	0.0003	0.0000	0.0000	0.0000
SiO_2	0.3703	0.3778	0.3601	0.3648	0.3748	0.3620
CaO	0.3470	0.3568	0.3394	0.3484	0.3546	0.3368
Al_2O_3	0.1041	0.1437	0.0378	0.0769	0.1262	0.0265
TiO_2	0.0115	0.0204	0.0011	0.0255	0.0157	0.0000
MgO	0.0007	0.0013	0.0007	0.0008	0.0009	0.0010
MnO	0.0076	0.0073	0.0027	0.0041	0.0061	0.0029
total	0.9936	1.0037	0.9964	1.0005	1.0019	0.9950
Cations per 12 oxygens						
$Na2+$	0.0000	0.0000	0.0000	0.0000	0.0000	0.0000
$Fe2+$	0.0000	0.0000	0.0000	0.0000	0.0000	0.0000
$Fe3+$	0.9177	0.5536	1.5874	1.0935	0.7322	1.6694
$K+$	0.0000	0.0020	0.0032	0.0000	0.0000	0.0000
$Si4+$	2.9759	2.9455	2.9948	2.9477	2.9544	3.0258
$Ca2+$	2.9880	2.9807	3.0246	3.0165	2.9951	3.0165
$Al3+$	0.9861	1.3206	0.3706	0.7324	1.1726	0.2611
$Ti2+$	0.0695	0.1196	0.0069	0.1550	0.0931	0.0000
$Mg2+$	0.0084	0.0151	0.0087	0.0096	0.0106	0.0125
$Mn2+$	0.0517	0.0482	0.0190	0.0281	0.0407	0.0205
total	7.9973	7.9852	8.0152	7.9828	7.9986	8.0057
% Ad	48.2	29.5	81.1	59.9	38.4	86.5
% Gr	50.8	69.0	18.8	39.6	60.5	13.4
% Sp+Alm	1.0	1.5	0.2	0.5	1.0	0.1

GARNET MICROPROBE DATA

Sample	205a	205b	205c	205d	205e	205f
Garnet type	banded	banded	banded	banded	banded	banded
Weight fraction						
Na2O	0.0001	0.0000	0.0001	0.0001	0.0001	0.0000
Fe2O3	0.1353	0.1501	0.2335	0.2468	0.1866	0.1848
K2O	0.0001	0.0002	0.0001	0.0000	0.0001	0.0001
SiO2	0.3796	0.3812	0.3674	0.3653	0.3775	0.3795
CaO	0.3483	0.3517	0.3406	0.3433	0.3452	0.3455
Al2O3	0.1187	0.1128	0.0503	0.0438	0.0943	0.0974
TiO2	0.0137	0.0087	0.0125	0.0045	0.0017	0.0031
MgO	0.0038	0.0031	0.0034	0.0024	0.0008	0.0009
MnO	0.0060	0.0057	0.0041	0.0029	0.0043	0.0065
total	1.0056	1.0135	1.0120	1.0091	1.0106	1.0178
Cations per 12 oxygens						
Na2+	0.0000	0.0000	0.0000	0.0000	0.0000	0.0000
Fe2+	0.0000	0.0000	0.0000	0.0000	0.0221	0.0193
Fe3+	0.8004	0.8853	1.4252	1.5186	1.0939	1.0775
K+	0.0010	0.0020	0.0010	0.0000	0.0010	0.0010
Si4+	2.9840	2.9883	2.9793	2.9875	3.0004	2.9929
Ca2+	2.9338	2.9542	2.9595	3.0083	2.9399	2.9196
Al3+	1.0998	1.0423	0.4808	0.4222	0.8834	0.9054
Ti2+	0.0810	0.0513	0.0762	0.0277	0.0102	0.0184
Mg2+	0.0445	0.0362	0.0411	0.0293	0.0095	0.0106
Mn2+	0.0400	0.0378	0.0282	0.0201	0.0289	0.0434
total	7.9846	7.9976	7.9912	8.0136	7.9894	7.9881
% Ad	42.1	45.9	74.8	78.2	55.3	54.3
% Gr	56.3	52.7	24.6	21.4	43.8	44.5
% Sp+Alm	1.6	1.3	0.6	0.4	0.9	1.1

GARNET MICROPROBE DATA

Sample	205g	205h	205i	205j	205k	205l
Garnet type	banded	banded	banded	banded	banded	banded
Weight fraction						
Na2O	0.0000	0.0003	0.0004	0.0005	0.0002	0.0000
Fe2O3	0.2049	0.1849	0.1814	0.1716	0.1977	0.2139
K20	0.0000	0.0001	0.0002	0.0000	0.0001	0.0000
SiO2	0.3717	0.3753	0.3743	0.3768	0.3722	0.3715
CaO	0.3474	0.3451	0.3480	0.3456	0.3460	0.3468
Al2O3	0.0784	0.0945	0.0946	0.1063	0.0800	0.0673
TiO2	0.0006	0.0000	0.0009	0.0007	0.0087	0.0033
MgO	0.0012	0.0006	0.0007	0.0011	0.0015	0.0023
MnO	0.0044	0.0060	0.0045	0.0052	0.0042	0.0038
total	1.0086	1.0068	1.0050	1.0078	1.0106	1.0089
Cations per 12 oxygens						
Na2+	0.0000	0.0000	0.0000	0.0000	0.0000	0.0000
Fe2+	0.0000	0.0000	0.0000	0.0035	0.0000	0.0000
Fe3+	1.2402	1.1114	1.0918	1.0206	1.1910	1.2993
K+	0.0000	0.0010	0.0020	0.0000	0.0010	0.0000
Si4+	2.9896	2.9973	2.9940	2.9882	2.9798	2.9987
Ca2+	2.9939	2.9532	2.9827	2.9368	2.9681	2.9995
Al3+	0.7433	0.8896	0.8919	0.9937	0.7549	0.6403
Ti2+	0.0036	0.0000	0.0054	0.0042	0.0524	0.0200
Mg2+	0.0144	0.0071	0.0083	0.0130	0.0179	0.0277
Mn2+	0.0300	0.0406	0.0305	0.0349	0.0285	0.0260
total	8.0150	8.0003	8.0067	7.9949	7.9938	8.0115
% Ad	62.5	55.5	55.0	50.7	61.2	67.0
% Gr	36.9	43.7	44.4	48.5	38.2	32.4
% Sp+Alm	0.5	0.7	0.6	0.8	0.6	0.6

GARNET MICROPROBE DATA

Sample	205m	205n	205o	205p	205q
Garnet type	banded	banded	banded	banded	banded
Weight fraction					
Na2O	0.0004	0.0008	0.0002	0.0000	0.0007
Fe2O3	0.2349	0.1466	0.1796	0.2961	0.2749
K2O	0.0000	0.0000	0.0000	0.0002	0.0000
SiO2	0.3699	0.3819	0.3777	0.3641	0.3639
CaO	0.3454	0.3514	0.3469	0.3341	0.3340
Al2O3	0.0539	0.1193	0.0942	0.0132	0.0324
TiO2	0.0014	0.0006	0.0004	0.0003	0.0002
MgO	0.0013	0.0009	0.0011	0.0002	0.0001
MnO	0.0028	0.0068	0.0047	0.0029	0.0053
total	1.0100	1.0083	1.0048	1.0111	1.0115
Cations per 12 oxygens					
Na2+	0.0000	0.0000	0.0000	0.0000	0.0000
Fe2+	0.0000	0.0000	0.0030	0.0278	0.0113
Fe3+	1.4359	0.8680	1.0762	1.8202	1.6905
K+	0.0000	0.0000	0.0000	0.0021	0.0000
Si4+	3.0050	3.0040	3.0160	3.0192	2.9931
Ca2+	3.0066	2.9618	2.9681	2.9685	2.9436
Al3+	0.5161	1.1061	0.8866	0.1290	0.3141
Ti2+	0.0086	0.0035	0.0024	0.0019	0.0012
Mg2+	0.0157	0.0106	0.0131	0.0025	0.0012
Mn2+	0.0193	0.0453	0.0318	0.0204	0.0369
total	8.0073	7.9993	7.9972	7.9915	7.9921
% Ad	73.6	44.0	54.8	93.4	84.3
% Gr	26.1	55.0	44.5	6.5	15.4
% Sp+Alm	0.3	1.0	0.7	0.1	0.3

PYROXENE MICROPROBE DATA

Sample	7-1a	7-1b	7a	7b	7c	7d
Core/Rim						
Weight fraction						
Na2O	0.0021	0.0010	0.0020	0.0019	0.0005	0.0037
FeO	0.1348	0.0669	0.1301	0.1409	0.0670	0.1403
K2O	0.0001	0.0000	0.0001	0.0003	0.0000	0.0001
SiO2	0.5208	0.5367	0.5212	0.5196	0.5387	0.5187
CaO	0.2441	0.2575	0.2418	0.2441	0.2519	0.2417
Al2O3	0.0018	0.0012	0.0011	0.0017	0.0006	0.0016
TiO2	0.0000	0.0002	0.0000	0.0001	0.0000	0.0000
MgO	0.0929	0.1320	0.1011	0.0903	0.1357	0.0906
MnO	0.0047	0.0137	0.0096	0.0056	0.0124	0.0075
total	1.0013	1.0092	1.0070	1.0045	1.0068	1.0042
Cations per 6 oxygens						
Na2+	0.0156	0.0072	0.0148	0.0141	0.0036	0.0276
Fe2+	0.4326	0.2076	0.4150	0.4523	0.2078	0.4508
K+	0.0005	0.0000	0.0005	0.0015	0.0000	0.0005
Si4+	1.9984	1.9914	1.9879	1.9945	1.9980	1.9929
Ca2+	1.0036	1.0238	0.9882	1.0040	1.0011	0.9951
Al3+	0.0081	0.0052	0.0049	0.0077	0.0026	0.0072
Ti2+	0.0000	0.0006	0.0000	0.0003	0.0000	0.0000
Mg2+	0.5314	0.7301	0.5748	0.5167	0.7503	0.5189
Mn2+	0.0153	0.0431	0.0310	0.0182	0.0390	0.0244
total	4.0056	4.0090	4.0172	4.0092	4.0024	4.0175
% Di	54.3	74.4	56.3	52.3	75.2	52.2
% Hd	44.2	21.2	40.7	45.8	20.8	45.3
% Jo	1.6	4.4	3.0	1.8	3.9	2.5

PYROXENE MICROPROBE DATA

Sample	124	205-12a	205-12b	205-12c	205-12d	205-12e
Core/Rim		core				
Weight fraction						
Na2O	0.0062	0.0017	0.0005	0.0000	0.0001	0.0002
FeO	0.0984	0.0705	0.0330	0.0336	0.0301	0.0303
K2O	0.0001	0.0000	0.0000	0.0003	0.0002	0.0001
SiO2	0.5208	0.5347	0.5447	0.5365	0.5414	0.5425
CaO	0.2393	0.2480	0.2558	0.2577	0.2596	0.2546
Al2O3	0.0056	0.0047	0.0022	0.0082	0.0043	0.0052
TiO2	0.0001	0.0000	0.0000	0.0007	0.0000	0.0010
MgO	0.1099	0.1309	0.1603	0.1552	0.1634	0.1573
MnO	0.0046	0.0101	0.0065	0.0074	0.0060	0.0067
total	0.9850	1.0006	1.0030	0.9996	1.0051	0.9979
Cations per 6 oxygens						
Na2+	0.0461	0.0123	0.0035	0.0000	0.0007	0.0014
Fe2+	0.3157	0.2200	0.1010	0.1034	0.0920	0.0930
K+	0.0005	0.0000	0.0000	0.0014	0.0009	0.0005
Si4+	1.9978	1.9955	1.9929	1.9741	1.9776	1.9917
Ca2+	0.9836	0.9917	1.0028	1.0160	1.0160	1.0016
Al3+	0.0253	0.0207	0.0095	0.0356	0.0185	0.0225
Ti2+	0.0003	0.0000	0.0000	0.0019	0.0000	0.0028
Mg2+	0.6284	0.7282	0.8743	0.8513	0.8897	0.8609
Mn2+	0.0149	0.0319	0.0201	0.0231	0.0186	0.0208
total	4.0126	4.0003	4.0041	4.0069	4.0140	3.9952
% Di	65.5	74.3	87.8	87.1	89.0	88.3
% Hd	32.9	22.4	10.1	10.6	9.2	9.5
% Jo	1.6	3.3	2.0	2.4	1.9	2.1

```
PYROXENE MICROPROBE DATA


Sample              205-12f
Core/Rim            12a rim
Weight fraction
Na2O                0.0019
FeO                 0.0330
K2O                 0.0002
SiO2                0.5447
CaO                 0.2546
Al2O3               0.0026
TiO2                0.0000
MgO                 0.1592
MnO                 0.0063
total               1.0025

Cations per 6 oxygens
Na2+                0.0135
Fe2+                0.1010
K+                  0.0009
Si4+                1.9940
Ca2+                0.9987
Al3+                0.0112
Ti2+                0.0000
Mg2+                0.8688
Mn2+                0.0195
total               4.0076

% Di                  87.8
% Hd                  10.2
% Jo                   2.0
```

AMPHIBOLE MICROPROBE DATA

Point #	PT 90	PT 91	PT 92	PT 93	PT 53	PT 54
Sample	84Ln78a	84Ln78b	84Ln78c	84Ln78d	EVE-2a	EVE-2b
Rock type	intrusive	intrusive	intrusive	intrusive	skarn	skarn
Weight fraction						
Na2O	0.0164	0.0155	0.0192	0.0153	0.0054	0.0083
FeO	0.1236	0.1143	0.1226	0.1114	0.1628	0.1792
K2O	0.0035	0.0033	0.0041	0.0021	0.0007	0.0002
SiO2	0.4794	0.4883	0.4722	0.4965	0.5379	0.5365
CaO	0.1100	0.1124	0.1102	0.1069	0.1172	0.1136
Al2O3	0.0766	0.0705	0.0806	0.0683	0.0085	0.0128
TiO2	0.0111	0.0099	0.0135	0.0102	0.0003	0.0003
MgO	0.1502	0.1551	0.1479	0.1573	0.1336	0.1230
MnO	0.0040	0.0047	0.0049	0.0042	0.0035	0.0026
total	0.9748	0.9740	0.9752	0.9722	0.9699	0.9765
Cations per 23 oxygens						
Na2+	0.4636	0.4363	0.5441	0.4289	0.1543	0.2371
Fe2+	1.5071	1.3876	1.4986	1.3468	2.0063	2.2076
K+	0.0651	0.0611	0.0764	0.0387	0.0132	0.0038
Si4+	6.9893	7.0880	6.9014	7.1774	7.9264	7.9028
Ca2+	1.7184	1.7482	1.7258	1.6559	1.8505	1.7930
Al3+	1.3163	1.2062	1.3885	1.1638	0.1476	0.2222
Ti2+	0.1217	0.1081	0.1484	0.1109	0.0033	0.0033
Mg2+	3.2643	3.3561	3.2223	3.3898	2.9348	2.7009
Mn2+	0.0494	0.0578	0.0607	0.0514	0.0437	0.0324
total	15.4952	15.4495	15.5662	15.3636	15.0802	15.1032
Atomic %						
Fe/Fe+Mg	31.6	29.3	31.7	28.4	40.6	45.0

AMPHIBOLE MICROPROBE DATA

Point #	PT 55	PT 56	PT 57	PT 58	PT 59
Sample	EVE-2c	EVE-2d	EVE-2e	EVE-2f	EVE-2g
Rock type	skarn	skarn	skarn	skarn	skarn
Weight fraction					
Na_2O	0.0052	0.0046	0.0135	0.0054	0.0103
FeO	0.1679	0.1643	0.2083	0.1654	0.1866
K_2O	0.0007	0.0004	0.0013	0.0003	0.0006
SiO_2	0.5346	0.5434	0.5204	0.5384	0.5350
CaO	0.1198	0.1224	0.1031	0.1190	0.1087
Al_2O_3	0.0140	0.0092	0.0245	0.0096	0.0139
TiO_2	0.0006	0.0000	0.0003	0.0006	0.0000
MgO	0.1347	0.1398	0.1032	0.1343	0.1212
MnO	0.0029	0.0034	0.0033	0.0034	0.0030
total	0.9804	0.9875	0.9779	0.9764	0.9793
Cations per 23 oxygens					
Na^{2+}	0.1475	0.1292	0.3910	0.1535	0.2943
Fe^{2+}	2.0540	1.9906	2.6021	2.0277	2.2998
K^+	0.0131	0.0074	0.0248	0.0056	0.0113
Si^{4+}	7.8199	7.8723	7.7732	7.8923	7.8843
Ca^{2+}	1.8777	1.9000	1.6501	1.8691	1.7165
Al^{3+}	0.2414	0.1571	0.4314	0.1659	0.2415
Ti^{2+}	0.0066	0.0000	0.0034	0.0066	0.0000
Mg^{2+}	2.9372	3.0191	2.2979	2.9347	2.6626
Mn^{2+}	0.0359	0.0417	0.0418	0.0422	0.0374
total	15.1331	15.1175	15.2156	15.0977	15.1477
Atomic %					
Fe/Fe+Mg	41.2	39.7	53.1	40.9	46.3

APPENDIX 3 - XRD ANALYSES

XRD (X-ray diffraction) samples were prepared by
making powder slide mounts of the selected mineral
(concentration > 70%) with an internal quartz standard.
Analyses were performed on a Rigaku Miniflex X-ray
diffractometer at the University of Alaska, Fairbanks,
using Ni-filtered Cu K alpha radiation and a scan speed of
1/2 degree per minute.

20 peaks were measured and were corrected using a
correction factor determined from the quartz standard. The
(400), (420), (422), (431), (521), (611), and (642) peaks
were used for garnet, the (111), (200), (220), and (311)
peaks were used for sphalerite, and the (101) and (112)
peaks were used for quartz. Peak position (d) were
calculated using

$$d_{hkl} = wavelength/2sinO$$

where wavelength = 1.5418 (for Cu K alpha) and O was taken
from the corrected 2O for that peak. Unit cell size (a_O)
for these cubic minerals was calculated using

$$a_O = d_{hkl}(h^2+k^2+l^2)^{\frac{1}{2}}$$

Andradite content in garnets was determined using
Winchell's (1958) determinative chart for garnets, and
assuming 0% almandine+spessartine, as supported by
microprobe analyses.

Fe content of sphalerite was calculated using the equation from Barton and Toulmin (1966)

$$\% \ FeS = 1774(a_O - 5.4093).$$

APPENDIX 3 - X-RAY DIFFRACTION RESULTS

GARNETS

SAMPLE NUMBER	GARNET TYPE	AVERAGE A SPACING	STANDARD DEVIATION	PERCENT ANDRADITE
DDH3-16	ISOTROPIC	12.004	0.006	77
DDH3-147	BANDED	12.028	0.005	90
DDH5-131	ISOTROPIC	12.010	0.007	80
51	BANDED	12.025	0.005	88
52	ISOTROPIC	12.024	0.003	88
195A	ISOTROPIC	12.038	0.004	95
195B	ISOTROPIC	12.050	0.007	100
196	ISOTROPIC	12.044	0.003	98
206-8	ISOTROPIC	12.049	0.012	100

SPHALERITE

SAMPLE NUMBER	ROCK TYPE	AVERAGE A SPACING	STANDARD DEVIATION	% FeS IN SPHALERITE
DDH3-47	VMS	5.4167	0.0025	13
DDH3-138	CU-ZN SKARN	5.4116	0.0024	4

APPENDIX 4 - MAJOR OXIDE ANALYSES

Major oxide analyses were performed by Bondar Clegg, Inc., Vancouver, B.C. and were determined using plasma emission spectrometry. Normative mineral compositions were calculated using IGPET geologic software. Abbreviations used in the table are as follows:

prop = propylitic

pot = potassic

ser = sericitic

LOI = loss on ignition.

APPENDIX 4 - MAJOR OXIDE ANALYSES

Sample #	79-Dn-57	79-Dn-57	79-Dn-57	DILLON
Rock type	Igneous	Igneous	Igneous	Igneous
Alteration	Fresh	Fresh	Fresh	Fresh
Wt. percent				
SiO2	64.08	64.98	67.21	65.42
Al2O3	15.52	15.91	14.25	15.23
Fe2O3	2.82	2.43	1.81	2.35
FeO	1.80	1.85	2.10	1.92
MgO	2.20	2.14	2.20	2.18
MnO	0.11	0.08	0.07	0.09
CaO	5.15	4.21	3.44	4.27
Na2O	3.37	3.50	3.29	3.39
K2O	2.23	2.27	2.99	2.50
TiO2	0.60	0.59	0.59	0.59
P2O5	0.40	0.35	0.33	0.36
LOI	1.80	2.00	1.10	1.63
Total	100.08	100.31	99.38	99.92

NORMATIVE MINERALS

Quartz	23.17	24.45	26.22	24.39
Orthoclase	13.18	13.42	17.67	14.77
Albite	28.52	29.62	27.84	28.69
Anorthite	20.64	18.60	14.91	18.83
Diopside	1.80			
Wollastonite				
Corundum		0.88	0.14	0.05
Hypersthene	4.83	5.89	7.00	6.21
Olivine				
Magnetite	4.09	3.52	2.62	3.41
Ilmenite	1.14	1.12	1.12	1.12
Hematite				
Apatite	0.93	0.81	0.76	0.83
Rutile				

APPENDIX 4 - MAJOR OXIDE ANALYSES

Sample #	84-Ln-2	85-Ln-56	84-Ln-146	84-Ln-21
Rock type	Igneous	Igneous	Igneous	Igneous
Alteration	Prop, Ser	Pot	Pot, Ser	Prop
Wt. percent				
SiO2	64.24	67.99	56.81	63.27
Al2O3	15.88	14.48	14.61	16.12
Fe2O3	2.48	1.95	1.51	2.21
FeO	1.80	2.20	5.25	1.60
MgO	2.15	0.99	4.29	2.06
MnO	0.08	0.09	0.11	0.06
CaO	4.14	2.26	6.10	4.28
Na2O	3.48	4.42	5.55	3.27
K2O	2.34	3.02	0.98	2.10
TiO2	0.58	0.54	1.06	0.55
P2O5	0.41	0.31	0.41	0.37
LOI	1.40	2.10	1.30	2.10
Total	98.98	100.35	97.98	97.99

NORMATIVE MINERALS

Quartz	23.92	24.50	2.70	24.87
Orthoclase	13.83	17.85	5.79	12.41
Albite	29.45	37.40	46.96	27.67
Anorthite	17.86	9.19	12.06	18.82
Diopside			12.66	
Wollastonite				
Corundum	1.08	0.57		1.57
Hypersthene	5.80	4.17	11.35	5.45
Olivine				
Magnetite	3.60	2.83	2.19	3.20
Ilmenite	1.10	1.03	2.01	1.04
Hematite				
Apatite	0.95	0.72	0.95	0.86
Rutile				

APPENDIX 4 - MAJOR OXIDE ANALYSES

Sample #	84-Ln-82	84-Ln-75	84-Ln-38	84-Ln-95B
Rock type	Igneous	Igneous	Igneous	Igneous
Alteration	Prop	Prop, Pot	Prop, Pot	Prop, Ser
Wt. percent				
SiO_2	60.08	64.20	65.72	66.73
Al_2O_3	15.02	15.89	15.23	11.16
Fe_2O_3	6.26	3.80	2.21	0.43
FeO	0.45	1.15	1.20	0.95
MgO	2.53	2.17	2.36	1.05
MnO	0.01	0.03	0.05	0.06
CaO	3.59	5.43	3.08	7.74
Na_2O	3.36	3.09	3.34	5.58
K_2O	2.17	1.64	2.39	0.38
TiO_2	0.59	0.51	0.47	0.24
P_2O_5	0.34	0.28	0.34	0.40
LOI	4.10	2.20	1.90	6.20
Total	98.49	100.39	98.29	100.92

NORMATIVE MINERALS

	84-Ln-82	84-Ln-75	84-Ln-38	84-Ln-95B
Quartz	21.73	25.97	27.99	22.10
Orthoclase	12.82	9.69	14.12	2.25
Albite	28.43	26.15	28.26	47.22
Anorthite	15.59	24.65	13.06	4.28
Diopside		0.36		7.72
Wollastonite				9.16
Corundum	1.43		2.36	
Hypersthene	6.30	5.24	5.88	
Olivine				
Magnetite		2.33	2.67	0.62
Ilmenite	0.97	0.97	0.89	0.46
Hematite	6.26	2.20	0.37	
Apatite	0.79	0.65	0.79	0.93
Rutile	0.08			

Major oxides determined by plasma emission spectrometry

APPENDIX 5 - TRACE ELEMENT ANALYSES

Sample Units Detection limit	Rock type	Alt'n type	Au ppb 5	Ag ppm 0.5	As ppm 5	Bi ppm 2	Co ppm 1
Dillon	Igneous	Fresh	5	1	7	13	7
Dillon	Igneous	Fresh	5	1	11	14	8
Dillon	Igneous	Fresh	5	1	9	15	8
Dillon avg	Igneous	Fresh	5	1	9	14	8
84-Ln-2	Igneous	Pr,ser	5	1	8	14	8
84-Ln-56	Igneous	Pot	5	1	5	11	6
84-Ln-146	Igneous	Pot,ser	5	1	16	14	11
84-Ln-21	Igneous	Pr	5	1	9	13	4
84-Ln-82	Igneous	Pr	5	1	5	6	20
84-Ln-75	Igneous	Pr,pot	5	1	9	10	12
84-Ln-38	Igneous	Pr,pot	5	1	6	14	11
84-Ln-95B	Igneous	Pr,ser	5	1	5	12	5
84-Ln-51A	Skarn	Gt	5	1	5	2	1
84-Ln-7	Skarn	Gt,ret px	220	4	56	2	20
84-Ln-7B	Skarn	Px,ret gt	5	1	5	10	7
84-Ln-5A	Skarn	Gt, px	5	1	5	6	4
84-Ln-124B	Skarn	Ret gt	55	5	14	2	10
84-Ln-205A	Skarn	Ret gt&px	10	1	6	5	8
84-Ln-205B	Skarn	Ret gt&px	5	1	5	11	4

Pr = propylitic, ser=sericitic, pot=potassic, gt=garnet, px=pyroxene,
ret=retrograde, avg=average values. Zr and Ba determined by X-ray
fluorescence. Hg determined by cold vapour atomic absorption. Au determined
by atomic absorption. All others by plasma emission spectrometry.

APPENDIX 5 - TRACE ELEMENT ANALYSES

Sample	Rock type	Alt'n type	Cr ppm	Cu ppm	Mn ppm	Mo ppm	Ni ppm
Detection limit			1	1	1	1	1
Dillon	Igneous	Fresh	41	43	230	1	11
Dillon	Igneous	Fresh	49	1	152	1	11
Dillon	Igneous	Fresh	47	41	82	2	15
Dillon avg	Igneous	Fresh	46	28	155	1	12
84-Ln-2	Igneous	Pr,ser	30	8	142	4	11
84-Ln-56	Igneous	Pot	45	15	500	1	8
84-Ln-146	Igneous	Pot,ser	21	288	149	1	13
84-Ln-21	Igneous	Pr	33	221	176	2	18
84-Ln-82	Igneous	Pr	25	15	22	1	33
84-Ln-75	Igneous	Pr,pot	29	46	113	1	24
84-Ln-38	Igneous	Pr,pot	29	465	154	13	26
84-Ln-95B	Igneous	Pr,ser	57	54	423	2	14
84-Ln-51A	Skarn	Gt	42	184	1168	1	17
84-Ln-7	Skarn	Gt,ret px	49	14803	877	10	33
84-Ln-7B	Skarn	Px,ret gt	32	864	928	1	12
84-Ln-5A	Skarn	Gt, px	109	26	1538	1	10
84-Ln-124B	Skarn	Ret gt	76	18898	617	79	40
84-Ln-205A	Skarn	Ret gt&px	71	486	1325	2	14
84-Ln-205B	Skarn	Ret gt&px	33	131	896	1	3

Pr = propylitic, ser=sericitic, pot=potassic, gt=garnet, px=pyroxene,
ret=retrograde, avg=average values. Zr and Ba determined by X-ray
fluorescence. Hg determined by cold vapour atomic absorption. Au determined
by atomic absorption. All others by plasma emission spectrometry.

APPENDIX 5 - TRACE ELEMENT ANALYSES

Sample	Rock	Alt'n	Pb	Sb	Se	W	Zn
Units	type	type	ppm	ppm	ppm	ppm	ppm
Detection limit			5	5	5	10	1
=================	====	=====	====	====	====	====	====
Dillon	Igneous	Fresh	5	5	5	10	10
Dillon	Igneous	Fresh	8	5	5	10	11
Dillon	Igneous	Fresh	18	5	5	10	7
Dillon avg	Igneous	Fresh	10	5	5	10	9
84-Ln-2	Igneous	Pr,ser	5	5	5	10	10
84-Ln-56	Igneous	Pot	15	5	5	10	33
84-Ln-146	Igneous	Pot,ser	5	5	5	10	11
84-Ln-21	Igneous	Pr	6	5	5	10	23
84-Ln-82	Igneous	Pr	8	5	5	10	1
84-Ln-75	Igneous	Pr,pot	5	5	8	10	13
84-Ln-38	Igneous	Pr,pot	8	5	5	10	17
84-Ln-95B	Igneous	Pr,ser	5	5	6	10	6
84-Ln-51A	Skarn	Gt	5	5	5	10	1
84-Ln-7	Skarn	Gt,ret px	9	5	5	19	48
84-Ln-7B	Skarn	Px,ret gt	5	5	5	10	11
84-Ln-5A	Skarn	Gt, px	5	5	8	10	2
84-Ln-124B	Skarn	Ret gt	10	5	7	10	171
84-Ln-205A	Skarn	Ret gt&px	5	5	5	10	9
84-Ln-205B	Skarn	Ret gt&px	5	5	5	10	1

Pr = propylitic, ser=sericitic, pot=potassic, gt=garnet, px=pyroxene, ret=retrograde, avg=average values. Zr and Ba determined by X-ray fluorescence. Hg determined by cold vapour atomic absorption. Au determined by atomic absorption. All others by plasma emission spectrometry.

APPENDIX 5 - TRACE ELEMENT ANALYSES

Sample	Rock type	Alt'n type	Hg ppb	Ba ppm	Nb ppm	Rb ppm	Sr ppm
Detection limit			5	20	5	5	5
Dillon	Igneous	Fresh	5	640	19	81	330
Dillon	Igneous	Fresh	5	720	15	94	320
Dillon	Igneous	Fresh	20	690	17	120	290
Dillon avg	Igneous	Fresh	10	683	17	98	313
84-Ln-2	Igneous	Pr,ser	5	710	17	67	360
84-Ln-56	Igneous	Pot	10	480	10	110	100
84-Ln-146	Igneous	Pot,ser	5	160	7	19	320
84-Ln-21	Igneous	Pr	40	560	18	96	370
84-Ln-82	Igneous	Pr	5	530	15	170	300
84-Ln-75	Igneous	Pr,pot	10	400	18	89	490
84-Ln-38	Igneous	Pr,pot	5	520	20	100	340
84-Ln-95B	Igneous	Pr,ser	5	40	12	9	360
84-Ln-51A	Skarn	Gt	10	20			
84-Ln-7	Skarn	Gt,ret px	190	20			
84-Ln-7B	Skarn	Px,ret gt	15	20			
84-Ln-5A	Skarn	Gt, px	10	40			
84-Ln-124B	Skarn	Ret gt	75	20			
84-Ln-205A	Skarn	Ret gt&px	15	20			
84-Ln-205B	Skarn	Ret gt&px	15	20			

Pr = propylitic, ser=sericitic, pot=potassic, gt=garnet, px=pyroxene,
ret=retrograde, avg=average values. Zr and Ba determined by X-ray
fluorescence. Hg determined by cold vapour atomic absorption. Au determined
by atomic absorption. All others by plasma emission spectrometry.

APPENDIX 5 - TRACE ELEMENT ANALYSES

Sample Units Detection limit	Rock type	Alt'n type	Zr ppm 5	Y ppm 5
Dillon	Igneous	Fresh	140	7
Dillon	Igneous	Fresh	130	12
Dillon	Igneous	Fresh	150	17
Dillon avg	Igneous	Fresh	140	12
84-Ln-2	Igneous	Pr,ser	120	5
84-Ln-56	Igneous	Pot	260	54
84-Ln-146	Igneous	Pot,ser	150	5
84-Ln-21	Igneous	Pr	140	11
84-Ln-82	Igneous	Pr	130	14
84-Ln-75	Igneous	Pr,pot	110	5
84-Ln-38	Igneous	Pr,pot	140	5
84-Ln-95B	Igneous	Pr,ser	64	5
84-Ln-51A	Skarn	Gt		
84-Ln-7	Skarn	Gt,ret px		
84-Ln-7B	Skarn	Px,ret gt		
84-Ln-5A	Skarn	Gt, px		
84-Ln-124B	Skarn	Ret gt		
84-Ln-205A	Skarn	Ret gt&px		
84-Ln-205B	Skarn	Ret gt&px		

Pr = propylitic, ser=sericitic, pot=potassic, gt=garnet, px=pyroxene,
ret=retrograde, avg=average values. Zr and Ba determined by X-ray
fluorescence. Hg determined by cold vapour atomic absorption. Au determined
by atomic absorption. All others by plasma emission spectrometry.

APPENDIX 6 - TYPICAL DEPOSIT CHARACTERISTICS

PORPHYRY COPPER DEPOSITS

TECTONIC SETTING

Porphyry copper deposits are formed near subduction zones in continental margins and island arcs. Calc-alkaline continental margin type deposits are associated with granodiorite to quartz monzonite porphyries, generally possess a well-developed sericitic alteration zone and are relatively high in Mo (>0.01%) and low in Au (<0.01 oz/ton) (Gilmour, 1982). Calc-alkaline island arc porphyry copper deposits, on the other hand, are associated with slightly more mafic intrusives (quartz diorites to granodiorites) and are relatively low in Mo (<0.01%) and high in Au (>0.01 oz/ton (0.32 ppm)) (Gilmour, 1982). Deposits hosted in alkaline plutonic rocks occur in both continental margin and island arc settings and can contain a variety of Au:Mo ratios (Gilmour, 1982). Sinclair and others (1982) suggest, however, that gold and molybdenum contents in porphyry copper deposits are a function of more than just tectonic environment, but may also be related to alteration assemblage and depth of formation.

TONNAGE AND GRADE

Porphyry copper deposits are low grade, high tonnage deposits. Primary copper grades generally range from about

0.3% to 0.8% Cu, with an average of 0.6% Cu (Gilmour, 1982). By-product metals average 0.015% Mo, 0.06 oz/ton (1.92 ppm) Ag, and 0.001 oz/ton (0.032 ppm) Au with considerable ranges, as discussed above. Tonnages range from 2 million tons to >3 billion tons of ore with an average of about 150 million tons.

ALTERATION TYPES

Titley (1982) and Beane (1982) described a number of hydrothermal alteration assemblages which occur in porphyry copper deposits.

1) Potassium silicate alteration consists of secondary biotite and K-feldspar. Magmatic biotite and hornblende are selectively replaced by secondary Fe- and Ti-poor biotite ± rutile; magmatic plagioclase is pervasively replaced by secondary potassium feldspar. This alteration type can also involve secondary biotite veinlets and K-feldspar veins ("A" and "B" veins - Gustafson and Hunt, 1975). Accessory minerals may include chlorite, anhydrite, apatite, magnetite, siderite, pyrite, chalcopyrite, bornite and/or molybdenite. Total sulfide abundances range from 2 to 5%.

2) Propylitic alteration consists of calcic plagioclase which is pervasively altered to epidote + calcite, with sodic plagioclase unaffected. Mafic minerals are altered to chlorite ± calcite ± actinolite ± sphene.

Minor chlorite - epidote - calcite veins may also be present. Accessory minerals include pyrite, magnetite and minor montmorillonite.

3) Sericitic alteration is characterized by the formation of quartz - pyrite veins with sericite envelopes ("D" veins - Gustafson and Hunt, 1975). Merging of these envelopes results in pervasive alteration of the rock to quartz-sericite-pyrite. Sulfide contents are high (10-15%) and pyrite to chalcopyrite ratios of >10:1 are typical. Sericitic alteration is the most texturally destructive alteration type in porphyry systems.

4)Hypogene argillic alteration occurs as both disseminated and fracture-controlled quartz, dickite, montmorillonite and pyrophyllite with minor (1-2%) pyrite. Argillic alteration is commonly not present, probably due to erosional removal.

ALTERATION-MINERALIZATION ZONING

The following discussion of alteration-mineralization zoning is based on work by Lowell and Guilbert (1970) and is summarized in Figure 27. Alteration zoning is characterized by a central core of potassic alteration, an intermediate zone of sericitic alteration, and a widespread outer zone of propylitic alteration. Argillic alteration, when present, is peripheral to and above the sericitic zone. The distribution of sulfide minerals is fairly
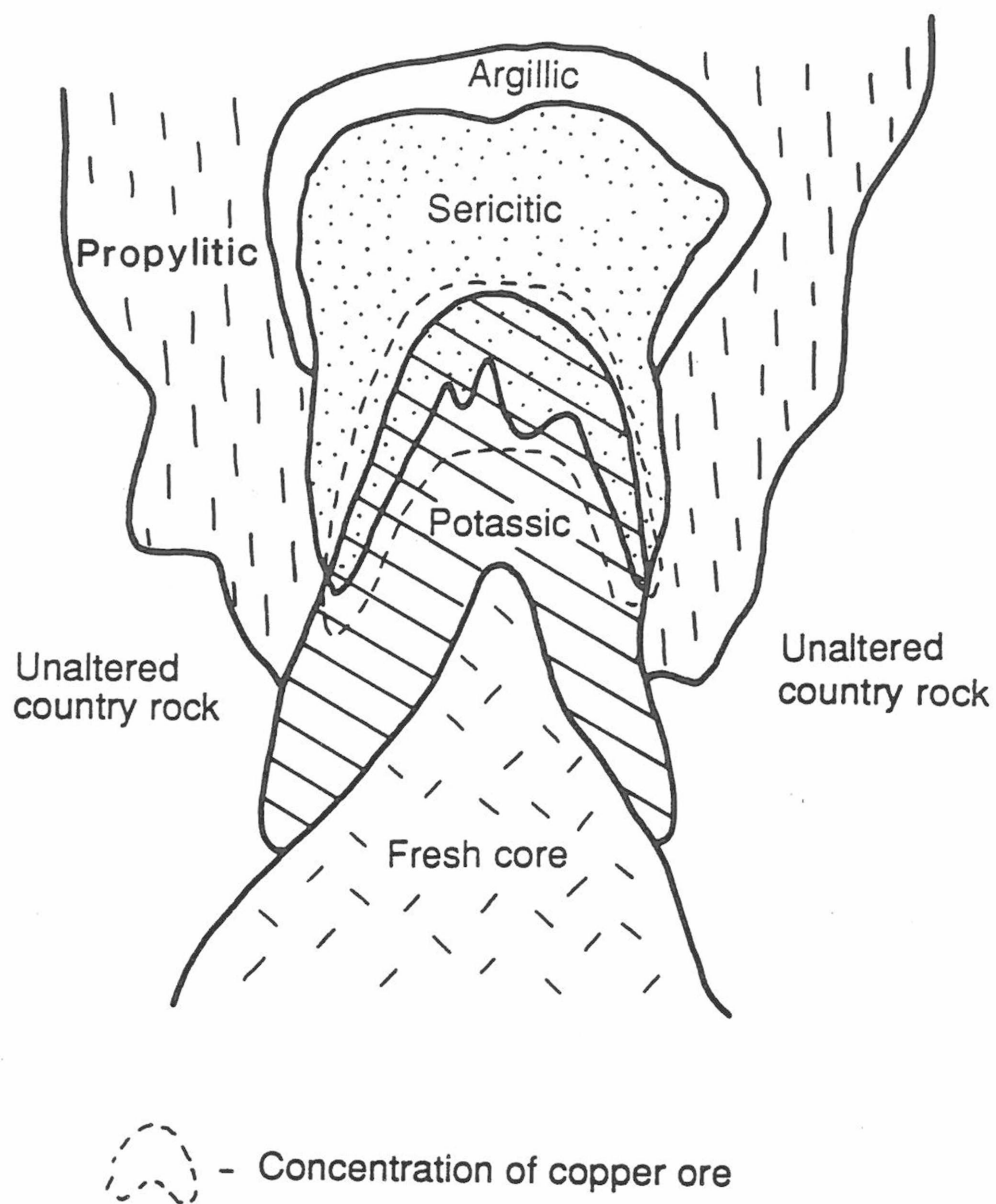
Porphyry Cu Deposit

Figure 27. Idealized cross section through a porphyry copper deposit. Note that copper ore is concentrated in areas where potassic and sericitic alteration overlap.

consistent in porphyry deposits, and the metals are zoned
laterally and vertically away from the central core. There
is generally an outward decrease in the abundance of
bornite and molybdenite, and an outward increase in the
abundance of pyrite. Bornite and molybdenite are generally
absent outside the potassic alteration zone, but
chalcopyrite is found in small quantities in the sericitic
zone. Pyrite is the dominant sulfide in the sericitic,
propylitic and argillic alteration zones. The highest
grade hypogene copper ore (0.5-1% Cu) is usually found in a
"shell" overlapping the contact between potassic and
sericitic alteration.

POST-ORE METAMORPHIC EFFECTS

Although a certain amount of deformation and a loss of
volatiles would be expected during metamorphism of porphyry
copper deposits, original hydrothermal alteration
assemblages should remain stable through high metamorphic
grades. The following discussion is based on a summary of
alteration mineral stabilities by Guilbert and Park (1986).
They suggest that argillic alteration clay minerals,
including kaolinite and montmorillonite, are dehydrated to
form aluminosilicates, such as andalusite or kyanite.
However, potassic alteration assemblages, which consist of
the same minerals as found in high grade granodioritic
gneisses (quartz, potassium feldspar, plagioclase, and

biotite) should survive to amphibolite metamorphic facies.
In addition, since propylitic alteration minerals are
equivalent to a greenschist metamorphic assemblage, they
should survive to at least upper greenschist facies
conditions. Sericitic alteration minerals (quartz and
muscovite) should be stable to amphibolite facies and
commonly form kink or chevron folded phyllites or muscovite
schists.

Because the above alteration assemblages are so
similar to metamorphic assemblages, criteria must be
established for discriminating between those which were
altered prior to metamorphism and those which were not.
Since large amounts of carbonate would not be expected as a
product of isochemical metamorphism of plutonic rocks, its
presence suggests introduction of CO_2 from outside the
system. Therefore, the occurrence of abundant calcite with
chlorite and epidote in the porphyry is more likely
indicative of propylitic alteration than of greenschist
metamorphism. Pyrite does not usually occur in
intermediate composition intrusive rocks unless introduced
by hydrothermal fluids (Burnham, 1979) and cannot be
introduced by greenschist metamorphism alone. The presence
of carbonates and sulfides in hydrothermally altered rocks
but not in unaltered meta-intrusive rocks at the Gibraltar

porphyry copper deposit, British Columbia (Drummond and others, 1973), supports these conclusions.

Metamorphic effects on sulfide minerals are also summarized by Guilbert and Park (1986). They point out that it is possible for sulfides to remain in a rock up to amphibolite facies of metamorphism without significant remobilization or recrystallization. They also suggest that, even when recrystallized and deformed, there is often little or no migration of metals and, therefore, metal values and distribution remain unchanged by metamorphism. Hence, although regional metamorphism of a porphyry copper deposit will result in deformation and recrystallization of the rocks, alteration and mineralization assemblages may still be recognizable.

PORPHYRY-RELATED COPPER SKARNS

Skarn refers to coarse grained calc-silicate rock which is formed in carbonate-rich host rocks near plutonic rocks by hydrothermal metasomatism. The following discussion is based primarily on papers by Einaudi and others (1981) and Einaudi (1982a and b).

Many of the same calc-silicate minerals are formed by both contact metamorphism and metasomatism of calcium-rich host rocks. There are a number of characteristics which can be used to distinguish between the two which are

summarized by Einaudi and others (1981). In general, metamorphic calc-silicates are finer grained and more Fe-poor than those formed by metasomatism. Also, metamorphic rocks generally preserve original compositional layering, whereas metasomatic calc-silicate veining may be completely destroy original layering.

Intense skarn development usually extends only 200-400 meters from the intrusive contact, but skarn-forming fluids can be focused along faults and dikes and cause localized skarn formation several kilometers from a causative pluton (e.g., Groundhog mine, N.M.; Meinert, 1987a).

SKARNOID

The term skarnoid applies to a calc-silicate rock whose origin is difficult to delineate and may involve mixed metamorphic and metasomatic processes (Zharikov, 1970). It is generally seen as grossular garnet replacement of interbedded carbonates and shales. This massive garnet rock resembles true skarn, but its Al-rich composition is significantly different from the andraditic garnets seen in porphyry copper-related metasomatic skarns. It is considered by Einaudi (1982b) to be a product of metamorphism and local diffusional metasomatism. In the Chandalar skarns, skarnoid consists of calc-silicate hornfels partially replaced and veined by metasomatic

skarn. Hence Chandalar skarnoid is gradational between a contact metamorphic rock and true skarn.

PROGRADE SKARN

This description of typical prograde and retrograde copper skarns is summarized from Einaudi and others (1981). In calcic copper skarns, the early calc-silicates formed are andraditic garnet, diopsidic pyroxene, wollastonite and, sometimes epidote. The first three commonly show a lateral zonation away from the intrusive: from garnet to pyroxene to wollastonite (see Figure 28). Epidote, where present, is next to or within the intrusive.

The garnets are color zoned from reddish brown near the intrusive to greenish farther out. They are ferric-rich garnets, ranging in composition from 80-100 mole % andradite ($Ca_3Fe_2Si_3O_{12}$; Ad) with negligible Mn contents. The clinopyroxenes have compositions ranging from 15-35% hedenbergite ($CaFeSi_2O_6$; Hd) and <3 percent manganese endmember, johannsenite ($CaMnSi_2O_6$; Jo).

Actinolite veins in pyroxene skarn are common in porphyry-related skarns. The actinolite generally contains 20-40 mole% ferro-actinolite.

Opaque minerals in skarn are both disseminated and vein controlled. Ore minerals are concentrated with retrograde alteration or in massive streaks and replacements at the marble front. Porphyry related skarns
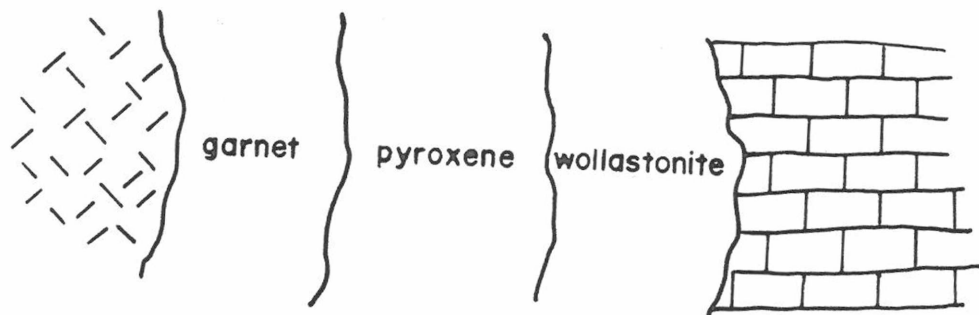
Figure 28.   Idealized calc-silicate zonation in a porphyry copper-related skarn.

generally contain from 2-15% sulfides and up to 10 % iron oxides.

Pyrite and chalcopyrite are the most common sulfides in the interior of the skarn. Chalcopyrite and bornite with minor sphalerite and pyrite are the dominant sulfides in "marble front" skarns (i.e., adjacent to marble). In some cases, e.g., Cananea, Mexico (Meinert, 1982), and the Groundhog, New Mexico (Meinert, 1987a), appreciable amounts of Zn-rich skarn are present 1-2 km from the center of high-Cu skarn. The most common primary iron oxide is magnetite, which is usually most abundant at contacts with the porphyry or marble and is an early-formed opaque mineral.

RETROGRADE ALTERATION

Retrograde alteration, a term used for lower-temperature skarn minerals, is usually well developed in porphyry copper related skarns. Where the prograde skarn minerals are andraditic garnet and diopsidic pyroxene, the stable retrograde assemblage usually consists of quartz, calcite, tremolite-actinolite, and iron oxides, with occasional epidote, talc and chlorite. The assemblage can appear as veins cross-cutting prograde skarn or as replacement of individual crystals.

POST-ORE METAMORPHIC AND DEFORMATIONAL EFFECTS

The effects of metamorphism and deformation on skarn deposits have not been well documented. However, Adams (1983) found that skarns formed adjacent to the regionally metamorphosed Arrigetch Peaks pluton in the central Brooks Range were not affected by the metamorphic foliation seen in the surrounding rocks. Furthermore, Newberry and others (1986) noted that in skarn prospects throughout the central Brooks Range, skarns were the only undeformed rocks.

VOLCANOGENIC MASSIVE SULFIDE DEPOSITS

The following discussion of undeformed volcanogenic massive sulfide (VMS) deposits is based upon a comprehensive paper by Franklin and others (1981). VMS deposits are found in rocks of all ages older than Tertiary. They are stratabound and mainly stratiform lenses of massive (>50%) sulfides associated with submarine volcanic rocks. These are high grade, generally low tonnage deposits, usually containing 0.1 - 50 million tons of 1-5% Cu, 5-20% Pb+Zn, with variable by-product Au and Ag. Several deposits are often found along strike within a particular stratigraphic unit. Where undeformed, the deposits are oval in plan view. They usually have a central, deep feeder zone of discordant veins and brecciation. This feeder zone is overlain by laminated

massive sulfide ore (up to 10 meters thick), which in turn
may be overlain by a sulfate-rich horizon generally
containing anhydrite and barite. Fewer than one half of
known VMS deposits contain a sulfate zone. A cherty, oxide
facies caps the deposits. Metal zonation is a common
feature in these deposits. Cu is usually deep and central,
whereas Pb, Zn, Au, and Ag are higher and farther from the
feeder zone. Sulfur isotopic ratios tend to vary by
approximately 2-8 per mil from the core to the margin of
the deposit. Their average $del^{34}S$ values are approximately
17 per mil lower than the values for contemporaneous
seawater (Sangster, 1968). Some unmetamorphosed massive
sulfide ores display textures (laminations, cross-bedding,
and framboids) interpreted as sedimentary; such textures
are generally destroyed during metamorphism. Figure 29
shows an idealized cross section through an undeformed VMS
deposit.

Typical alteration patterns in VMS deposits consist of
silicification at depth within a central feeder zone and
widespread chlorite, sericite, and/or talc alteration halos
below and sometimes above the main ore horizons. Abundance
and distribution of these alteration types varies widely
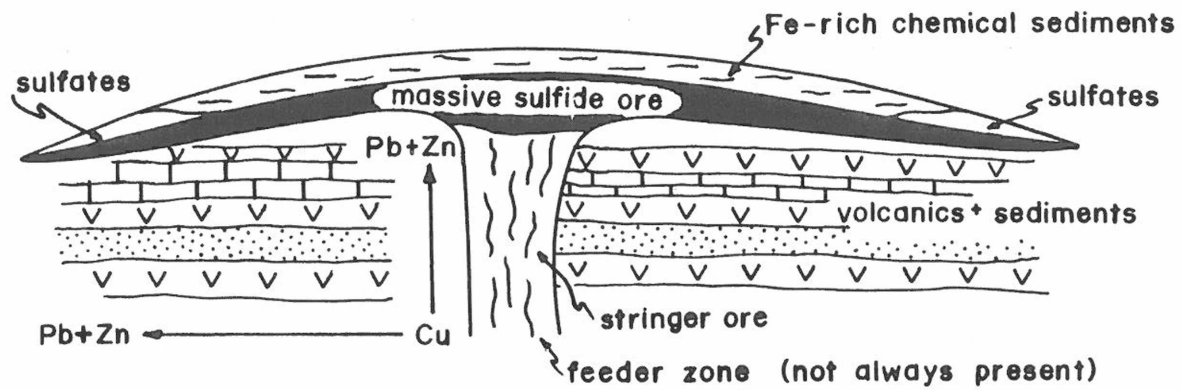between deposits.

Figure 29. Idealized cross section through a VMS deposit. Note the increase in Pb+Zn upward and away from the central feeder zone.

METAMORPHIC AND DEFORMATIONAL EFFECTS

Deposits older than Tertiary age are often deformed and metamorphosed, making them difficult to characterize. Effects of metamorphism on VMS deposits have been reviewed by Vokes (1969), Mookherjee (1976) and Rockingham and Hutchinson (1980). Mookherjee (1976) noted that during metamorphism, reactions occur between sulfides and silicates, exemplified by coronas of magnetite and pyrrhotite on silicate minerals. These become more conspicuous with increasing metamorphic grade.

Vokes (1969) and Rockingham and Hutchinson (1980) have shown that both textural and mineralogic changes occur with metamorphism. These include, with increasing metamorphic grade, 1) a progressive increase in grain size, 2) obliteration of sedimentary and diagenetic textures in the ores, 3) brittle deformation and rotation of harder sulfides, such as pyrite, 4) plastic deformation of softer sulfides, such as the remobilization of chalcopyrite and galena into fractures within pyrite, 5) annealing of sulfides around triple junctions, 6) increasing Fe content in sphalerite, and 7) coarsening of chalcopyrite and pyrrhotite blebs in sphalerite, which tend to lengthen and become rod shaped. Chemical and mineralogic changes are exemplified by the replacement of pyrite by pyrrhotite and then by magnetite.

During obduction of VMS deposits onto continental masses, they often become highly deformed (Sangster and Scott, 1976). Shearing may deform the deposit into an elongate flattened shape (Figure 30). The stringer zones may be turned into a "stratiform" disseminated sulfide zone and/or be translated away from the massive sulfide zone. Recumbent folding may destroy metal zoning patterns, or make them unrecognizable.

AMBLER DISTRICT DEPOSITS

An important set of VMS deposits to consider as an analogy to potential VMS mineralization in the Chandalar area are the Ambler district deposits in the southwestern Brooks Range, which are within the same lithostratigraphic terrane as the Chandalar study area. The following description is based on studies by Hitzman and others (1986) and Schmidt (1986).

The Ambler district consists of three major stratabound VMS deposits (Arctic, Sun and Smucker) and five smaller prospects (BT, Sunshine Creek, Bud, Cliff and Dead Creek). The majority of the ore bodies in the district are stratiform, laterally extensive, massive sulfide lenses (40-80% sulfides). The lenses range up to 14 meters in thickness with strike lengths of about 2.5 kilometers. Schmidt (1986) has described a chlorite-pyrite, sub-ore grade feeder zone at the Arctic deposit. The ores contain
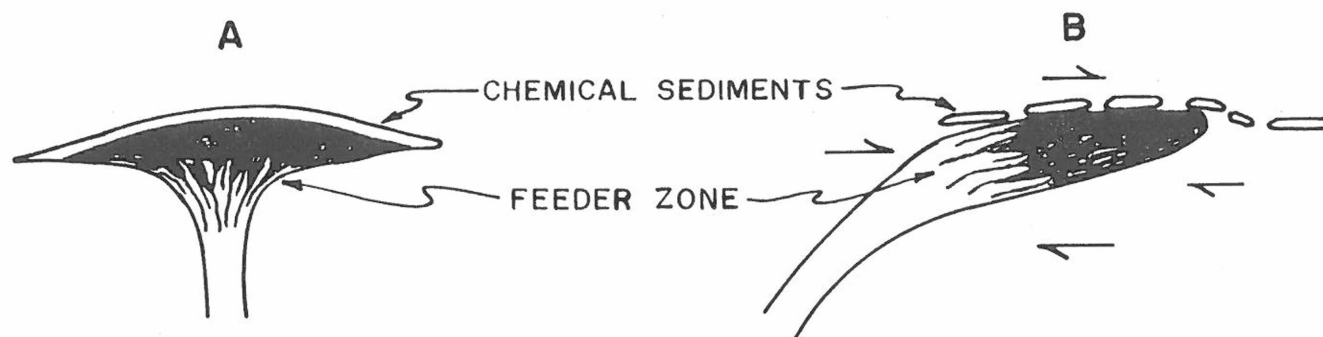
Figure 30. Schematic diagram showing the effects of deformation on a massive sulfide deposit. A. Undeformed massive sulfide deposit. B. Same deposit after shearing. After Sangster and Scott (1976).

varying proportions of pyrite, chalcopyrite, sphalerite, pyrrhotite, and galena with minor tennantite-tetrahedrite, bornite, and arsenopyrite. Average grades in the three major deposits range from 1 to 4% Cu, 5 to 7% Zn, 1 to 3% Pb and 2 to 7 oz/ton (64 to 224 ppm) Ag. Au grades are low, generally <0.02 oz/ton (<0.6 ppm). Gangue mineralogy consists of barite, quartz, phengite, phlogopite, chlorite, dolomite, talc, ankerite and calcite. Metamorphic textures predominate, especially the recrystallization of pyrite to coarse euhedral porphyroblasts. No large scale sulfide flowage is seen, although most primary textures have been obliterated.

Hydrothermal alteration in the Ambler deposits is exemplified by the Arctic deposit alteration patterns. In this deposit, Mg-rich chlorite ± sulfide are present in the footwall (below the ore horizon). Phengite-phlogopite-talc-carbonate alteration immediately surrounds the sulfide horizon (both below and above). Quartz-pyrite alteration is present in the hanging wall above the ore body.

The presence of lateral and vertical metal zoning varies within the Ambler deposits. When present, metals are zoned outward laterally from Cu to Zn to Pb and Ag and upward from Cu to Zn and Pb.

An additional metal-bearing rock type which occurs at the base of the Ambler sequence is informally named the

"gnurgle gneiss". It is a layered calc-silicate rock consisting of bands of quartz, actinolite, epidote, almandine-spessartine garnet and calcite with accessory magnetite, sphene and clinozoisite. It contains disseminated and banded masses of chalcopyrite, pyrite, sphalerite and galena. It was considered by Newberry and others (1986) to be the product of metamorphism of a layered Mn and base-metal rich chemical sediment, made up of chert, dolomite and limestone.

Although the mineralogy of the gnurgle gneiss is similar to that of a Cu-Zn skarn, a number of features distinguish the two. Low-Ca minerals are common in the gnurgle gneiss, including almandine and spessartine garnet, hornblende, biotite, stilpnomelane, and tourmaline. These are rarely seen in copper-zinc skarns. The silicates in the gnurgle gneiss form mono- and bi-mineralic layers which parallel schistosity and are often isoclinally folded. Sulfides are disseminated or concentrated in layers and lenses which parallel schistosity. Metamorphic fabrics dominate in the gnurgle gneiss. Elongate and platy minerals show parallel alignment and define schistosity. Garnets are poikiloblastic and slightly deformed, with long axes paralleling foliation (Newberry and others, 1986).

APPENDIX 7 - NON-MINERALIZED ROCK DESCRIPTIONS.

CALC-SILICATE HORNFELS

Calc-silicate hornfels is a banded rock which probably formed by contact metamorphism of calcareous shales and argillaceous limestones. It is composed of alternating 1-2 cm. wide green and light brown bands of very fine grained pyroxene-epidote hornfels and garnet-quartz hornfels, respectively. Primary sedimentary textures are absent, and the hornfels is often isoclinally folded.

BLACK HORNFELS

Black hornfels forms resistant layers which crop out adjacent to the Venus Creek meta-igneous body (Figure 3). It is a black, very fine grained, dense rock which is composed of quartz, muscovite and clays and often contains disseminated pyrite. West of Big Spruce Creek, it is interbedded with argillaceous marble. The protolith for this rock was probably a black, pyritic shale. No andalusite or cordierite is present, even immediately adjacent to granitic stocks.

SKAJIT MARBLE

The marble units within the study area form resistant outcrops up to 500 meters thick. These thick marble beds occur a number of times throughout the stratigraphic section and are interlayered with thick sequences of calc-

schist, quartz schist, and argillaceous marble. They are
light gray, massive to platy marbles with occasional
banding, identified by the presence of alternating layers
of very fine grained (0.02-0.05 mm) and fine grained (0.2-
1.0 mm) calcite. Platy marble consists of elongate calcite
grains and fine grained (0.01-0.02 mm) graphite, aligned
parallel to the metamorphic foliation in the surrounding
schists. This gray marble occasionally contains
disseminated pyrite. A second marble type, a 60 foot
thick, massive, clean white marble which contains numerous
pyrite stringers, is present in the Luna drill core but is
not seen in the Big Spruce Creek area. All relict
sedimentary textures have been destroyed, and the marbles
contain no discernable fossils.

CALCAREOUS SCHIST/ARGILLACEOUS MARBLE

Calc-schists and argillaceous marbles form a
compositional gradation between pelitic schist and pure
marble. As the calcite content increases, pelitic schist
grades into calc-schist, argillaceous marble, and then into
pure marble. Calc-schists are non-resistant and are rarely
exposed at the surface unless they are interlayered with a
more resistant rock type, such as argillaceous marble.
They are medium gray-green, sometimes crenulated schists
containing calcite and muscovite with minor quartz and
chlorite. Argillaceous marble consists of calcite with

minor muscovite and quartz. Where the protoliths were impure dolomites, the rocks contain sphene and biotite or phlogopite.

QUARTZ MUSCOVITE SCHIST

The quartz muscovite schist is a light greenish-gray, sometimes crenulated, schist consisting of predominantly muscovite with subordinate amounts of quartz and chlorite.

Croff and others (1979) examined thin sections of quartz sericite (felsic) schists from the Chandalar copper district and claimed that relict tuffaceous textures, including devitrified pumaceous material and subhedral plagioclase crystals, could be seen. No sample locations are given for these schists, however, and no photographic evidence was given. I have not observed unambiguous volcanic textures in any thin section or hand specimen.

CHLORITIC QUARTZ SCHIST

Chloritic quartz schists are gray green, fairly resistant units which are often interbedded with calc-schists and argillaceous marbles. They consist of variable amounts of quartz, feldspar (albite $\pm$ K-feldspar), chlorite, and muscovite with minor calcite and disseminated pyrite. The protolith for these rocks was probably a meta-graywacke or an andesitic tuff.

APPENDIX 8 - DISTRIBUTION OF IGNEOUS ALTERATION TYPES IN
THE BIG SPRUCE CREEK PROSPECTS

PROPYLITIC ALTERATION

In the southwestern portion of the Venus stock, propylitic alteration appears in two forms. The first is as veins of epidote, chlorite, actinolite and pyrite. The second is as chlorite and epidote replacing amphibole. Within the Venus Creek porphyry, propylitic alteration occurs as clusters of chlorite, calcite and epidote replacing the aphanitic groundmass. Propylitic alteration is present as veins of chlorite, epidote and pyrite. In the northeastern portion of this elongate stock, propylitic alteration appears as scaly masses of epidote, chlorite, and sphene. In one sample, there are broad bands containing intergrown epidote, chlorite, calcite and quartz and lacking noticeable igneous texture.

Columnar aggregates of epidote, calcite, and chlorite are present in the main body of the Victor stock. In a small outcrop of intrusive east of the main stock (either a separate fracture wedge or connected at depth), diopsidic pyroxene (remnant endoskarn?) is present and is partially replaced by epidote, calcite, sphene and muscovite. Veins of epidote are also present. A thick sill-like body of altered granodiorite is associated with the Eva prospect. Here, propylitic alteration appears as veins of calcite and

chlorite. Evidence for propylitic alteration is absent in the Evelyn Lee stock.

POTASSIC ALTERATION

In the southwestern Venus stock, potassic alteration occurs as veins of coarse grained potassium feldspar, quartz and pyrite. It also occurs as selective replacement of hornblende by biotite.

Within the main body of the Evelyn Lee stock, secondary potassium feldspar and fine-grained, fracture-controlled biotite indicate the presence of potassic alteration. In dikes which crop out north of the main body (and may connect to it at depth), potassic alteration is shown by selective replacement of hornblende by fine-grained biotite.

SERICITIC ALTERATION

Within Venus Creek, quartz-sericite-pyrite veins are present only locally. Along intrusive contacts, where foliation is more intense, sericitic alteration appears as lenses of quartz and muscovite with pyrite. In the northeastern portion of the Venus stock, along Alaska Creek, muscovite appears as selvages on quartz veins. Pyrite, although present, is not associated with these veins. Instead it is associated with propylitic veins of epidote and chlorite. In the main body of the Victor

stock, sericitic alteration again occurs as stacked bands of quartz and muscovite. In the granodiorite sill at Eva, veins of muscovite and pyrite indicate sericitic alteration.